

**AGE-RELATED CHANGES IN BONE:
VARIATION AND FACTORS INFLUENCING BONE FRAGILITY**

by

Dana Lynne Begun

**A dissertation submitted in partial fulfillment
of the requirements for the degree of
Doctor of Philosophy
(Anthropology and Biomedical Engineering)
in the University of Michigan
2015**

Doctoral Committee:

**Emeritus Professor Steven A. Goldstein, co-Chair
Professor Milford H. Wolpoff, co-Chair
Research Assistant Professor Andrea I. Alford
Assistant Professor Maureen J. Devlin
Professor Karl J. Jepsen**

© Dana L. Begun 2015
All Rights Reserved

DEDICATION



ACKNOWLEDGEMENTS

There have been so many people that have helped me get through my 25 years of schooling. The most important people, aside from having to deal with me the longest, are my parents and sister. Frank and Audrey Begun, my dad and mom, are the perfect combination of being normal enough to prevent me from becoming a serial killer but odd enough to keep things interesting. Though they may not always like the adults they are, they are both great examples of the dedication and persistence of continuing education and the good that can be achieved with it. My sister, Erica Begun-Veenstra, deserves a lot of credit, not least of all because she is the one who taught me to read (starting with the Bernstein Bears). She also has been my best friend and always there (except when she decided the swinging door and my face made a good combination). She has never shied away from being herself. Her passion for everything that she loves and lack of concern for whether those things are “cool” has always inspired me.

My aunt and uncle (Amy and Greg Grambeau) deserve a lot of credit for being a home-away-from-home. They not only dealt quite graciously with my taking over of their kitchen counter, but also the presence of my crazy squirrel-obsessed pup. Although, they did get some delicious scones out of the deal. My pseudo-uncle, Stan Stojkovic, has played many different roles throughout my life. Early on, he was my jungle gym (sorry about the tooth I kicked out) and skipping partner. He was also a great basketball teacher. Now, he is the best SCUBA diving buddy I could ask for. On the topic of almost family, I want to thank Kate Chamberlin for being the best friend someone could ever ask for since sophomore year of college when we tried to put together an “easy-to-assemble” shelf. Someday, we will live in the same city again! Hannah Osborn, though we only spent one ridiculous college year together, you are also a great friend

and I love how we can go without seeing each other for months and then pick up like it was yesterday.

I want to thank my advisor, Steve Goldstein. He agreed to take me on as a Master's student, not expecting to get stuck with me. Despite that, he has been an amazing mentor and a great example of how to approach problems that arise. He also has taken time out of his retirement to continue to mentor me. For all of his time, energy, and funding, I am supremely grateful. Milford Wolpoff deserves recognition for deciding that I was a worthy graduate student and accepting me into the program from the start. He also was the one that introduced me to Steve and the Orthopaedic Research Labs where I found my science home. Karl Jepsen has served as an honorary advisor the last few years. Since coming to the lab, he often provided day-to-day guidance, as well as letting me stink up his lab aisle with Trizol. Andrea Alford has played the role of friend and mentor. She is a good demonstration of how a successful woman in academia can also be fun. Maureen Devlin has not only provided wonderful arts and crafts supplies to the anthropology graduate students but also been a wonderful mentor. She was great at letting me in on the secret that nobody has a perfect graduate experience and you just have to deal with the problems that come at you. Ken Kozloff, although not officially on my committee, deserves some credit for helping to mentor me. He is always great at offering help with science and keeping things in perspective.

The Orthopaedic Research Labs has been my base of operations for my entire graduate career. The people I have met and gotten a chance to work with have been wonderful! The friends and coworkers that have passed through the lab mean so much to me and have made working there a blast. I specifically want to thank Jeff Meganck, Connie Soves, and Aaron Weaver. They were my lab big siblings that introduced me to the ORL and taught me pretty much everything I know about how to run experiments. The staff members at the ORL have also been crucial in helping get to this point, especially Kathy Sweet, who often got stuck for hours in a dark basement with me but made it bearable. Also, Peggy Piech who always looked out for me and let me rant and rave when I needed to.

I want to thank all of my friends that have kept me sane and entertained throughout this process. Zachary Cofran, Kristen Munnely, and Ben Sinder have been the best roomsters anyone could ask for. One of the best things about the Biological Anthropology program at Michigan is the ability to accept amazing people as students. Bethany Hansen has not only been a great pal but also brought back Sebo from Uganda, who quickly became my second favorite dog in the world and Reese's bestie. Caroline VanSickle and Crystal Meyer made the Wolpoff lab complete. Jess Beck needs to be thanked for all of her amazing food. Maire Malone, Marcela Benitez, Chelsea Fisher, Liz Johnson, Dave Pappano, Ashley Shubert, Colin Quinn, Alice Wright, Casey Barrier, Bryce Adams, Geoffy Hughes, Ethan Daley, and Eugene Manley, thanks for all of the hilarious times, you are wonderful friends!

Thank you everyone who has helped me over the years...GO BLUE!

TABLE OF CONTENTS

DEDICATION.....	ii
ACKNOWLEDGEMENTS	iii
LIST OF FIGURES	ix
LIST OF TABLES	xi
ABSTRACT	xii
CHAPTER I: INTRODUCTION	1
References: Chapter I	3
CHAPTER II: BONE FUNCTIONAL CHANGES VARY BETWEEN DIFFERENT INBRED MOUSE STRAINS	6
Introduction.....	6
Materials and Methods.....	7
<i>Animals.....</i>	<i>7</i>
<i>Micro-Computed Tomography (μCT)</i>	<i>9</i>
<i>Mechanical Testing</i>	<i>9</i>
<i>Statistical Analysis.....</i>	<i>9</i>
Results.....	10
<i>Experiment A: Mechanical Function</i>	<i>10</i>
<i>Experiment B: Causes of Functional Changes</i>	<i>12</i>
<i>BALB/c Mouse Parameter Relationships.....</i>	<i>12</i>
<i>C57Bl/6 Mouse Parameter Relationships</i>	<i>13</i>
<i>CBA/J Mouse Parameter Relationships.....</i>	<i>15</i>
<i>DBA/2 Parameter Relationships.....</i>	<i>17</i>
Discussion	18
<i>Future Work</i>	<i>21</i>
References: Chapter II	23
Figures: Chapter II	27
CHAPTER III: PATTERNS OF BONE AGING VARY BETWEEN MOUSE STRAINS	40
Introduction.....	40

Materials and Methods	41
<i>Animals</i>	41
<i>Micro-Computed Tomography (μCT)</i>	41
<i>Mechanical Testing</i>	42
<i>Statistical Analysis</i>	42
Results	42
<i>Mechanical Testing</i>	42
<i>Body Weight Relationship</i>	43
<i>General Linear Models: Mechanical Properties</i>	44
<i>Mechanical Parameter Relationships</i>	45
<i>Mechanics and Morphology</i>	47
<i>Trabecular Bone</i>	51
<i>General Linear Models: Femur</i>	53
<i>General Linear Models: Tibia</i>	55
<i>Trabecular and Cortical Relationships</i>	57
Discussion	58
<i>Models for Human Aging</i>	61
References: Chapter III	63
Figures: Chapter III	64
CHAPTER IV: DIFFERENTIAL AGE-RELATED CHANGES IN MECHANORESPONSE	87
Introduction	87
Materials & Methods	89
<i>Tibial Loading</i>	89
<i>Quantitative Real-Time PCR</i>	91
<i>Adaptive Loading</i>	93
<i>Statistics</i>	94
Results	94
<i>Periosteal Gene Expression</i>	94
<i>Cortical Gene Expression</i>	95
<i>Epiphyseal Gene Expression</i>	95
<i>Periosteal Dynamic Histomorphometry</i>	96
<i>Endosteal Dynamic Histomorphometry</i>	96
<i>Metaphyseal Dynamic Histomorphometry</i>	96

Discussion	97
References: Chapter IV.....	102
Figures: Chapter IV	108
CHAPTER V: CONCLUSIONS AND FUTURE WORK.....	118
Mouse Model for Human Bone Aging	118
Future Work.....	124
References: Chapter V.....	126
APPENDIX	128

LIST OF FIGURES

Figure 2. 1 - Changes in mechanical function parameters.	27
Figure 2. 2 - Graphical representation of general linear models.	29
Figure 2. 3 - Linear relationship between stiffness and ultimate load.	30
Figure 2. 4 - Load-displacement curves for 4-point bending.	31
Figure 2. 5 - Geometry comparisons between 3- and 18-month mice.	33
Figure 2. 6 - Alpha-blend comparisons of mineralization patterns between ages.	34
Figure 2. 7 - Summary of BALB/c results.	36
Figure 2. 8 - Summary of C57Bl/6 results.	37
Figure 2. 9 - Summary of CBA/J results.	38
Figure 2. 10 - Summary of DBA/2 results.	39
Figure 3. 1 - Femoral mechanical properties.	64
Figure 3. 2 - Tibial mechanical properties.	66
Figure 3. 3 - Average body weights in age groups.	67
Figure 3. 4 - Graphical representations of general linear models of mechanical properties.	69
Figure 3. 5 - Linear relationships between stiffness and ultimate load in four age groups.	70
Figure 3. 6 - Representative load-displacement curves for 4-point bending in four age groups.	71
Figure 3. 7 - Post-yield displacement means from 4-point bending.	72
Figure 3. 8 - MicroCT parameters influencing mechanics.	73
Figure 3. 9 - Cortical bone morphological measures in femur (left) and tibia (right).	76
Figure 3. 10 - Trabecular properties of the distal femur.	77
Figure 3. 11 - Trabecular stereology of the distal femur.	79
Figure 3. 12 - Trabecular properties of the proximal tibia.	80
Figure 3. 13 - Trabecular stereology of the proximal tibia.	81
Figure 3. 14 - General linear models of femoral trabecular parameters.	82
Figure 3. 15 - General linear models of femoral stereology.	83

Figure 3. 16 - General linear models of tibial trabecular parameters.	84
Figure 3. 17 - General linear models of tibial trabecular stereology.	85
Figure 3. 18 - Trabecular BMD and TMD regressed against weight.	86
Figure 4. 1 - Axial compressive loading system.	108
Figure 4. 2 - Periosteal gene expression.	109
Figure 4. 3 - Cortical gene expression.	111
Figure 4. 4 - Epiphyseal gene expression.	112
Figure 4. 5 - Periosteal dynamic histomorphometry.	113
Figure 4. 6 - Endosteal dynamic histomorphometry.	114
Figure 4. 7 - Metaphyseal trabecular dynamic histomorphometry.	116
Figure 4. 8 - Representative images of CBA/J diaphysis in control (left) and loaded (right) limbs.	117

LIST OF TABLES

Table 2. 1 - Femoral 4-point bending results.....	28
Table 2. 2 - Summary of mechanical testing data.	32
Table 2. 3 - Summary of microCT data results.	35
Table 3. 1 - Mean values of mechanical measures in femur and tibia.	68
Table 4. 1 - Preliminary results for mechanoresponse in tibial loading.....	108
Table 4. 2 – PrimeTime® qPCR primers and sequences.	108
Table A. 1 - Mean fold change in gene expression.....	128
Table A. 2 - Tibial dynamic histomorphometry data	129

ABSTRACT

Humans have a unique evolutionary trajectory that allows life past reproductive viability. Antagonistic pleiotropy and resource economics lead to the deterioration of physiological processes once beyond years in which natural selection is effective. As individuals age, bone becomes increasingly fragile and prone to fracture. Due to heterogeneity in human aging patterns, bone aging is a highly variable process. The ability to predict, diagnose, and treat age-related bone fragility has become an area of major focus in medical research, however, there is little consensus in the field as to the mechanisms behind bone aging. The lack of clarity in the causes of bone aging makes individualized medical approaches difficult. Studies of these mechanisms are complicated by the inherent variability in human biology and environment. The use of murine models provides greater experimental control but has previously not recognized the presence of variability in aging.

This work provides evidence for the utility of multiple inbred mouse strains in aging research. This approach provides high level of control but also allows investigation into the causes behind variable aging outcomes. The first aim of this project establishes differences in bone aging in the femora of four inbred mouse strains to demonstrate the range of intraspecies variability in bone aging. The BALB/c and C57Bl/6 strains lose mechanical functionality with age but in different ways. The CBA/J and DBA/2 strains maintain mechanical integrity with aging using different strategies. Different rates of remodeling, as well as mineralization, lead to the variation in mechanical function changes with age in the four strains. The second aim investigates the applicability of comparative mouse models of aging to humans. This aim applies modern theories of aging to the variable bone outcomes. The third aim demonstrates the potential influence age-related changes in mechanoresponse have on bone aging using a tibial axial loading model. The data in this thesis demonstrate the variability in bone aging in a mouse model, providing potential insight into human inter-individual aging variations. The work

presented also provides a platform for future aging experimentation investigating factors that influence how well bone ages.

CHAPTER I: INTRODUCTION

As individuals age, bone becomes increasingly fragile and prone to fracture [1, 2, 3]. With medical advances and lifestyle changes, the average human lifespan has increased from the mid-40's during the early 1900's to over 80 years in some countries [4]. With this change in demography, healthcare must address new medical issues, including age-related bone fragility leading to increased fracture rates. As a response to this need, the ability to predict, diagnose, and treat bone fragility has become an area of major focus in medical research.

The current standard for predicting fracture is dual-energy X-ray absorptiometry (DXA) measures of bone mineral density (BMD) [5]. Johnell *et al* estimate that every standard deviation away from the mean BMD increases the risk of fracture by 40% [6]. This provides a rapid method of predicting fracture risk. However, simplified guidelines such as BMD values are inherently flawed by not addressing the large range of variability in how people age. Cases in which BMD measures have proven ineffective include one study in which 1,012 elderly Chinese women were classified into three groups depending on DXA measures: osteoporotic, osteopenic, and normal. Within the normal group, 21.8% of the women suffered a fragility fracture [5]. This represents a large subgroup of the population that may pass screening and therefore receive no preventative measures, ultimately leading to preventable fractures. Another study demonstrating the complex nature of bone fragility was Aspray's 1996 study of Gambian and European women. This study compared BMD values of age-, height-, and weight-matched Gambian and European women. The Gambian women had BMD values 10-40% lower than values measured among the European group. However, incidents of fracture associated with aging were rare in the Gambian population compared to the European fracture rates [7].

A major reason for the lack of predictive accuracy in fracture risk assessment is the multifaceted phenomenon of increasing bone fragility with age. Bone aging patterns are

interrelated with a number of variables. Kanis *et al.* have compiled a list of factors that influence risk of fragility-related fracture [8]:

- Sex (females at higher risk)
- Age
- Low BMD
- Low body weight/BMI
- Ethnic origin (Asian or Caucasian)
- Previous fragility fracture
- Family history of fracture
- Glucocorticoid treatment
- High bone turnover
- Smoking
- High alcohol intake
- Long-term immobility
- Low calcium intake
- Vitamin D deficiencies
- Primary or secondary amenorrhea: surgery, chemotherapy, radiotherapy, anorexia nervosa, exercise, chronic illness, hyperprolactinemia
- Primary or secondary hypogonadism in males Klinefelter's syndrome, hypopituitarism, hyperprolactinemia, castration, prostate surgery
- Other related conditions: chronic liver disease, irritable bowel disease, hyperparathyroidism, organ transplant, renal failure, Cushing's syndrome, gastric surgery, neuromuscular disorders
- Fall risk factors: hemiparesis, Parkinson's dementia, vertigo, alcoholism, blindness/poor visual acuity, neuromuscular disorders

With the high number of interrelated and interacting risk factors of fragility fractures, it is difficult to get a clear and comprehensive understanding of the etiology of fragility fractures. This results in disparities in understanding how the function of bone changes with age progression. The lack of consensus as to the causes and effects relevant to bone aging hinders accurate characterization and diagnosis of fracture risk.

It is evident that guidelines for fracture risk cannot be universally applied to all populations and individuals. The insufficient understanding of the complex factors influencing bone fragility and fracture risk demonstrate the need for a method to investigate the sources of variability in bone aging. Human studies have inherent problems that hinder the ability to parse out individual factors in a controlled environment. Due to the limitations of human studies, it would be beneficial to develop a correlate for the bone aging variability evident in human populations.

Murine models for biomedical studies are some of the best characterized and easily accessible. One of the primary benefits of utilizing small rodent models, such as mice and rats,

is the ability to control and manipulate environmental factors. This level of control allows for a reduction in the confounding variables inherent in human research. Currently, most age-related research conducted in murine models has approached aging through either surgical and/or genetic modification methods [9]. One of the most widely used models of aging is the SAMP6 mouse strain [10, 11]. Unfortunately, this model—as well as the surgical models—does not demonstrate patterns of bone aging similar to that documented in humans [9].

Some aging work in mice has utilized the C57Bl/6 mouse strain to investigate various changes and influences on aging [9, 12]. The benefit to using untreated mouse models is that it may provide a more accurate correlate of true physiological aging than accelerated aging mouse models. However, one of the biggest benefits of using inbred mice in research may also be a large drawback in their utility for bone aging work. Inbred mouse strains are used due to the minimal variability, yet, it has been demonstrated that there is a large range of variability in human bone aging.

The first aim of this project is to establish that there are differences in the trajectory of bone aging in different inbred mouse strains. Many studies have given evidence of phenotype differences between various inbred mouse strains upon reaching maturity [13, 14, 15, 16, 17]. Despite clear phenotypic differences between inbred mouse strains, little work has been done comparing how the various strains might differ in aging patterns. The primary goal of this chapter is to determine if the four aged inbred mouse strains that are available experience similar or variable patterns of bone aging. If such variation is present, investigating the factors involved in the different outcomes may be a useful tool for parsing out the cause and effect of aging-related changes in humans.

The second aim is concerned with developing the mouse model of aging variation and investigating the applicability to humans. In general, age bone strength is lost with age through a combination of alterations to the mineralization, morphology, and composition. Before drawing connections between human and murine patterns of aging, we must first provide a comprehensive picture of how and when both strains change. This involves an understanding of the onset and rate of change occurring in both the cortical and trabecular bone regions. Furthermore, it is important to determine if these patterns are systemic to the skeletal system

or isolated to single bone locations. Once elucidated, we can begin to relate patterns of aging in the murine models to those in humans. This approach could provide avenues for experimentation regarding bone aging not possible in humans.

The third and final aim demonstrates the potential influence age-related changes in mechanoreponse have on bone quality. Mechanical stimulation is critical for maintenance of healthy bone [18]. The mechanoreponse system allows bone to sense and adapt to its loading environment. Studies investigating the role of mechanical responsiveness in aging bone health have produced confounding results [12, 19, 20, 21, 22, 23, 24]. Using the models of successful and at-risk bone aging, this chapter will determine if the ability to respond to load is altered with age. This knowledge will provide direction for future research into diagnostic and therapeutic measures to alleviate fracture risk due to aging.

References: Chapter I

- [1] A. L. Boskey and R. Coleman, "Aging and bone," *Journal of Dental Research*, vol. 89, no. 12, pp. 1333-1348, 2010.
- [2] S. M. Tommasini, P. Nasser and K. J. Jepsen, "Sexual dimorphism affects tibia size and shape but not tissue-level mechanical properties," *Bone*, vol. 40, pp. 498-505, 2007.
- [3] G. K. Chan and G. Duque, "Age-related bone loss: old bone, new facts," *Gerontology*, vol. 48, pp. 62-71, 2002.
- [4] National Institute on Aging, "Global Health and Aging," October 2011. [Online]. Available: http://www.nia.nih.gov/sites/default/files/global_health_and_aging.pdf. [Accessed 2014].
- [5] Y.-H. Deng, L. Zhao, M.-J. Zhang, C.-M. Pan, S.-X. Zhao, H.-Y. Zhao, L.-H. Sun, B. Tao, H.-D. Song, W.-Q. Wang, G. Ning and J.-M. Liu, "The influence of the genetic and non-genetic factors on bone mineral density and osteoporotic fracture in Chinese women," *Endocrine*, vol. 43, pp. 127-135, 2013.
- [6] O. Johnell, J. A. Kanis, A. Oden, H. Johansson, C. De Laet, P. Delmas, J. A. Eisman, S. Fujiwara, H. Kroger, D. Mellstrom, P. J. Meunier, L. J. Melton III, T. O'Neill, H. Pols, J. Reeve, A. Silman and A. Tenenhouse, "Predictive value of BMD for hip and other fractures," *Journal of Bone and Mineral Research*, vol. 20, no. 7, pp. 1185-1194, 2005.
- [7] T. J. Aspray, A. Prentice, T. J. Cole, Y. Sawo, J. Reeve and R. M. Francis, "Low bone mineral content is common but osteoporotic fractures are rare in elderly rural Gambian women," *Journal of Bone and Mineral Research*, vol. 11, p. 1019, 1996.
- [8] J. A. Kanis, "Diagnosis of osteoporosis and assessment of fracture risk," *Lancet*, vol. 359, pp. 1929-1936, 2002.

- [9] F. A. Syed and K. A. Hoey, "Integrative physiology of the aging bone: insights from animal and cellular models," *Annals of the New York Academy of Sciences*, vol. 1211, pp. 95-106, 2010.
- [10] O. Kajnekova, B. Lecka-Czernik, I. Gubrij, S. P. Hauser, K. Takahashi, A. M. Parfitt and e. al, "Increased adipogenesis and myelopoiesis in the bone marrow of SAMP6, a murine model of defective osteoblastogenesis and low turnover osteopenia," *Journal of Bone and Mineral Research*, vol. 12, pp. 1772-1779, 1997.
- [11] M. Matsushita, T. Tsuboyama, R. Kasai, H. Okumura, T. Yamamuro, K. Higuchi and e. al, "Age related changes in bone mass in the Senescence Accelerated Mouse (SAM) SAM-R/3 and SAM/6 as new models for osteoporosis," *American Journal of Pathology*, vol. 215, pp. 276-283, 1986.
- [12] V. Ferguson, R. Ayers, T. Bateman and S. Simske, "Bone development and age-related bone loss in male C57Bl/6 mice," *Bone*, vol. 33, pp. 387-398, 2003.
- [13] M. P. Akhter, Z. Fan and J. Y. Rho, "Bone intrinsic material properties in three inbred mouse strains," *Calcified Tissue International*, vol. 75, pp. 416-420, 2004.
- [14] K. J. Jepsen, O. Akkus, R. J. Majeska and J. H. Nadeau, "Hierarchical relationship between bone traits and mechanical properties in inbred mice," *Mammalian Genome*, vol. 14, pp. 97-104, 2003.
- [15] C. Price, B. C. Herman, T. Lufkin, H. M. Goldman and K. J. Jepsen, "Genetic variation in bone growth patterns defines adult mouse bone fragility," *Journal of Bone and Mineral Research*, vol. 20, no. 11, pp. 1983-1991, 2005.
- [16] J. E. Wergedal, M. H.-C. Sheng, C. L. Ackert-Bicknell, W. G. Beamer and D. J. Baylink, "Genetic variation in femur extrinsic strength in 29 different inbred strains of mice is dependent on variations in femur cross-sectional geometry and bone density," *Bone*, vol. 36, pp. 111-122, 2005.
- [17] I. Sabsovich, J. D. Clark, G. Liao, G. Peltz, D. P. Lindsey, C. R. Jacobs, W. Yao, T.-Z. Guo and W. S. Kingery, "Bone microstructure and its associated genetic variability in 12 inbred mouse strains: microCT study and in silico genome scan," *Bone*, vol. 42, no. 2, pp. 439-451, 2008.
- [18] D. Papachristou, K. Papachroni, E. Basdra and A. Papavassiliou, "Signaling networks and transcription factors regulating mechanotransduction in bone," *BioEssays*, vol. 31, pp. 794-804, 2009.
- [19] M. Willingham, M. Brodt, K. Lee, A. Stephens, J. Ye and M. Silva, "Age-related changes in bone structure and strength in female and male BALB/c mice," *Calcified Tissue International*, vol. 86, pp. 470-483, 2010.
- [20] M. Brodt and M. Silva, "Aged mice have enhanced endocortical response and normal periosteal response compared with young-adult mice following 1 week of axial tibial compression," *Journal of Bone and Mineral Research*, vol. 25, no. 9, pp. 2006-2015, 2010.
- [21] S. Srinivasan, S. Agans, K. King, N. Moy, S. Poliachik and T. Gross, "Enabling bone formation in the aged skeleton via rest-inserted mechanical loading," *Bone*, vol. 33, no. 6, pp. 946-955, 2003.
- [22] L. Meakin, G. Galea, T. Sugiyama, L. Lanyon and J. Price, "Age-related impairment of bones' adaptive response to loading in mice is associated with sex-related deficiencies in osteoblasts but no change in osteocytes," *Journal of Bone and Mineral Research*, vol. 29, no. 8, pp. 1859-1871, 2014.

- [23] N. Holguin, M. Brodt, M. Sanchez and M. Silva, "Aging diminishes lamellar and woven bone formation induced by tibial compression in adult C57Bl/6," *Bone*, vol. 65, pp. 83-91, 2014.
- [24] C. Turner, Y. Takano and I. Owan, "Aging changes mechanical loading thresholds for bone formation in rats," *Journal of Bone and Mineral Research*, vol. 10, no. 10, pp. 1544-1549, 1995.

CHAPTER II:

BONE FUNCTIONAL CHANGES VARY BETWEEN DIFFERENT INBRED MOUSE STRAINS

Introduction

In this chapter, I will address the present lack of understanding regarding the variability in mouse bone aging models. Published data provide evidence of phenotype differences between various inbred mouse strains upon reaching maturity [1, 2, 3, 4, 5]. Despite clear phenotypic differences between inbred mouse strains, little work has been reported comparing how the various strains might differ in aging patterns. The National Institute of Aging (NIA), a department of the National Institutes of Health (NIH), maintains a colony of aged inbred mouse strains, of which the BALB/c, C57Bl/6, CBA/J, and DBA/2 strains are available for research purposes. The primary aim of this study is to determine if these four aged inbred mouse strains experience different patterns of bone aging. If such variation is present, investigating the factors involved in the different outcomes will be a useful tool for parsing out the factors related to aging changes of bone functionality in humans.

Bone functionality is a poorly defined term. For the context of bone aging, we are concerned with the increase in fracture risk. No single measure can explain all the changes in risk of fracture, but we will use ultimate load (or maximum stress) as a correlate for the ability to resist fracture. Stiffness and ultimate load are highly correlated in healthy adult humans with coefficients of determination (R^2) around 0.92 for cortical bone in tension [6]. Whether this relationship holds up with aging will provide clues as to the underlying factors driving differences in mechanical properties. Mechanical changes with aging may be due to a number of morphological and/or material properties of the bone. By comparing changes in these properties to the mechanical outcomes we can begin to elucidate the size, shape, and mineralization factors that might be leading to the variation between the mouse strains in terms of how their bones are aging.

The primary null hypothesis of this first aim is that there are no differences in ultimate load of the femora from 3-month and 18-month mice in any of the strains. This will be tested using 4-point mechanical loading. If our data do not support the primary null hypothesis, the secondary null hypothesis is that there are no differences in the percent change in ultimate load with age when comparing the four strains. We will test this second hypothesis using linear modeling. In the final part of this chapter, we will then attempt to correlate morphological measures to the changes in function.

Materials and Methods

Animals

All animals used in this study are male mice procured through the NIA/NIH aged colonies. Inbred strains were chosen to provide a sample of phenotypically diverse mice but with less animals required than in a heterogeneous study design. Mice reach bone maturity around 3-months of age [7, 8, 9]. Age-related loss of bone stiffness and maximum load has been reported by 12-months in C57Bl/6 mice [7]. Therefore, we opted for a sample of young mice consisting of 3-month males. The old mouse sample was comprised of 18-month old males. The 18-month time point was chosen since it falls after the 12-month peak in mechanics but before the mean life expectancies of the four strains. While in the future, both sexes should be studied, resources limited this work to the males only. Males were chosen due to lower lifespans in the female of some strains [10]. Furthermore, within the four inbred strains, the survival curves for female mice had much higher ranges of variability [11].

BALB/c mice are the second most widely utilized general-purpose inbred mouse strains, behind C57Bl/6. BALB/c has been recognized as an independent stock since 1913. This strain is notable for high cage activity and male aggression [12]. One study estimates average male lifespan at 620 days [13] and another at 662 days [11]. Ackert *et al* (2008), through the Nathan Shock Center for Aging Research, published data on 32 inbred strains of mice. At 6 months, BALB/c males have an average body weight of 30.3 grams, 19% of which is fat, and a DEXA estimated BMD of 0.0522 g/cm². Average male body weight at 12 months is 31.9 grams, 20% of this is fat, and the average BMD is 0.0574 g/cm² [14].

C57Bl/6 mice are used in a large number of fields of study. This strain dates back to 1921, developed by C.C. Little. Notably, C57Bl/6 may have 6.5% genome from *Mus spretus*. The C57Bl/6 mice are described as having high cage activity. Reports from Jackson puts average lifespan of males around 795 days [15] to 894 days [11]. These mice reportedly develop metabolic syndrome easily and are highly susceptible to diet-induced obesity and diabetes. Other relevant points of interest include the lower bone density and delayed hematopoietic stem cell senescence in this strain [16]. Ackert's report for C57Bl/6 6-month old male mice estimates average body weight at 30.7 grams, 18% being fat, and mean BMD of 0.0524 g/cm². The 12-month averages are 35.5 grams for body weight, 28% fat percentage, and 0.0547 g/cm² for BMD [14].

The CBA/J mouse strain was first developed by Strong in 1920 through a cross of a female Bagg albino and a DBA male. Handlers report low cage activity and large proportion of time spent sleeping. Male lifespan is estimated at 527 days in one study [17] and 647 days in the Yuan report [11]. Researchers describe this strain as having high systolic blood pressure and high cell turnover [18]. Ackert's 2008 estimates for 6-month male CBA/J means are 36.0 grams for body weight, 29% of that is fat, and 0.0570 g/cm² for BMD. The 12-month body weight mean is 40.4 grams, 33% which is fat, and mean BMD is 0.0616 g/cm² [14].

DBA/2 is the oldest inbred strain and was isolated by C.C. Little in 1909. Male lifespan is estimated around 700 days [19] in one study and 641 in another [11]. DBA/2, as reported by Ackert, have the smallest body weight of 29.5 grams at 6 months, 20% is fat, and 27.4 grams at 12 months, 15% is fat. Mean BMD values are 0.0536 g/cm² at 6 months and 0.0544 g/cm² at 12 months [14].

We analyzed each strain cross-sectionally at 3 and 18 months. The 3-month animals were euthanized upon arrival, and their femora excised and frozen in PBS. The oldest age at which all strains were available was 17 months. Therefore, animals were group-housed for four weeks. During this time, four of the BALB/c and four of the DBA/2 old mice died either of natural causes or were euthanized due to poor health. After the 4-week waiting period, all 18-month animals were euthanized and their femora extracted and frozen. The premature death of four 18-month mice from each of the BALB/c and DBA/2 strains resulted in a sample size of

six, which was insufficient to produce adequate power, since a power analysis showed a recommended sample size of 7-8 animals per group.

Micro-Computed Tomography (μ CT)

All bones were scanned with a GE Medical eXplore Locus SP scanner (GE Medical, Waukesha, WI) at 18 μ m voxel size using a beam flattener. Specimens were scanned in a custom designed 8-bone holder to maximize throughput. The size of each region of interest (ROI) for cortical bone was defined as 10% of total bone length and was situated so that the most proximal point centered at the mid-diaphysis (50% of total bone length). Using GE MicroView 2.2 ABA software, an auto-thresholding algorithm was employed and morphological measures recorded.

Mechanical Testing

Bones were tested in 4-point bending with a custom designed system controlled using a Mini Bionix II servohydraulic system (MTS; Eden Prairie, MN). Femora were oriented such that load was applied in the anterior-posterior direction with the posterior surface in tension. Load was applied using a constant displacement rate of 0.05 mm/s. A custom MATLAB script was written to extract critical data from the load-displacement curves. Primary outcome measures of interest were ultimate load, fail load, and stiffness. Yield load, yield, ultimate, fail and post-yield displacements, and total, elastic, and plastic energies were also recorded. Yield point was defined as the point when the slope of the linear region changes by 10% between two consecutive slope estimate iterations. Ultimate load was defined as the maximum load point of the entire test. Fail load was defined as the first point where the slope of the iteration is less than -100. Yield, ultimate, and fail points were visually verified before values were recorded.

Statistical Analysis

All statistics were run using commercially available software packages SPSS v22 (IBM corp., Armonk, NY) and GraphPad Prism 6 (GraphPad Software, San Diego, CA). All mechanical and morphological measures (including weight) were compared between 3- and 18-month animals within each strain using *t*-tests. Outcome measures were standardized by dividing by

body weight. Simple linear regressions were fitted to look at relationships between the primary outcome measures and weight. The coefficient of determination is presented as R^2 .

Additionally, simple linear regressions were also run between stiffness and ultimate load for each strain and each age within strains. General linear models (GLMs) were designed to investigate strain differences in changes with age. The model was run including age and strain as factors and the interaction term: age+strain+age*strain. Bivariate correlations were run between measured parameters and Pearson's correlation coefficient reported (R). All statistics were run with significance level defined at $p<0.05$.

Results

Experiment A: Mechanical Function

Mechanical testing was employed to measure differences in bone strength and stiffness with age. Mean ultimate load values were lower in the BALB/c and C57Bl/6 18-month old mice compared to the 3-month mice, but there was no difference in age means in the CBA/J or DBA/2 mice. In 4-point bending of the femur (Table 2.1)¹, the 18-month BALB/c mice exhibited a 24% lower mean ultimate load but no significant difference in stiffness compared to their 3-month counterparts. The C57Bl/6 group showed dramatic age-related differences in mechanical function in the femur. Femoral ultimate load and stiffness were 34% and 26% lower, respectively, between the 3- and 18-month groups. Aging CBA/J mice appeared to be more successful in maintaining mechanical function compared to BALB/c and C57Bl/6. In the femur, there were no significant changes in ultimate load but a 39% greater stiffness. The femora of DBA mice showed no difference based on age in ultimate load but, similar to CBA/J mice, they exhibited a 41% greater stiffness (Figure 2.1 – A, B, C). These data demonstrate that not all strains change functionality with age similarly.

In order to demonstrate changes in mechanical function, we tested for body size effects on the 4-point bending results. The ability for bone to adapt to mechanical loading has a large impact on bone health and remodeling [20, 21, 22, 23]. Therefore, it is important to consider the role weight change may have on the mechanical properties within the four mouse strains.

¹ Complete table of data in Table 2.2 with unstandardized means.

BALB/c mice had an average 15% ($p=0.003$) greater body weight in the 18-month group compared to the 3-month animals. The 18-month C57Bl/6 animals, despite looking hunched and scruffy, also had body weights greater by 10% ($p<0.001$) than the 3-month mice. The most dramatic difference in weight was seen between the 3- and 18-month CBA/J mice, with a mean 20% greater weight ($p<0.001$). The DBA/2 strain, however, showed no significant differences in body weight by age (Figure 2.1 – D).

The consistent t -test outcomes before and after standardizing for weight suggested that weight was not significantly influencing the mechanical changes with age in each strain. To verify this, regressions between weight and mechanical parameters were run. In both BALB/c and C57Bl/6 mice, when age groups were pooled, weight did not change consistently with ultimate load or stiffness. In the CBA/J mice, ultimate load was not significantly related to weight. However, stiffness increased linearly with weight ($R^2=0.335$, $p<0.001$). In the DBA/2 strain, the regressions between weight and ultimate load and stiffness were not significant. Due to the fact that different strains seem to have different relationships with weight, standardizing values to body mass will remove bias from a weight interaction that might be different between strains.

The two strains that had lower ultimate load means with age (BALB/c and C57Bl/6) may be losing strength at different rates. To test this, we ran general linear models as a full factorial model with age and strain as factors for ultimate load (Figure 2.2 – A) and stiffness (Figure 2.2 – B). By comparing the slopes of the age*strain interaction term, we were able to determine if age influences ultimate load and stiffness differently in the four mouse strains. For ultimate load, the age+strain+age*strain model was significant ($p<0.001$). The interaction of age and strain on ultimate load was not significantly different between the BALB/c and C57Bl/6 strains. However, values for BALB/c and C57Bl/6 mice differed in slope from values for CBA/J ($p=0.004$; $p=0.002$, respectively) and DBA/2 mice ($p=0.016$; $p=0.022$, respectively). This was expected based on the lack of change in ultimate load means with age in the CBA/J and DBA/2 strains.

The model was also significant for estimating stiffness ($p<0.001$). As with ultimate load, the age-strain interaction was similar in the BALB/c and C57Bl/6 mice due to indistinguishable slopes. Again, BALB/c and C57Bl/6 mice showed different relationships between stiffness and

age compared to CBA/J ($p=0.006$; $p<0.001$) and DBA/2 mice ($p=0.003$; $p<0.001$). The change in stiffness was similar when CBA/J and DBA/2 were compared.

Despite having different means at the 3-month time point in femoral ultimate load, the same age-related slope appeared for BALB/c and C57Bl/6 strains. This suggests that BALB/c and C57Bl/6 mice may engender similar patterns of bone aging relative to their starting values. CBA/J and DBA/2 mice also demonstrate similar aging patterns to each other, but display very different methods of aging when compared to the BALB/c and C57Bl/6 patterns.

Experiment B: Causes of Functional Changes

In Experiment A, we determined that the BALB/c and C57Bl/6 strains have less strength with age. Furthermore, the CBA/J and DBA/2 strains maintain strength with age. Our next goal was to determine the underlying causes behind the differential changes in ultimate load with age. To do this, we first investigated the contributions pre-yield and post-yield mechanics had on bone strength. The second part of this experiment compared the mechanical outcomes to morphological measures. The goal of this step was to consider the age-related changes in morphology and how they are influencing bone strength changes.

BALB/c Mouse Parameter Relationships

In BALB/c mouse aging, ultimate load was significantly lower in the 18-month mice compared to the 3-month mice with no difference in stiffness. In the 3-month mice, the regression between stiffness and ultimate load had an $R^2 = 0.64$ ($p=0.006$). This relationship was not significant in the 18-month group (Figure 2.3 – A). An ANCOVA was run to test the similarity of intercepts and slopes between the two ages. The intercepts were significantly different ($p=0.028$) but the slopes followed similar trajectories. The offset of the intercept with invariant slopes indicated that at the same stiffness values, the older bones broke at lower loads. Since morphology would have influenced stiffness, the ANCOVA results suggest matrix alterations and post-yield changes leading to lower ultimate loads in the older animals. Average post-yield displacement (PYD) was 60% lower ($p=0.002$) in the older animals compared to younger animals. Furthermore, ultimate displacement was highly correlated with PYD ($R=.924$, $p<0.001$) but had no significant correlation with yield displacement. These data, in combination with the

lack of variant stiffness, all point to a dramatic change in post-yield properties leading to the weaker bone strength (Figure 2.4 – A).

Comparing the 18-month mice to the 3-month mice, tissue mineral density (TMD) was 11% lower ($p=0.026$) (Figure 2.6 – A), cortical thickness mean was 24% lower ($p<0.001$), and second moment of area (I_y) mean did not vary with age. There was no significant distinction between mean endosteal circumference between ages but there was a very small increase (2%) in marrow area ($p=0.034$). Average periosteal circumference was 9% greater in the aged animals ($p=0.019$), but there was an overall 17% reduction in average cortical area ($p=0.001$) (Figure 2.5 – A).²

The marrow area did not increase greatly with aging in this strain. Therefore, periosteal expansion was not required to compensate for endosteal resorption. However, bone is able to adapt to changes in material properties by altering morphology [24]. The drop in TMD may be an explanation for small periosteal expansion that was measured as there tends to be a relationship between mineralization change and periosteal deposition [24]. The stiffness of the BALB/c femora does not seem to change statistically with age. Thus, the BALB/c femur is maintaining stiffness through minimizing endosteal resorption but still reducing ultimate load. The loss in strength is not likely due to major shape changes but rather differences in mineralization and alterations in collagen and/or porosity. Nyman (2007) asserts that non-enzymatic collagen crosslinking and collagen content have a large effect on the age-related decrease in post-yield toughness [25]. Further study on the BALB/c mice should include assessment of the collagen and other matrix properties.

C57Bl/6 Mouse Parameter Relationships

Comparisons between femora of 18-month and 3-month C57Bl/6 mice demonstrated lower mean values of ultimate load and stiffness under 4-point bending in the 18-month mice compared to the 3-month group. The stiffness values were highly correlated with ultimate load ($R^2 = 0.609$, $p<0.001$) in the 3-month mice, however, as in the BALB/c mice, this relationship was not present in the 18-month group (Figure 2.3 – B). ANCOVA results demonstrated a

² Table of all microCT data with unstandardized means available in Table 2.3.

significant difference in both the intercepts ($p<0.001$) and slopes ($p=0.008$) of the ultimate load-stiffness regressions. The average PYD was 25% less in the 18-month mice compared to 3-month mice ($p=0.004$). Ultimate and post-yield displacements had a strong correlation ($R^2=0.737$, $p<0.001$) whereas ultimate and yield displacements did not (Figure 2.4 – B). These results suggest large morphological *and* matrix changes occurring between the 3- and 18-month periods leading to a disconnect between stiffness and ultimate load.

Compared to the 3-month mean, the 18-month average TMD was 8% lower ($p<0.001$) (Figure 2.6 – B). When mean values for the two ages were compared, the 18-month mice had 23% thinner cortices ($p<0.001$), 3% larger second moment of area ($p=0.045$), and 5% greater endosteal circumference ($p=0.025$) leading to a 25% larger marrow area ($p<0.001$) compared to the 3-month mice. Mean periosteal circumference was not different between ages. The greater marrow area accompanied by the lack of periosteal expansion led to a 16% lower cortical area in the 18-month mice than the 3-month mean ($p<0.001$) (Figure 2.5 – B).

Reduced mineralization and an inadequate change in second moment of area led to less stiff bones in the 18-month C57Bl/6 mice than the 3-month mice. This was tested by estimating the increase in second moment of area required to compensate for the reduced TMD.

First, we set up a simplified system assuming modulus was only dependent on TMD:

$$S = I_y \times \text{TMD}$$

We calculated the stiffness of the 3-month C57Bl/6 group:

$$\begin{aligned} S_{3\text{mo}} &= I_{y\ 3\text{mo}} \times \text{TMD}_{3\text{mo}} \\ S_{3\text{mo}} &= .0058 \times 34.63 \\ S_{3\text{mo}} &= .2009 \end{aligned}$$

Now, we solved for the required second moment of area at 18 months to keep stiffness constant, accounting for the change in TMD:

$$\begin{aligned} .2009 &= I_{y\ 18\text{mo}} \times \text{TMD}_{18\text{mo}} \\ .2009 &= I_{y\ 18\text{mo}} \times 31.89 \\ I_{y\ 18\text{mo}} &= .0063 \end{aligned}$$

Interestingly, the estimated necessary second moment of area value was almost exactly the same as the actual average second moment of area value at 18 months. Yet, stiffness was still smaller in the 18-month animals. This simplified model ignores the fact that bone is a

composite material. The true elastic modulus is dependent upon mechanical changes in mineral and matrix. Therefore, it is possible that mineral density is an insufficient correlate for the modulus of the mineral phase, or that the matrix modulus is changing enough to alter the total elastic modulus. This lends support for the need to further investigate differences in matrix properties in the aging mouse strains.

The lower bending stiffness was likely contributing to the overall lower mechanical stability as evidenced by the correlation between stiffness and ultimate load. However, as C57Bl/6 mice aged, the strong relationship between stiffness and ultimate load disappeared, suggesting other factors were also causing the lower ultimate load. The loss in ultimate load was likely also caused by changes in the post-yield region, supported by the strong correlation between ultimate displacement and PYD. In addition to the hypothesized alteration to post-yield properties, the C57Bl/6 mice also had mineralization and shape differences that led to less stiff bones in the 18-month mice than 3-month mice. An interesting aspect of C57Bl/6 mechanical properties was the very long post-yield region in both age groups. This is suggestive of a strong reliance on matrix properties and organization to resist fracture. If aging alters collagen and other matrix properties, as has been proposed, the mouse strain most dependent on post-yield properties experiences the largest drop in ultimate strength without adequate shape adaptations.

Unlike the BALB/c mice, the second moment of area in the C57Bl/6 mice was greater in the 18-month mice compared to the 3-month mice. This difference was not sufficient to balance the lowered cortical thickness, cortical area, mineralization, and post-yield modifications. While aging in the BALB/c mice seemed to be dominated by post-yield changes with little morphological difference, C57Bl/6 mice experienced decreased stiffness and post-yield properties in addition to marrow expansion.

CBA/J Mouse Parameter Relationships

The CBA/J strain of mice experienced no significant difference in ultimate load when comparing the 3- and 18-month groups but stiffness was 16% greater in the 18-month animals ($p=0.033$). In the CBA/J strain, the femur had a significant regression between stiffness and ultimate load in both the 3-month group ($R^2 = 0.682$, $p < 0.001$) and the 18-month group

($R^2=0.488$, $p=0.002$) (Figure 2.3 – C). The ANCOVA results showed no difference in either the intercepts ($p=0.704$) or the slopes ($p=0.956$) of the lines. However, PYD undergoes a dramatic 65% drop in CBA/J with aging ($p<0.001$) and ultimate displacement had a strong relationship to PYD ($R^2=0.816$, $p<0.001$) (Figure 2.4 – C). Interestingly, when the 18-month group was considered independently, the relationship between ultimate displacement and PYD was no longer significant. The 3-month mechanical properties seemed dependent upon both pre- and post-yield mechanics, however, the PYD approached zero in the 18-month animals. The loss of ductility could have led to the need to increase stiffness to maintain ultimate load.

The increase in stiffness was not likely due to mineralization increase, since TMD decreased 13% ($p<0.001$) with age (Figure 2.6 – C). We set up a simplified system to test if stiffness is maintained through morphology:

$$\begin{aligned} S &= I_y \times TMD \\ S_{3mo} &= I_{y\ 3mo} \times TMD_{3mo} \\ S_{3mo} &= .00316 \times 37.95 \\ S_{3mo} &= .1199 \end{aligned}$$

Next, we solved for the required second moment of area at 18 months to keep stiffness constant, accounting for the change in TMD:

$$\begin{aligned} .1199 &= I_{y\ 18mo} \times TMD_{18mo} \\ .1199 &= I_{y\ 18mo} \times 32.83 \\ I_{y\ 18mo} &= .0037 \end{aligned}$$

In order to maintain stiffness and compensate for the drop in mineral density, CBA/J mice would have required a new second moment of area value of .0037. The actual 18-month second moment of area value is .0049, suggesting that CBA/J aged animals were more than compensating for the drop in mineralization by adaptations to geometry.

In reality, second moment of area increased with age 53% ($p<0.001$). This was driven by changes on the endosteal and periosteal surfaces. The circumference of the endosteal surface increased by 12% ($p<0.001$) resulting in a 43% increase in marrow area ($p<0.001$). Periosteal circumference did not change significantly but total area increases 10% ($p<0.001$). This led to an overall 13% drop in cortical thickness ($p<0.001$) but no change in cortical area (Figure 2.5 – C).

The CBA/J mice are able to accommodate both the loss of TMD and endosteal resorption by adding bone on the periosteal surface.

DBA/2 Parameter Relationships

DBA/2 mice experienced no age-related loss in ultimate load but stiffness increased 23% ($p=0.026$). The femora of DBA/2 mice had a strong relationship between stiffness and ultimate load at 3-months of age ($R^2=0.535$, $p=0.016$). This relationship is maintained in the 18-month group, as well ($R^2 = .983$, $p<0.001$) (Figure 2.3 – D). The ANCOVA resulted in no difference in the intercepts ($p=0.428$) or slopes ($p=0.332$) of the regression lines. In contrast with the other three strains, DBA/2 mice did not exhibit a drop in PYD as they aged. While CBA/J mice seem to have increased stiffness but lost ductility, the DBA/2 strain appeared to increase stiffness while maintaining ductility (Figure 2.4 – D). The increased stiffness of CBA/J mice may be at the expense of ductility. Furthermore, the increase in stiffness could be compensation for the loss of ductility. In the DBA/2 mice, stiffness increased but post-yield properties did not change. This trend demonstrates that the change in stiffness is accomplished without affecting ductility. The stiffness increase of DBA/2 old mice was, therefore, primarily geometric rather than compositional and/or organizational since most of these changes would result in modified post-yield properties, as well.

This was supported by the lack of change in TMD value in the 18-month DBA/2 animals compared to 3-month mice (Figure 2.6 – D). Additionally, second moment of area increased a dramatic 96% ($p<0.001$) with age. In the previous strains, it was assumed that the loss of mineral density prompted the geometry changes leading to stiffness changes. However, in the DBA/2 strain, we saw no change in mineral density but still a large increase in both second moment of area and stiffness. If not a response to changing material properties, the increased second moment of area could have been a result of compensation for endosteal resorption.

To support this theory, we set up the second moment of area at 3 months and at 18 months to be equal:

$$I_{y\ 18mo} = I_{y\ 3mo}$$

Adding the equation for I_y :

$$(d_{peri18}^4 - d_{endo18}^4) = (d_{peri3}^4 - d_{endo3}^4)$$

Filling in our averages at 3 months and the change in endosteal surface:

$$\begin{aligned}(d_{\text{peri18}}^4 - .0351^4) &= (.0439^4 - .0276^4) \\ (d_{\text{peri18}}^4) &= (.0439^4 - .0276^4 + .0351^4) \\ (d_{\text{peri18}}^4) &= .0464\end{aligned}$$

Multiplying this by π we found the required periosteal circumference required to accommodate the endosteal resorption common in aging. The minimum required value to, at least, maintain second moment of area is 0.146. The actual average periosteal circumference in the DBA/2 18-month animals is 0.157 (Figure 2.5 – D). The DBA/2 mice were capable of responding to age-related endosteal resorption by adding bone to the periosteal surface, therefore providing support to maintain bone strength.

Discussion

The first hypothesis of this work asks if the four mouse inbred strains exhibit changes in bone strength with aging. We found that two of the strains, BALB/c and C57Bl/6, lose functionality with age and two, CBA/J and DBA/2 maintain functionality with age. The second hypothesis is proposed to determine if age-related changes in strength are parallel in the four strains. The linear models show that the two strains that lost strength have similar relative rates of loss. The last question investigated in this chapter asks if the changes in strength occur due to similar changes in morphology. The data demonstrate that the causes behind the loss of strength in the BALB/c and C57Bl/6 strains are different. Similarly, the CBA/J and DBA/2 strains, which maintained bone strength, also did so in two distinct ways.

Those that lost strength either did not add or insufficiently added bone on the periosteal surface. The BALB/c mice maintained stiffness but had significant losses of post-yield displacement that led to the reduced strength. The combination of mechanical and morphological data indicates a loss of strength due to non-geometric changes. The reduced strength is due to the lower mineralization and matrix changes reducing post-yield properties. In the C57Bl/6 mice, the mechanical data demonstrate a reduction in strength, stiffness, and ductility. The loss of strength can be attributed to both the mineralization and matrix changes,

as in BALB/c, but also to geometric changes. The loss of strength and stiffness is partly due to the marrow expansion without adequate periosteal compensation.

In contrast to the first two strains, the CBA/J and DBA/2 mice maintained strength with age, in part, by increasing stiffness. In the CBA/J strain, the loss of mineralization, post-yield displacement, and endosteal bone are compensated for by periosteal expansion in CBA/J aging. The increase in periosteal bone led to the greater stiffness, however, the bones became much more brittle. Unique to the DBA/J mice, the older animals did not experience altered PYD or TMD. This indicates minimal changes to the composition of the bone throughout the aging process. However, the old mice do experience dramatic changes to their bone geometry. Similar to the CBA/J mice, the DBA/2 strain is able to compensate for the endosteal resorption by adding bone to the periosteal surface.

With respect to the first hypothesis, the results of this chapter differ slightly from previous work published on aging mouse strains. In one study, BALB/c males reportedly have a steady increase in stiffness throughout aging [27]. Our data found no change in stiffness in the male BALB/c mice with age. Reports of C57Bl/6 aging have shown no decline in stiffness or strength in the femur after 12 months [7]. Our data demonstrate a loss in both stiffness and ultimate load in this strain. One major difference in methodology is the use of standardized values to account for weight differences which would reduce variance in the samples. However, running the *t*-tests on unstandardized values produced the same significant trends. Another possible source of disagreement may be due to cohort and/or seasonality effects. Furthermore, variation in housing practices could lead to different results.

The age-related changes reported in this paper, compared to previous work for BALB/c and C57Bl/6 strains, are more representative of changes documented in humans. In human bone aging, cortical bone strength declines with age [27, 28, 29, 30, 31]. The results of this work demonstrate that there are different ways to lose bone strength. Strength can be lost due to changes on the material level. This includes changes to collagen organization and cross-linkage and crystallinity, among others. Most current diagnostic approaches in assessing human fracture risk measure bone morphological changes. Unfortunately, as evidenced by the BALB/c aging patterns, loss of bone strength may be caused by matrix composition and organization

changes that are not commonly measured in clinical settings. Therefore, in order to better assess fracture risk, clinicians need methods of measuring both changes in morphology and material properties. One method that is currently being investigated is the use of RAMAN spectroscopy. RAMAN measures can provide information on material-level properties such as mineral and matrix profiles [32]. A combination of RAMAN and DXA diagnostics could provide more accurate predictions of fracture risk.

There is a scarcity of research that reports on the maintenance of bone strength with age across mouse strains. The CBA/J and DBA/2 mouse strains could provide a useful model for humans that age without incurring an age-related fracture. Again, the maintenance of mechanical integrity can be attained in multiple ways. The CBA/J mice were able to compensate for aging changes by increasing periosteal diameter but potentially at the cost of ductility. The DBA/2 mice had large increases in second moment of area without compromising ductility. In human aging, there is a positive relationship between loss of mineralization and periosteal deposition [33]. This is supported when comparing CBA/J bone aging with BALB/c and C57Bl/6 aging. The CBA/J mice had the greatest loss in TMD with age and experienced periosteal bone growth whereas BALB/c and C57Bl/6 did not expand periosteally. However, when comparing the CBA/J and DBA/2 aging patterns, this relationship is no longer valid. The DBA/2 mice did not lose mineralization with age as the CBA/J did, yet both strains had large amounts of periosteal bone growth. This suggests that the TMD loss may be related to periosteal growth but not necessary for the deposition to occur.

In human bone aging, expansion occurs at both the endosteal and periosteal surfaces [34, 35, 36, 37, 38, 39]. Men tend to maintain bone strength better than women during aging [36, 37]. This is in part due to the geometry differences, where men have more robust bones, on average, than women. Therefore, periosteal deposition in men has a greater influence on second moment of area than in women [33]. Interestingly, the BALB/c and C57Bl/6 have more robust bones compared to the CBA/J and DBA/2 mice, yet the latter two strains are better at maintaining strength. This is contrary to what would be expected based on sex differences in humans.

Since there are no female mouse data in this study, direct conclusions cannot be drawn regarding sex differences in bone aging. It has been suggested that women are less able to maintain strength with age compared to men due to inherent geometric limitations. Periosteal deposition on a robust (male-like) individuals has a greater impact on second moment of area than it would have on a slender (more female-like) individual [33]. However, the finding that the more slender mouse strains maintain strength suggests that the inability for women to add sufficient bone periosteally is not due to the bone size and shape. Thus, the lack of periosteal expansion in some women may have other biological causes (e.g. hormonal differences). Following studies should investigate the aging patterns in the female mice of these strains. It is possible that we will see similar ability to maintain strength in the CBA/J and DBA/2 mice, compared to their male counterparts. If this is the case, we can begin to investigate what is unique in humans that leads to the loss of strength due to inadequate periosteal growth.

The results of this chapter also provide a reason for using caution when studying mouse models as analogs for human aging. Most studies of mouse aging have been conducted on individual inbred strains or genetically modified strains [7, 9, 10, 27, 34]. The conclusions made concerning mouse bone aging will largely differ if one group using the C57Bl/6 strain only while another group studies the CBA/J strain. Therefore, it must be understood that results from single-strain studies are not representative of the range of variation possible in the mouse species.

One drawback to the cross-sectional approach taken in this work is the assumption that differences in mean values between the two age groups are representative of changes within an individual as they age. Despite this limitation, many age-related studies are cross-sectional in design in order to expedite results. In one such study, researchers compared cross-sectional and longitudinal results from the same cohort. The authors conclude that cross-sectional study design may underestimate the age-related changes [26]. Therefore, the use of cross-sectional measures in this work provides a more conservative approach.

Future Work

Due to the limitations on the breadth of this thesis, these data do not illuminate the underlying biological causes of the variability in bone aging outcomes. However, having defined

the patterns of variation here will allow for future work to address the causative factors. In humans, individuals with greater resorption rates tend to have larger bone cross-sectional geometry. The ability to resorb bone may be allowing for increased periosteal expansion [38] in the CBA/J and DBA/J strains. The high amounts of resorption on the endosteal surface could permit associated periosteal deposition. Bone is a metabolically expensive tissue. With limited resources, the freeing of minerals bound to the endosteal surface of the bone may allow these to be recycled and added to the periosteal surface.

Bone aging variation could also be due to age-related changes in the adaptive response to load. BALB/c, C57Bl/6, and CBA/J mice all increase body weight with age. The adaptive response to increased load should lead to changes in bone morphology and composition that increase resistance to failure. The fact that BALB/c and C57Bl/6 mice do not have the weight-induced expected adaptive response, suggests that the mechanoresponse system is lost or modified with age in these strains.

Variation in aging could also be due to metabolic and life history patterns that differ between the strains. The C57Bl/6 strain has the longest average lifespan of the four inbred strains used in this study, but the most significant loss in bone mechanical stability [14]. This strain could be reallocating resources towards organism survival at the cost of bone function. In support of this, the C57Bl/6 strain tends to have high body fat and low BMD compared to the other strains [14]. Tests were run using data from the Ackert-Bicknell and Yuan data reported on phenome.jax.org [11, 14]. Comparing the mean changes in BMD and body fat in the males of 23 strains shows a strong negative correlation between these parameters ($R=-0.587$, $p=0.003$). The lower life expectancy of CBA/J mice could be due to the strain's strategy of investing in body fat AND bone. This approach to aging could lead to over-expenditure of resources in bone and fat, at the expense of maintaining the integrity of other vital systems thus reducing life expectancy. This is supported by work not presented in this thesis. In a heterogeneous population of mice, those with larger bones at 4-months of age had a shorter lifespan [42].

Future work should also include a better understanding of the variability in human aging. We have shown that within a single species, different genetic backgrounds and/or life histories can lead to variations in organism aging. We need to measure how variable human

bone aging is in order to provide adequate predictive, diagnostic, and treatment approaches that accounts for the heterogeneity inherent in humans. The biological causes of the difference in aging pattern are unknown. However, with evidence of variant aging patterns in the mouse strains, comparative studies between mice that lose mechanical integrity and those that do not may provide integral information as to the intrinsic and external influences leading to bone aging variation. Inferences from this future work could allow for a better understanding of the relationships between variables known to influence human bone aging and their effect on skeletal fragility and fracture risk.

References: Chapter II

- [1] M. P. Akhter, Z. Fan and J. Y. Rho, "Bone intrinsic material properties in three inbred mouse strains," *Calcified Tissue International*, vol. 75, pp. 416-420, 2004.
- [2] K. J. Jepsen, O. Akkus, R. J. Majeska and J. H. Nadeau, "Hierarchical relationship between bone traits and mechanical properties in inbred mice," *Mammalian Genome*, vol. 14, pp. 97-104, 2003.
- [3] C. Price, B. C. Herman, T. Lufkin, H. M. Goldman and K. J. Jepsen, "Genetic variation in bone growth patterns defines adult mouse bone fragility," *Journal of Bone and Mineral Research*, vol. 20, no. 11, pp. 1983-1991, 2005.
- [4] J. E. Wergedal, M. H.-C. Sheng, C. L. Ackert-Bicknell, W. G. Beamer and D. J. Baylink, "Genetic variation in femur extrinsic strength in 29 different inbred strains of mice is dependent on variations in femur cross-sectional geometry and bone density," *Bone*, vol. 36, pp. 111-122, 2005.
- [5] I. Sabsovich, J. D. Clark, G. Liao, G. Peltz, D. P. Lindsey, C. R. Jacobs, W. Yao, T.-Z. Guo and W. S. Kingery, "Bone microstructure and its associated genetic variability in 12 inbred mouse strains: microCT study and in silico genome scan," *Bone*, vol. 42, no. 2, pp. 439-451, 2008.
- [6] D. P. Fyhrie and D. Vashishth, "Bone stiffness predicts strength similarly for human vertebral cancellous bone in compression and for cortical bone in tension," *Bone*, vol. 26, no. 2, pp. 169-173, 2000.
- [7] V. L. Ferguson, R. A. Ayers, T. A. Bateman and S. J. Simske, "Bone development and age related bone loss in male C57Bl/6 mice," *Bone*, vol. 33, pp. 387-398, 2003.
- [8] M. Brodt and M. Silva, "Aged mice have enhanced endocortical response and normal periosteal response compared with young-adult mice following 1 week of axial tibial compression," *Journal of Bone and Mineral Research*, vol. 25, no. 9, pp. 2006-2015, 2010.

- [9] V. Glatt, E. Canalis, L. Stadmeier and M. Bouxsein, "Age-related changes in trabecular architecture differ in female and male C57BL/6J mice," *Journal of Bone and Mineral Research*, vol. 22, pp. 1197-1207, 2007.
- [10] S. Ali, C. Xiong, J. Lucero, M. Behrens, L. Dugan and K. Quick, "Gender differences in free radical homeostasis during aging: short-lived female C57BL/6 mice have increased oxidative stress," *Aging Cell*, vol. 5, no. 6, pp. 565-574, 2006.
- [11] R. Yuan, C. Ackert-Bicknell, B. Paigen and L. L. Peters, "Aging study: Lifespan and survival curves for 31 inbred strains of mice," 2007. [Online]. Available: <http://phenome.jax.org/db/q?rtn=projects/projdet&reqprojid=234>. [Accessed 12 December 2014].
- [12] JAX(R) Mice database, "BALB/cJ," The Jackson Laboratory, 2014. [Online]. Available: <http://jaxmice.jax.org/strain/000651.html>. [Accessed 12 December 2014].
- [13] JAX(R) Mice database, "Physiological Data Summary - BALB/cJ (000651)," 13 December 2007. [Online]. Available: <http://jaxmice.jax.org/support/phenotyping/BALBcJdata000651.pdf>. [Accessed 12 December 2014].
- [14] C. Ackert-Bicknell, W. Beamer, C. Rosen and J. Sundberg, "Aging study: bone mineral density and body composition of 32 inbred strains of mice MDP:Ackert1," The Jackson Laboratory, 2008. [Online]. Available: <http://phenome.jax.org/db/q?rtn=projects%2Fdetails&sym=Ackert1&mlistmode=strainvalues&reqstrainid=8&indivmeas=no&x=15&y=0>. [Accessed 12 December 2014].
- [15] JAX(R) Mice database, "Physiological Data Summary - C57BL/6J (000664)," 13 December 2007. [Online]. Available: <http://jaxmice.jax.org/support/phenotyping/B6data000664.pdf>. [Accessed 12 December 2014].
- [16] JAX(R) Mice database, "C57BL/6J," The Jackson Laboratory, 2014. [Online]. Available: <http://jaxmice.jax.org/strain/000664.html>. [Accessed 12 December 2014].
- [17] JAX(R) Mice database, "Physiological Data Summary - CBA/J (000656)," 13 December 2007. [Online]. Available: <http://jaxmice.jax.org/support/phenotyping/CBAJdata000656.pdf>. [Accessed 12 December 2014].
- [18] JAX(R) Mice database, "CBA/J," The Jackson Laboratory, 2014. [Online]. Available: <http://jaxmice.jax.org/strain/000656.html>. [Accessed 12 December 2014].
- [19] JAX(R) Mice database, "DBA/2J," The Jackson Laboratory, 2014. [Online]. Available: <http://jaxmice.jax.org/strain/000671.html>. [Accessed 12 December 2014].
- [20] E. Ozcivici, Y. K. Luu, B. Adler, Y.-X. Zin, J. Ruben, S. Judex and C. T. Rubin, "Mechanical signals as anabolic agents in bone," *Nature Reviews: Rheumatology*, vol. 6, pp. 50-59, 2010.
- [21] A. G. Robling, A. B. Castillo and C. H. Turner, "Biomechanical and molecular regulation of bone remodeling," *Annual Review of Biomedical Engineering*, vol. 8, pp. 455-498, 2006.
- [22] C. H. Turner, "Skeletal adaptation to mechanical loading," *Clinical Reviews in Bone and Mineral Metabolism*, vol. 5, pp. 181-194, 2007.
- [23] C. H. Turner and A. G. Robling, "Mechanisms by which exercise improves bone strength," *Journal of Bone and Mineral Metabolism*, vol. 23, no. Supp1, pp. 16-22, 2005.

- [24] K. J. Jepsen, B. Hu, S. M. Tommasini, H.-W. Courtland, C. Price, M. Cordova and J. H. Nadeau, "Phenotypic integration of skeletal traits during growth buffers genetic variants affecting the slenderness of femora in inbred mouse strains," *Mammalian Genome*, vol. 20, pp. 21-33, 2009.
- [25] J. S. Nyman, A. Roy, J. H. Tyler, R. L. Acuna, H. J. Gayle and X. Wang, "Age-related factors affecting the postyield energy dissipation of human cortical bone," *Journal of Orthopaedic Research*, vol. 25, no. 5, pp. 646-655, 2007.
- [26] J. Desrosiers, R. Hebert, G. Bravo and A. Rochette, "Comparison of cross-sectional and longitudinal designs in the study of aging of upper extremity performance," *Journal of Gerontology: Biological Sciences*, vol. 53A, no. 5, pp. B362-B368, 1998.
- [27] M. D. Willingham, M. D. Brodt, K. L. Lee, A. L. Stephens, J. Ye and M. J. Silva, "Age related changes in bone structure and strength in female and male BALB/c mice," *Calcified Tissue International*, vol. 86, pp. 470-483, 2010.
- [28] A. Burstein, D. Reilly and M. Martens, "Aging of bone tissue: mechanical properties," *Journal of Bone and Joint Surgery American*, vol. 58, pp. 82-86, 1976.
- [29] R. McCalden, J. McGeough, M. Barker and C. Court-Brown, "Age-related changes in the tensile properties of cortical bone: The relative importance of changes in porosity, mineralization, and microstructure," *Journal of Bone and Joint Surgery American*, vol. 75, pp. 1193-1205, 1993.
- [30] X. Wang, X. Shen, X. Li and C. Agrawal, "Age-related changes in the collagen network and toughness of bone," *Bone*, vol. 31, pp. 1-7, 2002.
- [31] P. Zioupos and J. Currey, "Changes in the stiffness, strength, and toughness of human cortical bone with age," *Bone*, vol. 22, pp. 57-66, 1998.
- [32] O. Akkus, A. Polyakova-Akkus, F. Adar, and M. B. Schaffler, "Aging of microstructural compartments in human compact bone," *Journal of Bone and Mineral Research*, vol. 18, no. 6, pp. 1012-1019, 2003.
- [33] K. J. Jepsen and N. Andarawis-Puri, "The amount of periosteal apposition required to maintain bone strength during aging depends on adult bone morphology and tissue-modulus degradation rate," *Journal of Bone and Mineral Research*, vol. 27, no. 9, pp. 1916-1926, 2012.
- [34] O. Kajnekova, B. Lecka-Czernik, I. Gubrij, S. P. Hauser, K. Takahashi, A. M. Parfitt and e. al, "Increased adipogenesis and myelopoiesis in the bone marrow of SAMP6, a murine model of defective osteoblastogenesis and low turnover osteopenia," *Journal of Bone and Mineral Research*, vol. 12, pp. 1772-1779, 1997.
- [35] H. Ahlborg, O. Johnell, C. Turner, G. Rannevik and M. Karlsson, "Bone loss and bone size after menopause," *New England Journal of Medicine*, vol. 349, pp. 327-334, 2003.
- [36] M. Buxsein, K. Myburgh, M. van der Meulen, E. Lindenberger and R. Marcus, "Age-related differences in cross-sectional geometry of the forearm bones in healthy women," *Calcified Tissue International*, vol. 54, pp. 113-118, 1994.
- [37] R. Martin and P. Atkinson, "Age and sex-related changes in the structure and strength of the human femoral shaft.," *Journal of Biomechanics*, vol. 10, pp. 223-231, 1977.

- [38] C. Ruff and W. Hayes, "Sex differences in age-related remodeling of the femur and tibia," *Journal of Orthopaedic Research*, vol. 6, pp. 886-896, 1988.
- [39] P. Szulc, E. Seeman, F. Duboeuf, E. Sornay-Rendu and P. Delmas, "Bone fragility: failure of periosteal apposition to compensate for increased endocortical resorption in postmenopausal women," *Journal of Bone and Mineral Research*, vol. 21, pp. 1856-1863, 2006.
- [40] B. Riggs, L. Melton, R. Robb, J. Camp, E. Atkinson, J. Peterson, P. Rouleau, C. McCollough, M. Bouxsein and S. Khosla, "Population-based study of age and sex differences in bone volumetric density, size, geometry, and structure at different skeletal sites," *Journal of Bone and Mineral Research*, vol. 19, pp. 1945-1954, 2004.
- [41] J. Kemp, A. Sayers, L. Paternoster, D. Evans, K. Deere, B. St Pourcain, N. Timpson, S. Ring, M. Lorentzon, T. Lehtimäki, J. Eriksson, M. Kahonen, O. Raitakari, M. Laaksonen, H. Sievanen, J. Viikari, L.-P. Lyytikäinen, G. Smith, W. Fraser, L. Vandenput, C. Ohlsson and J. Tobias, "Does bone resorption stimulate periosteal expansion? A cross-sectional analysis of beta-C-telopeptides of type I collagen (CtX), genetic markers of the RANKL pathway, and periosteal circumference as measured by pQCT," *Journal of Bone and Mineral Research*, vol. 29, no. 4, pp. 1015-1024, 2014.
- [42] R. Miller, J. Kreider, A. Galecki and S. Goldstein, "Preservation of femoral bone thickness in middle age predicts survival in genetically heterogeneous mice," *Aging Cell*, vol. 10, no. 3, pp. 383-391, 2011.

Figures: Chapter II

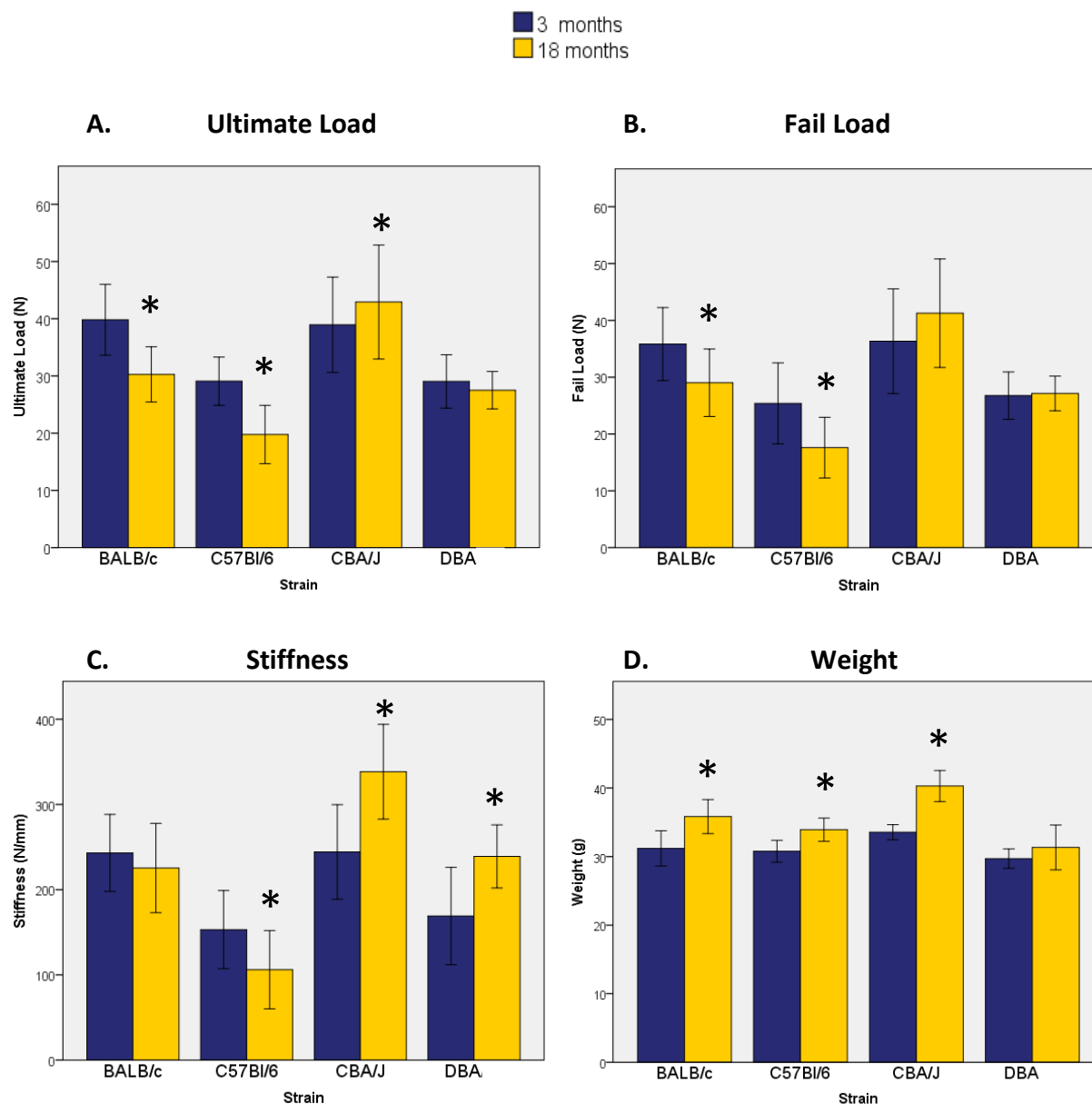


Figure 2. 1 - Changes in mechanical function parameters.

T-tests were run within strains—BALB/c, C57Bl/6, CBA/J, and DBA/2—comparing 3- and 18-month groups. **A)** Ultimate load; **B)** Fail load; **C)** Stiffness; **D)** Body weight * $p < 0.05$ ± 1 SD

Table 2. 1 - Femoral 4-point bending results.

Numerical data reporting ultimate load, fail load, and stiffness changes in all 4 inbred strains. T-test are considered significant at $p < 0.05$. Percent change = $(18 \text{ month mean} - 3 \text{ month mean}) / (3 \text{ month mean}) * 100$.

Strain	Age	n	Ultimate Load (N)				Fail Load (N)			
			Mean	Stdev	p-value	% Change	Mean	Stdev	p-value	% Change
BALB	3	10	39.82	6.19	0.006	-23.98	35.83	6.43	0.054	-19.01
	18	6	30.28	4.83			29.03	5.93		
C57Bl/6	3	18	29.09	4.23	<0.001	-29.89	25.39	7.14	0.001	-29.38
	18	17	20.39	4.71			17.92	5.14		
CBA/J	3	20	38.95	8.34	0.195	10.19	36.34	9.21	0.12	13.57
	18	17	42.92	9.96			41.26	9.55		
DBA/2	3	8	29.06	4.94	0.515	-5.3	26.78	4.43	0.863	1.37
	18	6	27.52	3.28			27.15	3.05		

Strain	Age	n	Stiffness (N/mm)			
			Mean	Stdev	p-value	% Change
BALB	3	10	243.08	45.17	0.486	-7.28
	18	6	225.39	52.39		
C57Bl/6	3	18	153.1	45.84	0.008	-27.19
	18	17	111.48	40.06		
CBA/J	3	20	244.26	55.51	<0.001	38.55
	18	17	338.43	55.63		
DBA/2	3	8	185.49	25.29	0.005	28.87
	18	6	239.03	37.02		

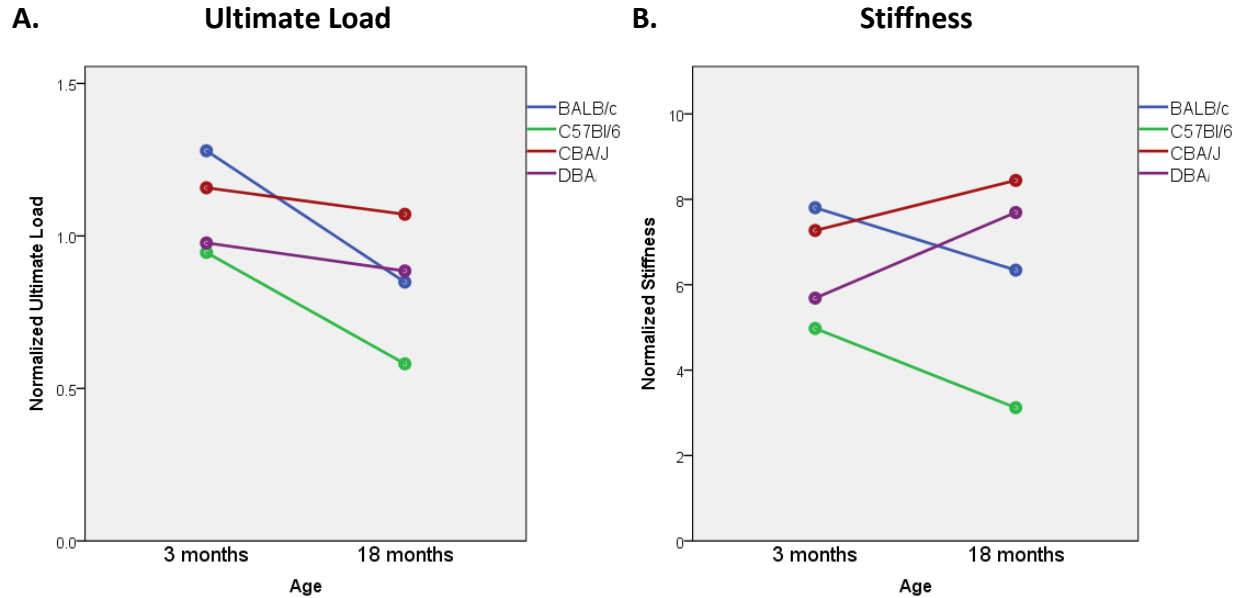


Figure 2. 2 - Graphical representation of general linear models.

General linear modeling was run with age and strain as factors and including the interaction term (age*strain). **A)** The linear model shows that the rate of change in BALB/c and C57Bl/6 are statistically similar to each other but both are different from CBA/J and DBA/2, as there is no difference in ultimate load in these strains. **B)** The model estimated slopes of stiffness change are not different between BALB/c and C57Bl/6. These two strains experience a similar relative loss of stiffness with age. The slopes are significantly divergent from the CBA/J and DBA/2 rates of change, regardless of starting values. CBA/J and DBA/2 stiffness increases with age.

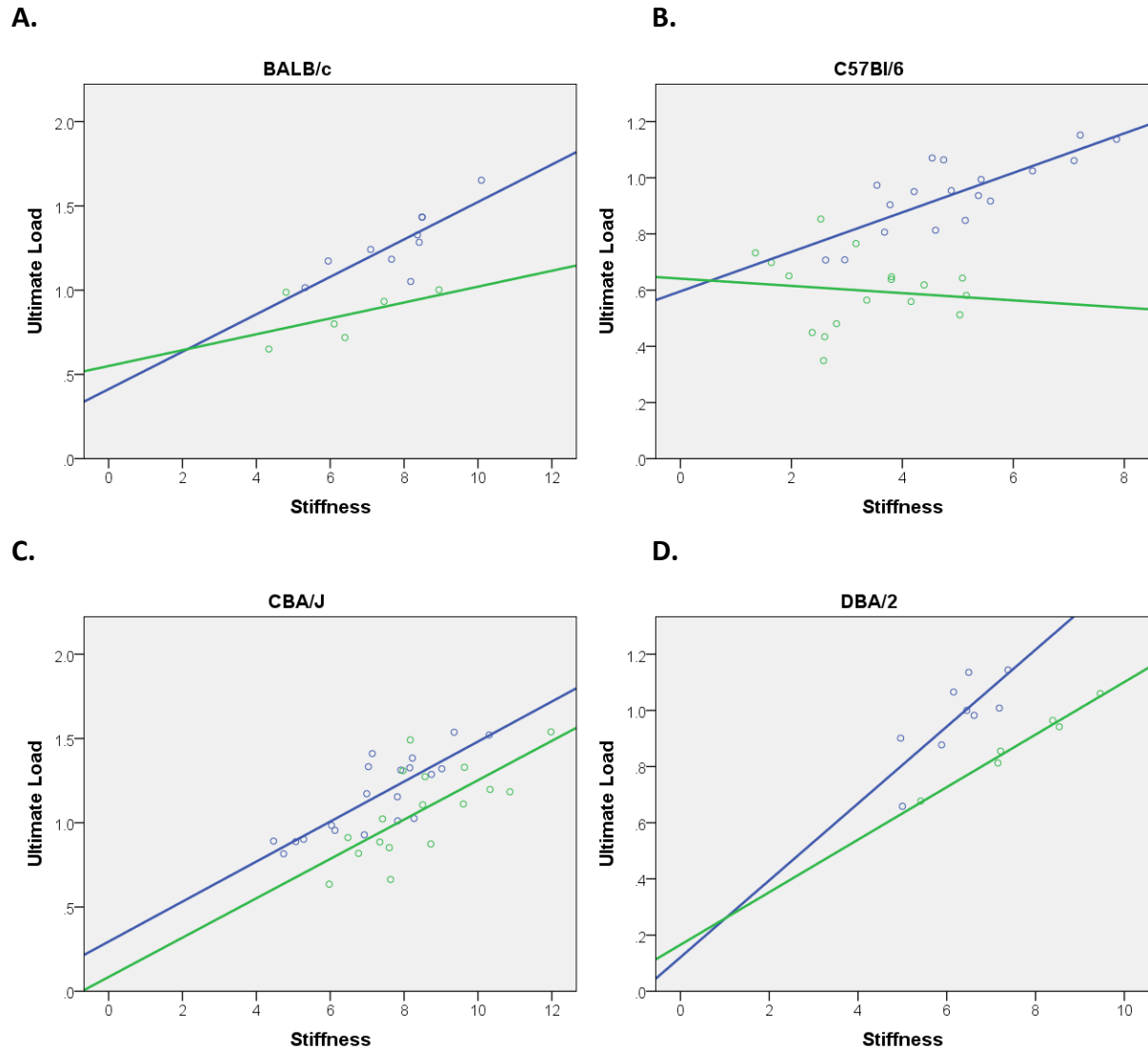


Figure 2. 3 - Linear relationship between stiffness and ultimate load.

Regressions were run for the 3 month and 18 month groups of all four strains. The blue lines represent the 3-month regressions and the green lines represent the 18-month regressions. **A)** At 3 months, the BALB/c femoral stiffness is linearly related with ultimate load ($R^2=0.636$, $p=0.006$). In the 18-month sample, the relationship is no longer significant. **B)** The 3-month C57Bl/6 stiffness-ultimate load relationship is also significant ($R^2=0.609$, $p<0.001$). The 18-month femora do not maintain this relationship. **C)** The linear relationship between stiffness and ultimate load is stronger in the CBA/J younger mice ($R^2=0.682$, $p<0.001$) than the older mice ($R^2=0.488$, $p=0.002$). The linear relationship is weaker in the DBA/2 younger mice ($R^2=0.535$, $p=0.016$) when compared to the older animals ($R^2=0.983$, $p<0.001$).

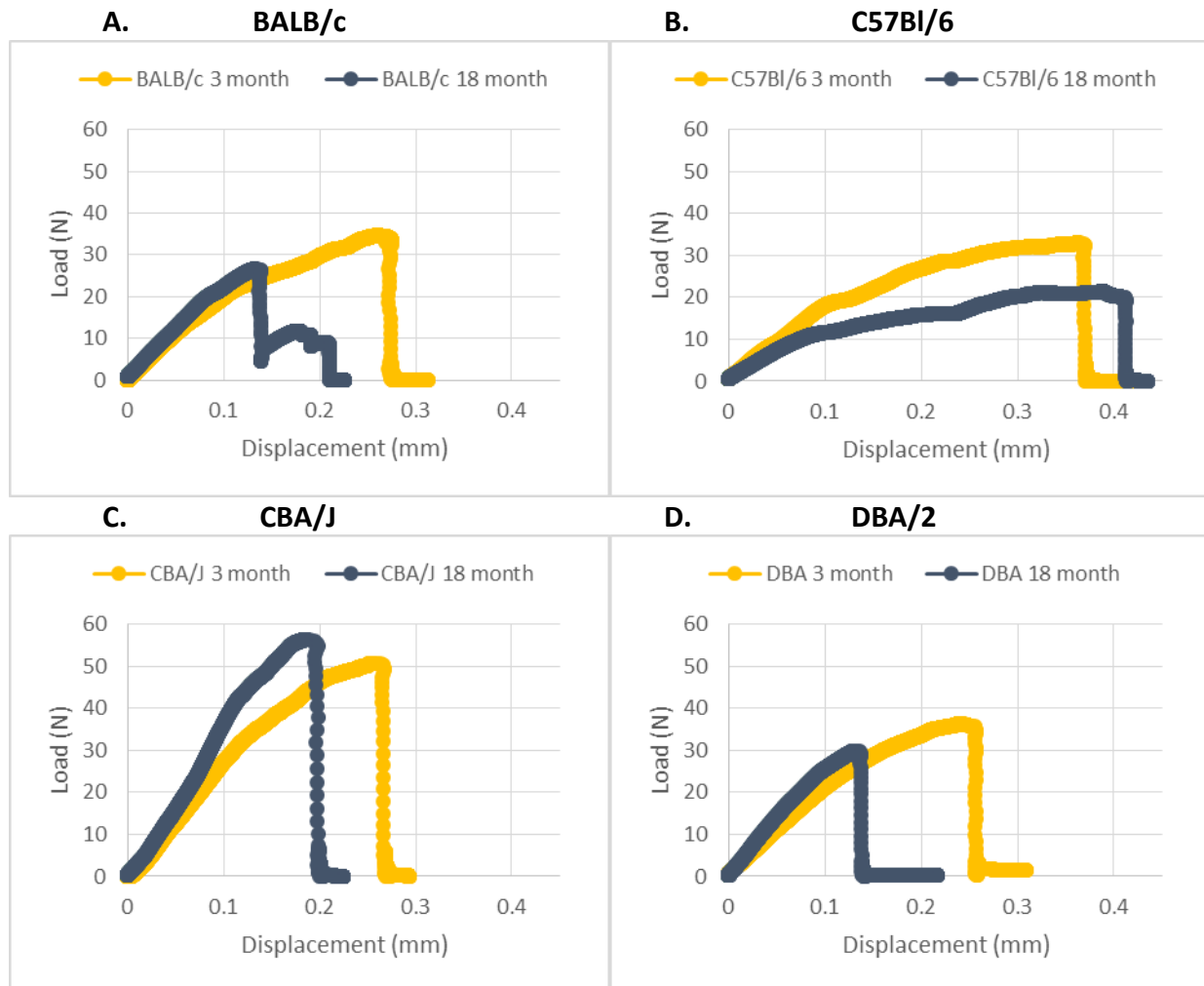


Figure 2. 4 - Load-displacement curves for 4-point bending.

Maize markers represent data points on the load-displacement curves of a representative 3-month animal for each strain. Blue markers are representative animals at 18 months. **A)** BALB/c have similar stiffness between ages but a lower ultimate load in the older animals. There is no difference in yield load or displacement. The older mice have a mean ultimate displacement that is 41% less ($p < 0.001$) and a PYD that is 60% less ($p = 0.002$) than the 3-month mean. **B)** C57Bl/6 femora have lower ultimate load and stiffness means in the older mice compared to younger. The 18-month yield load is 26% lower ($p = 0.002$) than that of the 3-month mice. The old mice have a 13% lower ultimate displacement mean ($p = 0.053$) and a 25% lower PYD mean ($p = 0.004$) than the 3-month mice. Yield displacement is invariant between the age groups. **C)** The 18-month CBA/J mice have greater stiffness with similar ultimate and yield load averages compared to the 3-month mice. In the old mice, yield displacement is 25% less ($p = 0.025$), ultimate displacement is 45% less ($p < 0.001$) and PYD is 65% less ($p < 0.001$) than the 3-month means. **D)** DBA/2 mice have greater stiffness in the older femora but there is no difference in ultimate, yield, or fail loads when compared to the 3-month means. Yield displacement is 42% lower in the older mice than the younger mice ($p = 0.002$), ultimate displacement is 35% lower ($p < 0.001$), but there is no difference in PYD.

Table 2. 2 - Summary of mechanical testing data.

Data is presented in unstandardized form. Means are given ± 1 SD. Values highlighted in **BOLD** represent 18-month means that were significantly different from the 3-month means in *t*-test with significance determined $p \leq 0.05$.

	BALB/c		C57Bl/6		CBA/J		DBA/2	
	3 months	18 months	3 months	18 months	3 months	18 months	3 months	18 months
N	10	6	18	19	20	17	10	6
Ultimate Load	39.82 ± 6.19	30.28 ± 4.83	29.09 ± 4.23	19.87 ± 4.96	38.95 ± 8.34	42.92 ± 9.96	29.05 ± 4.66	27.52 ± 3.28
Yield Load	21.90 ± 5.09	21.80 ± 6.70	14.13 ± 4.43	11.45 ± 5.28	25.76 ± 6.64	31.44 ± 9.58	21.42 ± 8.88	20.96 ± 5.22
Fail Load	35.83 ± 6.43	29.03 ± 5.93	25.39 ± 7.14	17.51 ± 5.21	36.34 ± 9.21	41.26 ± 9.55	26.75 ± 4.18	27.15 ± 3.05
Stiffness	243.08 ± 45.17	225.39 ± 52.39	153.10 ± 45.84	103.87 ± 45.62	244.26 ± 55.51	338.43 ± 55.63	169.06 ± 57.15	239.03 ± 37.02
Ultimate Displacement	.26 \pm .03	.18 \pm .04	.36 \pm .05	.34 \pm .08	.24 \pm .04	.16 \pm .03	.23 \pm .03	.15 \pm .02
Yield Displacement	.10 \pm .02	.10 \pm .03	.10 \pm .04	.14 \pm .12	.12 \pm .04	.11 \pm .04	.14 \pm .04	.09 \pm .02
Fail Displacement	.29 \pm .06	.19 \pm .05	.51 \pm .17	.37 \pm .16	.30 \pm .15	.17 \pm .04	.25 \pm .05	.16 \pm .02
Total Energy	8.00 ± 2.75	3.72 ± 1.58	10.77 ± 3.34	4.40 ± 2.03	7.33 ± 2.98	4.18 \pm 1.51	4.56 ± 1.64	2.58 \pm .91
Elastic Energy	1.20 $\pm .49$	1.26 \pm .84	.80 \pm .63	.61 \pm .43	1.77 $\pm .29$	1.85 \pm .88	1.61 \pm .92	.95 \pm .53
Plastic Energy	6.80 ± 2.71	2.46 ± 1.97	9.97 ± 3.39	3.79 ± 2.20	5.56 ± 2.83	2.33 \pm 1.81	2.95 ± 1.81	1.63 \pm 1.01

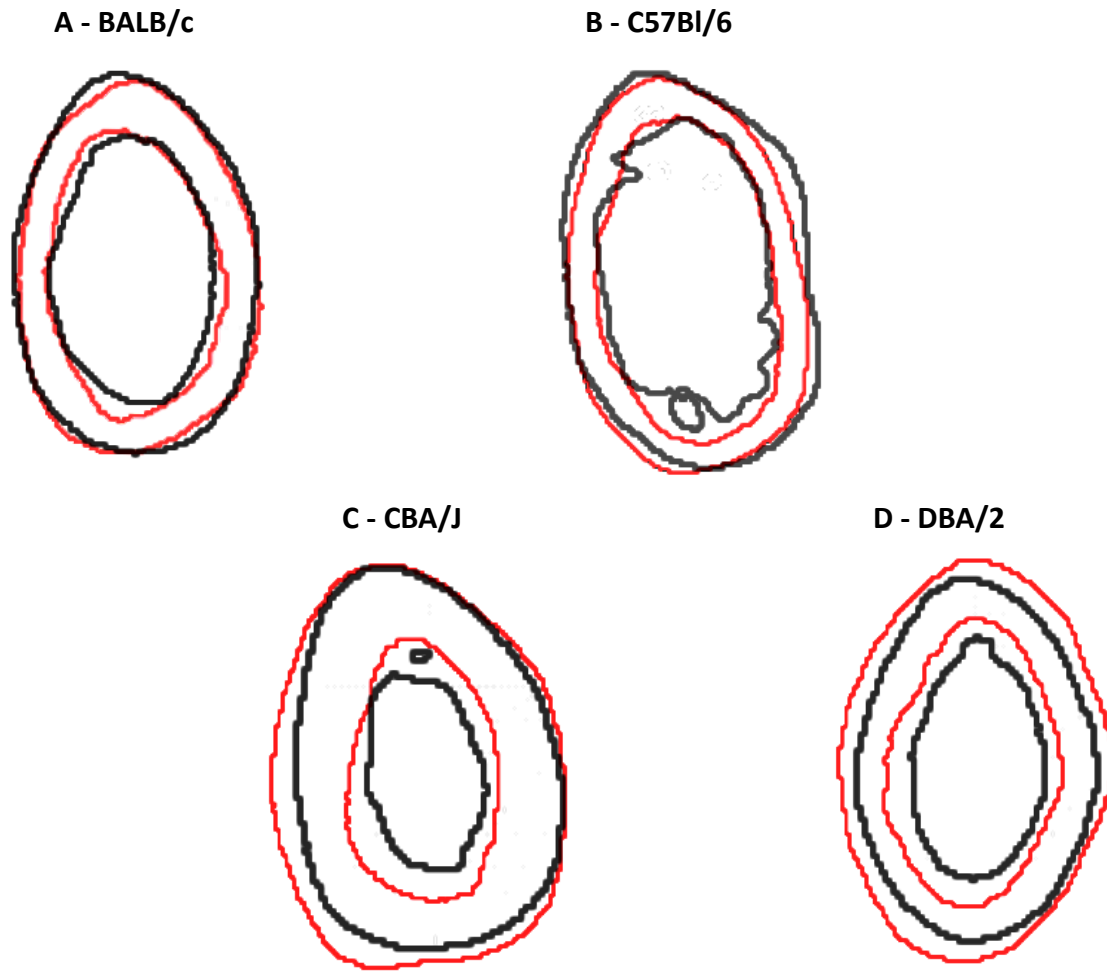


Figure 2. 5 - Geometry comparisons between 3- and 18-month mice.

Geometric outlines from μ CT images demonstrate size and shape changes that occur with aging. Black outlines represent a typical 3 month animal and the red outlines are of a typical 18 month animal. Centroids of representative individuals from both time points are aligned. **A)** Compared to the 3-month means, BALB/c 18-month cortical thickness is 24% lower ($p<0.001$), cortical area is 17% lower ($p=0.001$), endosteal circumference is no different, marrow area is 2% larger ($p=0.034$), periosteal circumference is 9% larger ($p=0.019$), resulting in no difference in second moment of area (I_y). **B)** Compared to the 3-month means, C57Bl/6 18-month have a 23% smaller cortical thickness ($p<0.001$), 16% smaller cortical area ($p=0.001$), 5% greater endosteal circumference ($p=0.025$), 25% greater marrow area ($p<0.001$), and no difference in periosteal circumference, resulting in a 3% increase in I_y ($p=0.045$). **C)** Compared to the younger mice, CBA/J old mice have a 13% smaller cortical thickness ($p<0.001$), no difference in cortical area, 12% greater endosteal circumference ($p<0.001$), 43% greater marrow area ($p<0.001$), no difference in periosteal circumference, and a 10% greater total area ($p<0.001$), resulting in a 53% increase in I_y ($p<0.001$). **D)** Compared to the younger mice, DBA/2 old mice have a 10% smaller cortical thickness ($p=0.014$), 14% greater cortical area ($p=0.002$), 27% greater endosteal circumference ($p<0.001$), 82% greater marrow area ($p<0.001$), 14% greater periosteal circumference ($p=0.003$), and a 38% greater total area ($p<0.001$), resulting in a 96% increase in I_y ($p<0.001$).

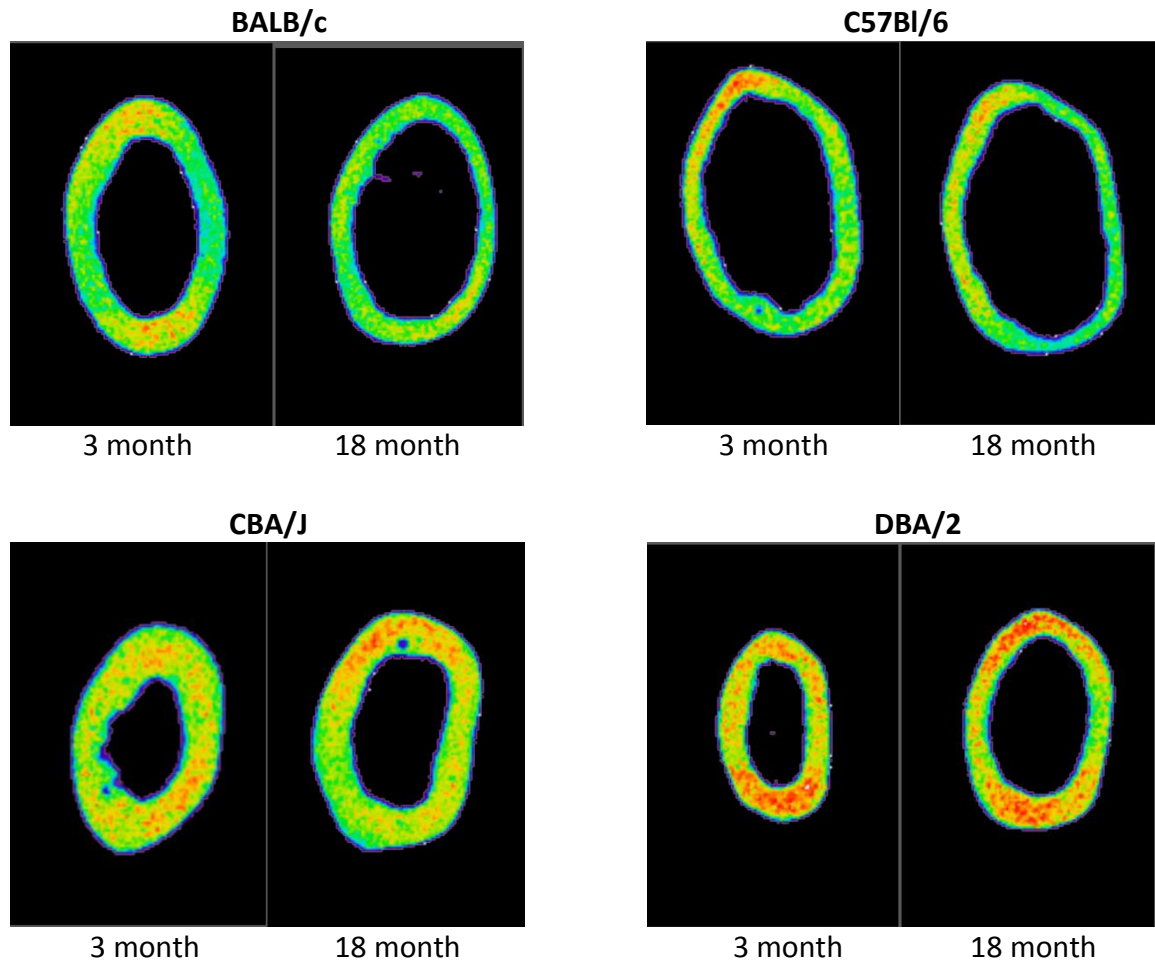


Figure 2. 6 - Alpha-blend comparisons of mineralization patterns between ages.

From μ CT data, mineralization is visualized on a colorimetric scale with regions highlighted red having the most mineralized tissue. **A)** In the BALB/c old mice, TMD is 11% less than the younger mice ($p=0.026$). **B)** The old C57Bl/6 mice have an 8% lower TMD than the 3-month mean ($p<0.001$) **C)** The CBA/J old mice have a 13% lower mean TMD than the younger mice ($p<0.001$). **D)** DBA/2 young and old mice have TMD means that are not significantly different.

Table 2. 3 - Summary of microCT data results.

Data is presented in unstandardized form. Means are given ± 1 SD. Values highlighted in **BOLD** represent 18-month means that were significantly different from the 3-month means in *t*-test with significance determined $p \leq 0.05$.

	BALB/c		C57Bl/6		CBA/J		DBA/2	
	3 months	18 months	3 months	18 months	3 months	18 months	3 months	18 months
N	10	6	19	19	20	17	10	6
TMC (mg)	3.42 $\pm .34$	3.34 $\pm .43$	2.55 $\pm .26$	2.48 $\pm .22$	3.11 $\pm .47$	4.11 $\pm .38$	2.18 $\pm .11$	2.61 $\pm .20$
TMD (mg/cc)	1218.87 ± 24.22	1251.85 ± 14.34	1064.26 ± 44.38	1084.76 ± 60.24	1273.13 ± 74.22	1318.68 ± 36.64	1242.95 ± 25.92	1251.66 ± 21.89
Cortical Thickness (mm)	.28 $\pm .02$.24 $\pm .02$.22 $\pm .01$.19 $\pm .01$.34 $\pm .02$.34 $\pm .03$.25 $\pm .01$.24 $\pm .01$
Ix (mm ⁴)	.40 $\pm .09$.41 $\pm .09$.37 $\pm .05$.41 $\pm .05$.23 $\pm .04$.37 $\pm .04$.15 $\pm .01$.28 $\pm .04$
Iy (mm ⁴)	.15 $\pm .03$.19 $\pm .03$.18 $\pm .02$.21 $\pm .02$.11 $\pm .01$.19 $\pm .03$.06 $\pm .01$.13 $\pm .02$
Ixy (mm ⁴)	.009 $\pm .026$.001 $\pm .018$.02 $\pm .04$.02 $\pm .04$.01 $\pm .02$.01 $\pm .01$.01 $\pm .01$.002 $\pm .005$
Endosteal Circumf. (mm)	3.51 $\pm .29$	4.02 $\pm .27$	4.17 $\pm .21$	4.82 $\pm .17$	2.38 $\pm .14$	3.19 $\pm .29$	2.60 $\pm .12$	3.44 $\pm .23$
Periosteal Circumf. (mm)	5.28 $\pm .32$	5.53 $\pm .32$	5.56 $\pm .25$	5.96 $\pm .19$	4.57 $\pm .20$	5.44 $\pm .27$	4.12 $\pm .10$	4.88 $\pm .22$
Marrow Area (mm ²)	.82 $\pm .12$	1.11 $\pm .15$	1.15 $\pm .10$	1.58 $\pm .09$.38 $\pm .05$.65 $\pm .10$.43 $\pm .03$.82 $\pm .10$
Cortical Area (mm ²)	1.14 $\pm .13$	1.09 $\pm .11$.99 $\pm .06$.92 $\pm .06$	1.10 $\pm .08$	1.30 $\pm .09$.77 $\pm .03$.92 $\pm .07$
Total Area (mm ²)	1.97 $\pm .23$	2.20 $\pm .22$	2.14 $\pm .15$	2.50 $\pm .11$	1.48 $\pm .10$	1.94 $\pm .11$	1.20 $\pm .05$	1.73 $\pm .16$

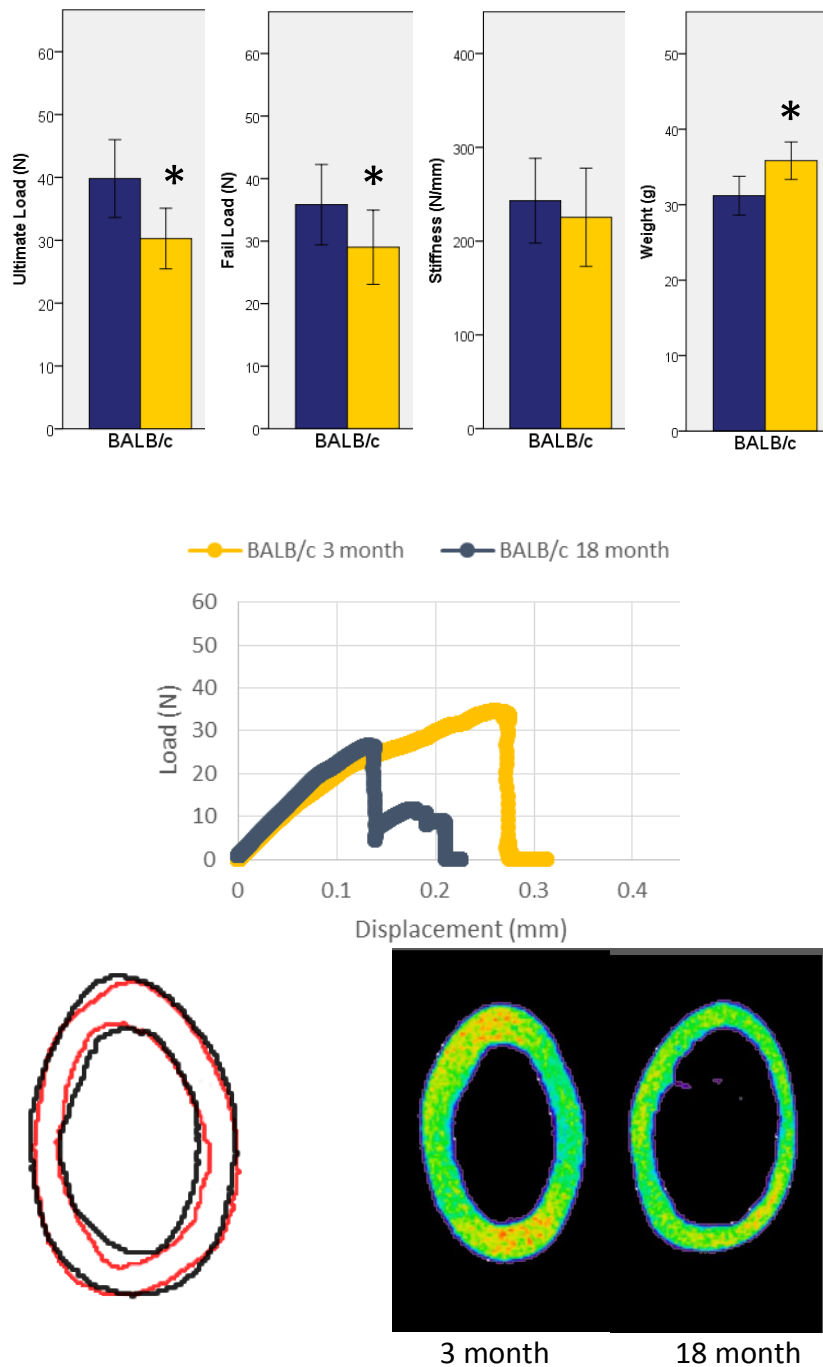


Figure 2. 7 - Summary of BALB/c results.

Visualizations combined to summarize the findings for the BALB/c femora at 3 and 18 months. BALB/c-18 month mice have lower mean ultimate load and fail load. Stiffness is not different and weight increases with age. There is little morphological differences between ages. TMD is 11% less in the older mice compared to 3-month mice. This, in addition to load-displacement curves, suggest loss in mechanical stability is primarily due to decreased mineralization and matrix changes leading to brittleness.

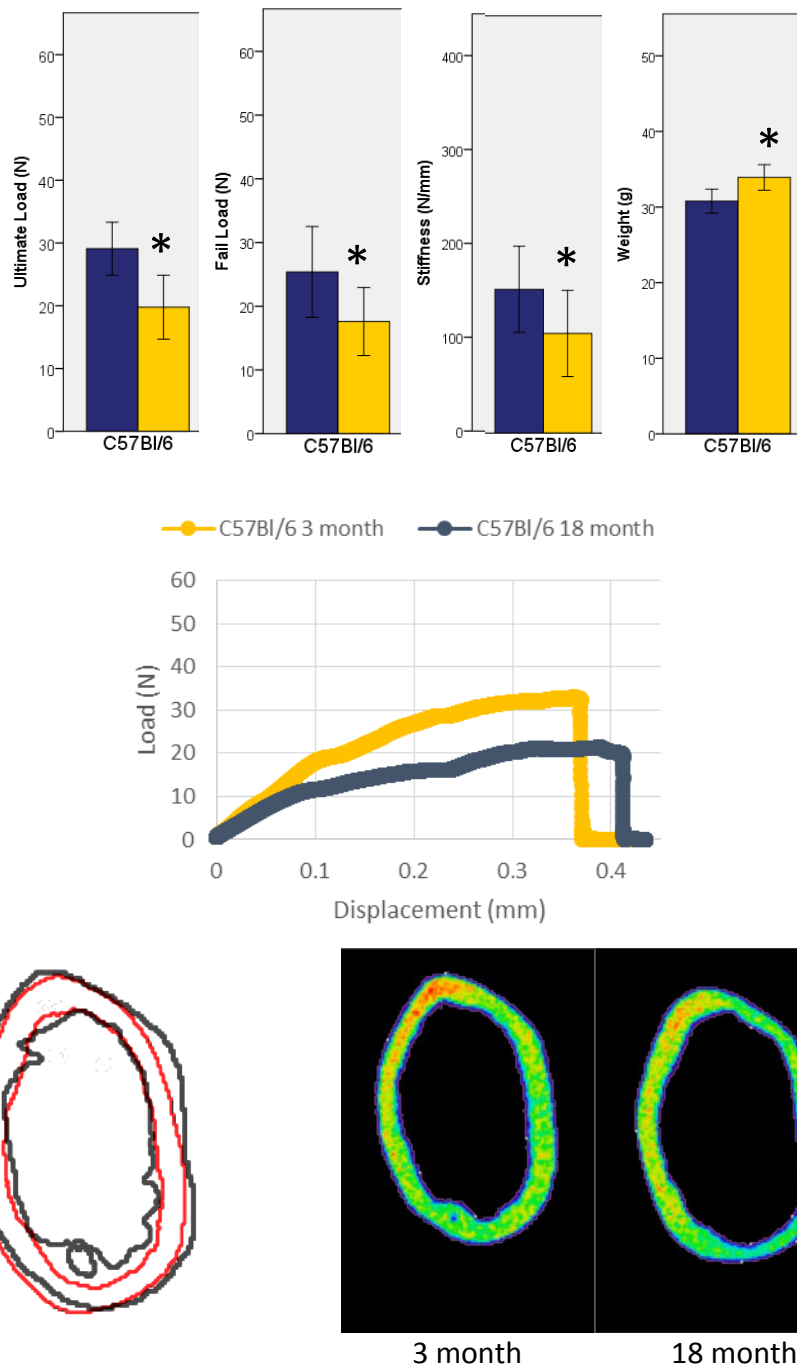


Figure 2. 8 - Summary of C57Bl/6 results.

Visualizations combined to summarize the findings for the C57Bl/6 femora at 3 and 18 months. 18-month mice have lower mean ultimate load, fail load, and stiffness. Weight increases with age. TMD is less in the older mice and geometry is unable to adapt appropriately to maintain stiffness. The loss of mineralization, the lack of morphology adaptation, and a slight loss of ductility contribute to the reduced mechanical properties in the 18-month mice compared to the 3-month mice.

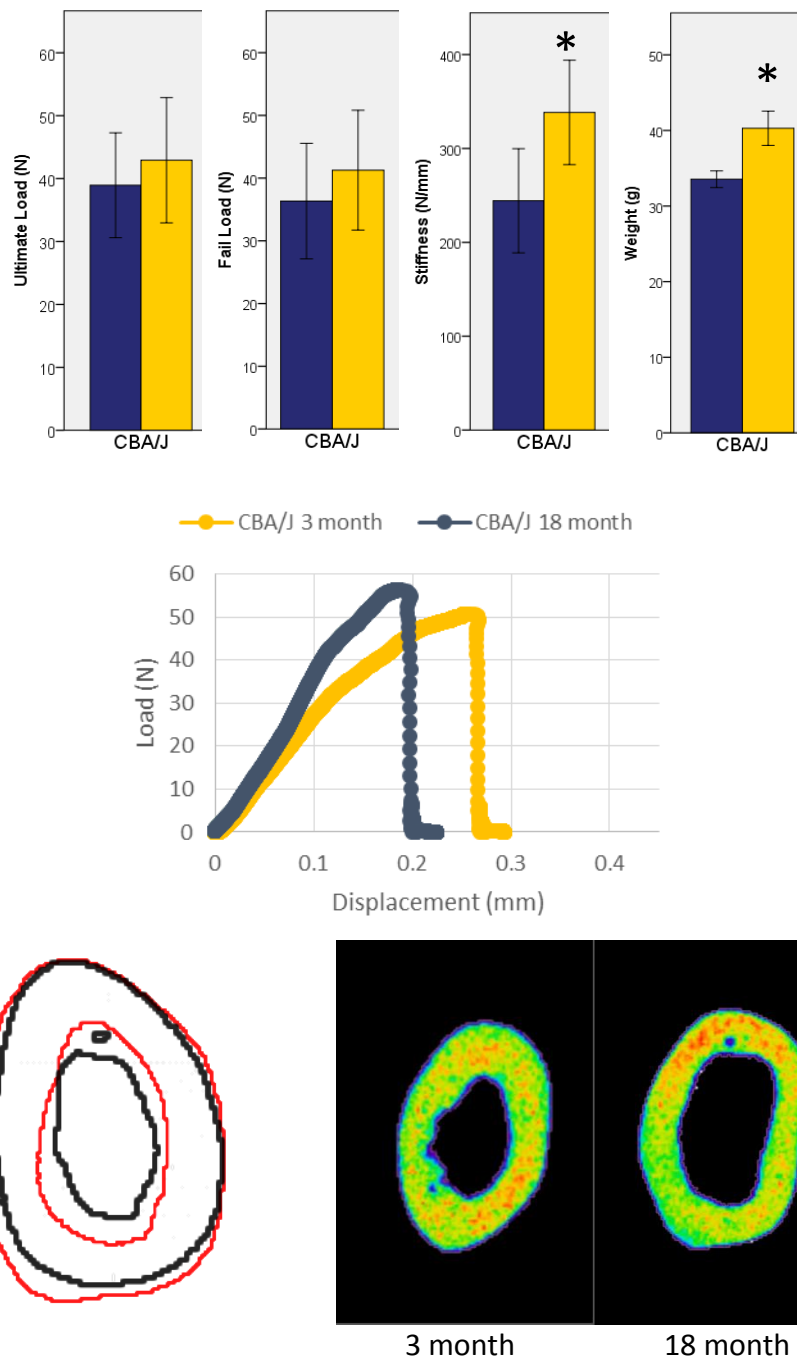


Figure 2. 9 - Summary of CBA/J results.

Visualizations combined to summarize the findings for the CBA/J femora at 3 and 18 months. 18-month mice have no difference in ultimate or fail loads compared to the 3-month mice. Stiffness and weight are both greater in the older animals. There is large amount of marrow expansion, which is compensated for through periosteal apposition. The periosteal expansion leads to an increase in second moment of area that recovers the stiffness lost from a lower TMD in the older mice. This increase in stiffness maintains ultimate load but may occur at the expense of ductility.

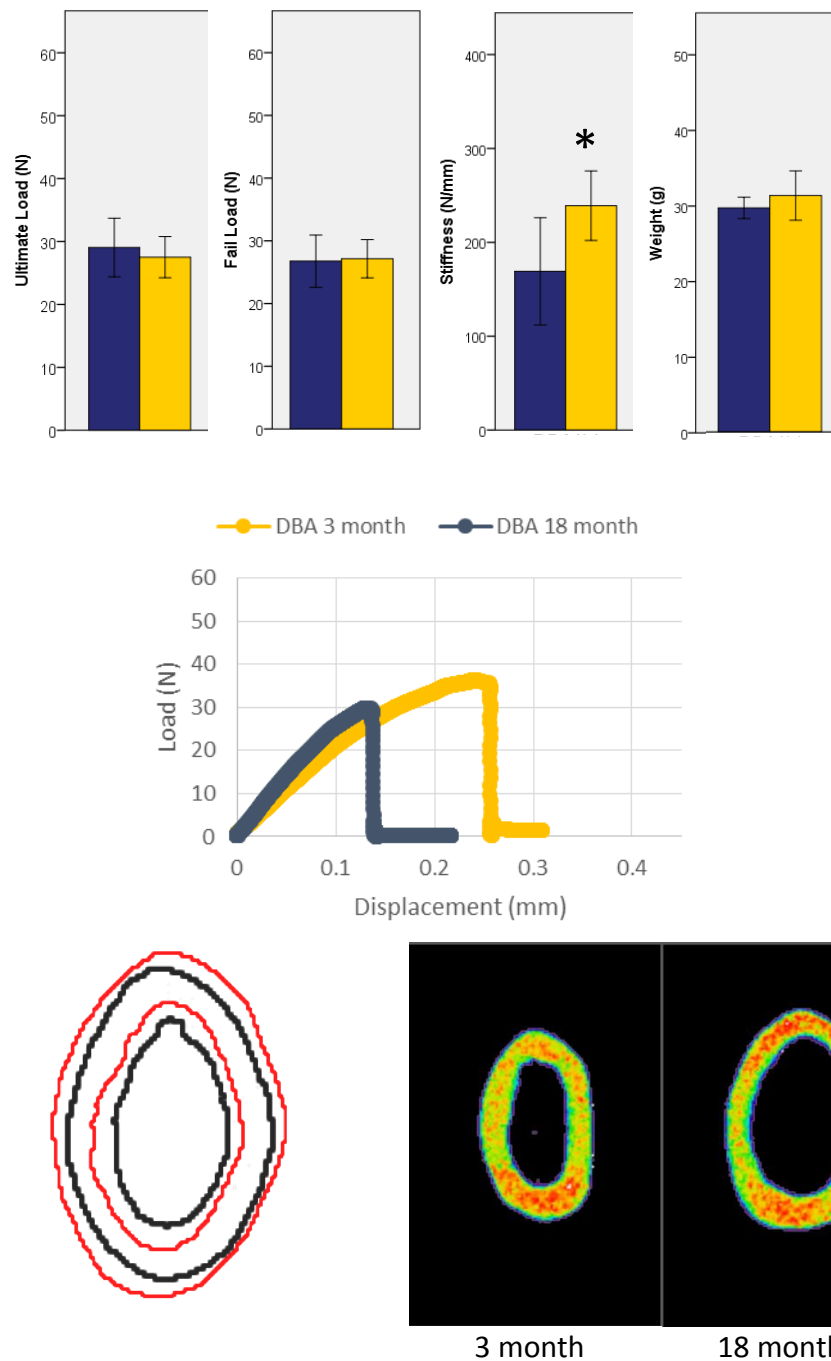


Figure 2. 10 - Summary of DBA/2 results.

Visualizations combined to summarize the findings for the DBA/2 femora at 3 and 18 months. DBA/2 18-month mice have no difference in ultimate load, fail load, or weight when compared to the 3-month mice but have a greater stiffness. There is no difference in TMD between the ages. Therefore, periosteal expansion is possibly in response to endosteal resorption. The increase in stiffness and maintenance of ultimate load suggest appropriate adaptive response to age-related marrow expansion.

CHAPTER III: PATTERNS OF BONE AGING VARY BETWEEN MOUSE STRAINS

Introduction

The previous chapter demonstrated that there are differing strategies to bone aging in the various inbred mouse strains. The two mouse strains with the most dissimilar aging outcomes are the C57Bl/6 and CBA/J mice. Due to limited availability of the aged mice, in this chapter, we will only investigate these two strains. Future work should expand to include the BALB/c and DBA/2 strains, as well as female mice. When comparing the age extremes – 3 and 18 months – the C57Bl/6 mice do not maintain the same level of bone strength and stiffness. The CBA/J mice have mechanical properties that provide consistent ultimate load values at 3 and 18 months.

The results from the first chapter suggest that the inbred mouse strains do, in fact, undergo different patterns of aging that lead to variable changes in mechanical functionality. However, in comparing 3- and 18-month mice, it is unclear as to the onset and continuity of age-related bone changes. That approach also prevents inference on which features of bone aging occur in response to changes in others. This chapter will include data from 10-month and 14-month animals for more precise understanding of the onset and progression of the bone aging changes.

In this chapter, I will test two primary hypotheses. The first hypothesis is that age-related changes in mouse bone will not occur at the same rate and timing in both strains. We predict that the C57Bl/6 mice will begin to lose mechanical properties and bone quantity earlier than the CBA/J mice. If this is not supported and both strains undergo bone changes simultaneously, we suggest that C57Bl/6 mice will lose bone properties at a faster rate.

The second hypothesis that will be tested in this chapter is that changes in cortical bone with aging will be correlated with changes in trabecular bone with aging. Many fragility fractures occur in highly trabeculated regions such as the femoral neck. Therefore, it is critical

to compare the aging strategies in the two mouse strains with respect to the trabecular compartments. In human aging, cortical and trabecular bone changes do not always coincide. In order to utilize the comparative approach to variability in bone aging, the trabecular patterns of aging must be elucidated.

The more complete examination of bone aging in the two mouse strains, will provide a stronger model for understanding the factors that impact bone aging. By enumerating a large array of age-related changes in the bones of the two mouse strains, we can determine if these strains are appropriate models for patterns of human bone aging.

Materials and Methods

Animals

All animals used were male mice procured through the NIA/NIH aged colonies. The two inbred strains utilized are C57Bl/6 and CBA/J. Each strain was analyzed cross-sectionally at 3, 10, 14, and 18 months. The 3, 10, and 14 month animals were euthanized upon arrival and femora and tibiae excised and frozen in PBS. The oldest age at which both strains were available was 17 months. Therefore, animals were group housed for 4 weeks. After the 4 week waiting period, all 18 month animals were euthanized and bones extracted and frozen.

Micro-Computed Tomography (μ CT)

All bones were scanned with a GE Medical eXplore Locus SP scanner (GE Medical, Waukesha, WI) at 18 μ m voxel size using a beam flattener. Specimens were scanned in a custom designed 8-bone holder to maximize throughput. The size of each region of interest (ROI) for cortical bone was defined as 10% of total bone length. The ROI was situation so the proximal-most point centered at 50% of length. Trabecular ROI was defined as 10% of total bone length. The most proximal point of the trabecular ROI coincided with the termination of the growth plate. Using GE MicroView 2.2 ABA software, an auto-thresholding algorithm was employed and morphological measures recorded.

Mechanical Testing

Bones were tested in 4-point bending with a custom designed system controlled using a Mini Bionix II servohydraulic system (MTS; Eden Prairie, MN). Femora were oriented such that load was applied in the anterior-posterior direction with posterior in tension. Based on the curvature of the tibiae, they were loaded also in the anterior-posterior direction but with the anterior surface in tension. The fibula was separated prior to testing. Load was applied using a constant displacement rate of 0.05 mm/s. A custom MATLAB script was written to extract critical data from the load-displacement curves. Primary outcome measures of interest were ultimate load, fail load, and stiffness.

Statistical Analysis

All statistics were run using commercially available software packages SPSS (IBM corp., Armonk, NY) and GraphPad Prism (GraphPad Software, San Diego, CA). ANOVA analysis were used to compare parameters age groups within strains. A Games-Howell post-hoc analysis was used due to variation in sample size and variance. Simple linear regression was employed to quantify relatedness of various measures. General linear modeling was also used in order to identify differences between the strains in timing and scale of bone aging changes. All results are considered significant when $p < 0.05$.

Results

Mechanical Testing

In 4-point bending of the C57Bl/6 femur, ultimate load averages were significantly different between age groups ($p < 0.001$) (Figure 3.1—A). More specifically, the 18-month ultimate load mean was 32% lower than the 3-month mean ($p < 0.001$) and 29% lower than the 10-month means ($p < 0.001$). The average stiffness values for C57Bl/6 femora differed between ages ($p < 0.001$). The 10-month mean was 42% greater than the 3-month mean ($p < 0.001$). The 18-month mean stiffness was 32% lower than the 3-month mean ($p = 0.012$), 52% lower than the 10-month mean ($p < 0.001$), and 43% lower than the 14-month mean ($p = 0.008$). Mean ultimate load values in C57Bl/6 tibiae were not statistically different between age groups ($p = 0.234$). For the mean stiffness, the ANOVA was significant when comparing the C57Bl/6 ages ($p = 0.039$). The

only pair-wise comparison that was significant is the 10-month and 14-month difference ($p=0.047$).

Results of 4-point bending in the CBA/J mice demonstrated similar average ultimate load values when comparing age groups ($p=0.099$) (Figure 3.1—A). The mean stiffness values of the CBA/J mice were significantly different ($p<0.001$) (Figure 3.1—C). Comparing the age-groups individually, the 3-month mean was 46% less than the 10-month mean ($p=0.046$), 36% less than the 14-month mean ($p=0.002$), and 29% less than the 18-month mean ($p<0.001$). The average ultimate load of the CBA/J tibiae demonstrated no difference in means between the age groups ($p=0.258$) (Figure 3.2—A). The mean stiffness of the CBA/J tibiae were significantly different ($p=0.034$) with a 10-month mean that is 27% greater than the 3-month mean stiffness ($p=0.012$) (Figure 3.2—C).

Body Weight Relationship

Running an ANOVA test for weight differences in the C57Bl/6 age groups demonstrated an average 12% greater body weight in the C57Bl/6 18-month mice than the 3-month group ($p<0.001$). The CBA/J average body weights were also different between the age groups ($p<0.001$), with the 18-month mice being 23% heavier than the 3-month mice ($p<0.001$) (Figure 3.3). When femoral ultimate load and stiffness values were normalized by body weight, ANOVA results for C57Bl/6 remained the same (Figure 3.1—B, D). The tibial ultimate load values became significantly different when standardized to weight ($p=0.002$). Following normalization, the 18-month mean ultimate load is 20% lower than the 3-month mean ($p=0.003$) (Figure 3.2—B). The total ANOVA remained significant when stiffness was normalized by body weight ($p=0.030$), however, no pairwise comparisons reached significance (Figure 3.2—D).

The ANOVA results for ultimate load and stiffness remained the same after normalizing the CBA/J data to body weight (Figure 3.1—B, D). However, the 3-month comparison to the 14- and 18-month means was no longer significant (Figure 3.1—D). The comparison in tibial ultimate load in the CBA/J was not significant prior to standardizing to weight, but showed statistically significant differences after ($p=0.029$). Following standardization, the 18-month tibial ultimate load was 16% less than that recorded in the 3-month mice ($p=0.026$) (Figure 3.2—B). Where ultimate load comparisons gained significance following standardization in

CBA/J, the comparisons of mean tibial stiffness lost significance following standardization ($p=0.801$) (Figure 3.2—D).³

General Linear Models: Mechanical Properties

General linear modeling is a useful tool to determine if the manner in which age influences bone properties is different between the C57Bl/6 and CBA/J mouse strains. We ran the model using the weight-normalized values to eliminate the different impact weight had on the outcome variables. We used a model looking at the effects of age, strain, and the interaction of age and strain on both ultimate load and stiffness. In the femur, this model for ultimate load was significant with $R^2=0.594$ ($p<0.001$). Strain, alone, significantly influenced ultimate load ($R^2=0.435$, $p<0.001$) with CBA/J mice having greater mean ultimate load at all ages compared to C57Bl/6 means. Independent of strain, age also had an individual influence on the ultimate load values ($R^2=0.254$, $p<0.001$). The interaction term between strain and age was not significant ($p=0.287$). This suggested that the age-related changes in ultimate load are similar in the C57Bl/6 and CBA/J strains within each time interval. However, cumulatively, there was a loss of ultimate load in the C57Bl/6 strain by 18-months but not in the CBA/J mice (Figure 3.4 – A).

Similar to the GLM results for ultimate load, the model for femoral stiffness was significant $R^2=0.733$ ($p<0.001$). Strain and age, alone, had an effect on stiffness ($R^2=0.576$, $p<0.001$ and $R^2=0.291$, $p<0.001$, respectively). Unlike the ultimate load model, the interaction term was significant ($R^2=0.117$, $p=0.012$). This suggests that the strains differed in how age influences stiffness of the femur. Post-hoc tests were run in order to determine when, during the aging process, the two strains differ. The slopes for C57Bl/6 and CBA/J mice were not distinct between 3 and 10 months ($p=0.854$), 10 and 14 months ($p=0.103$), or 14 and 18 months ($p=0.445$). However, slopes between 3 and 18 months were significantly divergent ($p=0.004$), as were the slopes between 10 and 18 months ($p=0.022$). This suggests a cumulative difference in aging effects that occur between 10 and 18 months of age (Figure 3.4 – B).

³ Note: The remaining statistics are run using the normalized values unless otherwise stated.

These models were also run on the ultimate load and stiffness in the tibiae. The model was significant for tibial ultimate load with $R^2=0.247$ ($p<0.001$). However, in this model, age was the only factor that significantly influenced ultimate load ($R^2=0.216$, $p<0.001$). The strains did not differ in either the values for ultimate load or how these values changed with age (Figure 3.4 – C). The model for tibial stiffness was also significant with $R^2=0.260$ ($p<0.001$). Strain was the only factor significantly influencing the model ($R^2=0.151$, $p<0.001$). The stiffness of the tibia does not appear to change in either strain as age increases (Figure 3.4 – D).

Mechanical Parameter Relationships

C57 Femur:⁴ The ultimate load did not significantly drop until the 18-month. Femoral stiffness in the C57BL/6 mice was greatest in the 10-month group. Ultimate load, when all ages were pooled, was linearly correlated with stiffness ($R=0.649$, $p<0.001$). When the 3-month animals were isolated, ultimate load was still correlated with stiffness ($R=0.779$, $p<0.001$). In the 10-month-only group, ultimate load and stiffness had a relationship approaching significance ($R=0.813$, $p=0.094$), as well as in the 14-month mice ($R=0.844$, $p=0.072$). Ultimate load was not significantly related to stiffness ($p=0.523$) in the 18-month age group. Running pairwise ANCOVA, we determined that the 18-month intercept was significantly different from all other time points. None of the slopes were significantly different, however. (Figure 3.5 – A). This suggests a change in the ultimate load and stiffness relationship occurring between the 14- and 18-month times, likely due to matrix-level changes. Post-yield displacement differed between 3 months and the other age groups ($p=0.004$). The 3-month mean was 46% greater than the 14-month mean ($p=0.001$) and 30% greater than the 18-month mean ($p=0.030$) (Figure 3.7 – A).

C57 Tibia:⁵ The ultimate load did not significantly drop until the 18-month group where it was 20% lower than at 3 months. Tibial stiffness in the C57BL/6 mice was invariant, statistically, when the ages are compared. Ultimate load, when all ages were pooled, was linearly correlated with stiffness ($R=0.544$, $p<0.001$). When the 3-month and 14-month animals were isolated, ultimate load was no longer correlated with stiffness. In the 10-month and 18-

⁴ Load-displacement curve visualized in Figure 3.6 – A.

⁵ Load-displacement curve visualized in Figure 3.6 – C.

month groups, ultimate load and stiffness had a significant relationship ($R=0.889$, $p=0.044$ and $R=0.616$ $p=0.007$). As in the C57Bl/6 femur, the ANCOVA revealed no difference in slopes of the ultimate load – stiffness relationship. However, the 18-month intercept was significantly different from all other time points (Figure 3.5 – B). Post-yield displacement was different between the age groups ($p=0.054$) (Figure 3.7 – B). The 10-month mean was 53% greater than the 18-month mean ($p=0.035$). The mechanical trends, again, suggest matrix-level changes affecting the ultimate load – stiffness relationship.

CBA Femur:⁶ The ultimate load did not differ between the age groups. Femoral stiffness was statistically different when comparing age groups, however, most of the post-hoc pair-wise comparisons disappeared when normalizing for weight. Ultimate load, when all ages are pooled, was linearly correlated with stiffness ($R=0.616$, $p<0.001$). When the 3-month animals were isolated, ultimate load was still correlated with stiffness ($R=0.701$, $p=0.001$). The 10-month and 14-month relationships were not significant. However, ultimate load was significantly related to stiffness in the 18-month age group ($R=0.711$, $p=0.001$). The ANCOVA resulted in no significant differences in intercept or slope of the regression lines at the different ages (Figure 3.5 – C). Post-yield displacement differed between 3 months and the other age groups ($p<0.001$) (Figure 3.7 – A). The 3-month mean was 41% greater than the 10-month mean, 74% greater than the 14-month mean ($p=0.012$) and 69% greater than the 18-month mean ($p<0.001$). The mechanical data suggest that the loss of PYD did not influence the relationships between ultimate load and stiffness.

CBA Tibia:⁷ The ultimate load did not significantly drop until the 18-month group and tibial stiffness in the mice was invariant when normalized to weight. Ultimate load, when all ages were pooled, was linearly correlated with stiffness ($R=0.491$, $p<0.001$). When the 3-month animals were isolated, ultimate load was still correlated with stiffness ($R=0.708$, $p<0.001$). The 10-month-only group had a relationship approaching significance ($R=0.866$, $p=0.058$). The 14-month and 18-month mice did not have a significant relationship between ultimate load and stiffness (Figure 3.5 – D). Unlike the femoral ANCOVA, the 18-month intercept of the regression

⁶ Load-displacement curve visualized in Figure 3.6 – B.

⁷ Load-displacement curve visualized in Figure 3.6 – D.

line was significantly different from those at all other ages, though the slopes were invariant. Post-yield displacement also was invariant across the age groups (Figure 3.7 – B).

Mechanics and Morphology

C57Bl/6 Femur: In the C57Bl/6 femora, the means for TMD differed between the age groups ($p<0.001$) with the 18-month mean being 9% lower than the 3-month mean ($p<0.001$) and 10% lower than the 10-month mean ($p=0.018$) (Figure 3.8 – A). C57Bl/6 cortical thickness was different when age groups were compared ($p<0.001$), with the 3-month mean being 15% greater than the 14-month mean ($p<0.001$) and 26% greater than the 18-month mean ($p<0.001$). The 10-month mean was 11% greater than the mean at 14 months ($p=0.035$) and 22% greater than the mean at 18 months ($p<0.001$). The 14-month mean was 13% greater than the 18-month mean ($p=0.002$) (Figure 3.8 – C). C57Bl/6 age groups had different means for second moment of area (I_y) in the bending direction ($p=0.003$). The 14-month mean was 21% greater than the 3-month mean ($p=0.003$), 23% greater than the 10-month mean ($p=0.017$), and 14% greater than the 18-month mean ($p=0.052$) (Figure 3.8 – E). The age-related changes in mechanical function (loss of ultimate load and stiffness) were largely related to the reduction in both amount and mineralization of bone. The slight increase in I_y that occurred in the older age groups was not sufficient to mechanically accommodate the loss of function from cortical thinning and decreased TMD.

The ANOVA demonstrated differences in endosteal perimeter means ($p=0.032$), however, none of the post-hoc comparisons reached significance (Figure 3.9 – A). The periosteal perimeter means were invariant between age groups ($p=0.066$) (Figure 3.9 – C). Despite the lack of statistical evidence of periosteal or endosteal surface change, both marrow area and cortical area differed between the age groups ($p<0.001$). The 3-month marrow area mean was 24% less than the 14-month mean ($p<0.001$) and 23% less than the 18-month mean ($p<0.001$). The 10-month mean was 30% lower than the 14-month mean ($p<0.001$) and 28% lower than the 18-month mean ($p<0.001$) (Figure 3.9 – E). The mean cortical area in the 18-month group was 18% lower than the 3-month mean ($p<0.001$), 12% lower than the 10-month mean ($p=0.001$), and 11% lower than the 14-month mean ($p=0.005$) (Figure 3.9 – G).

C57Bl/6 Tibia: The mean TMD values in the C57Bl/6 tibiae were different when comparing the age groups ($p=0.016$) with the 3-month mean being 8% greater than the 18-month mean ($p=0.006$) (Figure 3.8 – B). This pattern was similar to the pattern of change measured in the tibial ultimate load. The C57Bl/6 tibiae undergo little functional change until after the 14-month time point, at which time TMD decrease may account for much of the loss of ultimate load. However, with a decrease in TMD, we would expect an associated decrease in stiffness, yet this did not occur in the samples compared here. Therefore, the lower ultimate load was possibly due to changes influencing the post-yield mechanics without influencing the pre-yield measures. Cortical thickness also varied between age groups ($p<0.001$). The 3-month mean was 20% greater than the 14-month mean ($p<0.001$) and 27% greater than the 18-month mean ($p<0.001$). Additionally, the 14-month mean was 9% greater than the 18-month mean ($p=0.026$) (Figure 3.8 – D). However, this should also have influenced stiffness values which did not change. This is further evident by the lack of variation in the I_y values between age groups (Figure 3.8 – F). The mineralization and shape changes that were measured did not influence stiffness. The lack of change in stiffness might be due to interactions with the fibula that were not investigated.

The lower cortical thickness was due to greater endosteal perimeter ($p<0.001$) with the 3-month mean being 14% less than the 14-month mean ($p=0.016$) and 10% less than the 18-month mean ($p<0.001$) (Figure 3.8 – B). This led to an expansion of marrow area ($p<0.001$). The 3-month mean was 12% lower than the 10-month mean ($p=0.039$), 36% lower than the 14-month mean ($p=0.001$), and 29% lower than the 18-month mean ($p<0.001$). The 10-month mean was 21% less than the 14-month mean ($p=0.007$) and 15% less than the 18-month mean ($p=0.012$) (Figure 3.9 – F). This loss of bone on the endosteal surface was not compensated through periosteal apposition. The periosteal circumference means varied between ages ($p<0.001$), however the difference in means was due to a 4% drop, rather than increase, between the 3- and 18-month age groups ($p=0.010$) (Figure 3.9 – D). This resulted in a significant difference in cortical area between ages ($p<0.001$). The 3-month mean was 12% greater than the 14-month mean ($p=0.004$) and 19% greater than the 18-month mean ($p<0.001$) (Figure 3.9 – H).

CBA/J Femur: In the femora of the CBA/J mice, the age groups demonstrated different mean TMD, cortical thickness and I_y values ($p<0.001$). The 3-month mean TMD was 16% greater compared to the 18-month mice (Figure 3.8 – A). The 3-month mean cortical thickness was 19% greater than the 18-month mean ($p<0.001$) (Figure 3.8 – C). Despite the lower TMD and cortical thickness, the ultimate load and stiffness means remained fairly constant. This was likely due to the increasing I_y values with age. The 3-month I_y mean was 11% less than the 10-month mean ($p=0.045$), 19% less than the 14-month mean ($p=0.045$), and 50% less than the 18-month mean ($p<0.001$). The 10-month mean was 36% less ($p<0.001$) and the 14-month mean was 26% less ($p=0.005$) than the 18-month mean (Figure 3. 8 – E).

Using the mean values for TMD and I_y , we assessed how well the CBA/J femur was able to accommodate age-related loss of mineralization with size/shape changes. The normalized TMD values for 3, 10, 14, and 18 months were 38.86, 35.27, 36.95, and 32.76, respectively.⁸ The normalized values for I_y are 0.0032, 0.0036, 0.0039, and 0.0048, respectively. Assuming a simplified tissue modulus where E is only based on mineralization, we used the equation for stiffness:

$$K = \text{TMD} \times I_y$$

The calculated arbitrary stiffness value at 3 months was equal to 0.1256. We added in the TMD and I_y values to see if changes in shape accounted for the maintenance of stiffness despite a decrease in TMD.

$$K_3 = (38.86) \times (.0032) = .1243$$

$$K_{10} = (35.27) \times (.0036) = .1270$$

$$K_{14} = (36.95) \times (.0039) = .1441$$

$$K_{18} = (32.76) \times (.0048) = .1572$$

Thus, it seems that using a simplified model for stiffness, the age-related increase in I_y was able to compensate for the loss of mineralization also evident with age increase. The CBA/J mean endosteal and periosteal perimeters did not differ between age groups (Figure 3.9 – A, C). Differences in marrow area were significant between ages ($p<0.001$), where the 3-month mean

⁸ Note: due to the values being standardized by weight, the true unit is mg/mm³/g. However, we will treat it as dimensionless for ease of calculation.

was 39% lower than the 18-month mean ($p<0.001$) (Figure 3.9 – E). Although, there was no significant differences in cortical area means in the CBA/J femora (Figure 3.9 – G).

CBA/J Tibia: TMD means in the CBA/J tibiae differed between ages ($p<0.001$), with the 3-month mean being 12% greater than the 18-month mean ($p<0.001$) (Figure 3.8 – B). The lower TMD value paralleled the changes measured in CBA/J tibial ultimate load. Additionally, the differences in cortical thickness between age groups ($p<0.001$) occurred in a pattern similar to the ultimate load differences. The 3-month cortical thickness mean was 15% greater than the mean at 14-months ($p=0.010$) and 21% greater than the mean at 18 months ($p<0.001$) (Figure 3.8 – D). The loss of TMD and cortical thickness are driving the reduction in mean ultimate load in the CBA/J tibia. The TMD and cortical thickness patterns did not seem to greatly influence stiffness. The lack of change to stiffness might have been due to the 12% greater I_y mean at 3 months compared to 18 months ($p=0.047$) (Figure 3.8 – F). Using the same formula for stiffness as above, we tested if stiffness was being maintained due to appropriate compensation in shape to offset the loss of TMD. Since the only significant difference in TMD occurred between the 3- and 18-month groups, we limited our calculations to those:

$$K_3 = (36.52) \times (.002213) = .0808$$

$$K_{18} = (32.21) \times (.002477) = .0800$$

It seems that the increase in I_y was able to accommodate the loss of mineralization to maintain stiffness. This fact suggests that the decrease in ultimate load is occurring due to changes influencing the post-yield properties.

The age groups had different endosteal perimeter means in the CBA/J mice ($p=0.010$) with the 3-month mean being 7% smaller than the 18-month mean ($p=0.010$). The CBA/J periosteal perimeter means were not statistically distinguishable (Figure 3.9 – D).

Marrow area means were also significantly different ($p<0.001$). The 3-month mean was 38% lower than the 14-month mean ($p=0.012$) and 41% lower than the 18-month mean ($p<0.001$) (Figure 3.9 – F). Cortical area in the CBA/J age groups had different means, as well ($p=0.007$). The 3-month mean was 9% larger than both the 14-month mean ($p=0.045$) and the 18-month mean ($p=0.003$) (Figure 3.9 – H).

Trabecular Bone

C57Bl/6 Distal Femur: Mean trabecular BMD (tBMD) was different when C57Bl/6 ages were compared ($p<0.001$). The 3-month mean was 43% greater than the 14-month mean ($p<0.001$) and 40% greater than the 18-month mean ($p<0.001$). The 10-month mean was 35% greater than the 14-month mean ($p=0.010$) and 32% greater than the 18-month mean ($p=0.003$) (Figure 3.10 – A). Mean trabecular TMD (tTMD) values also differed when the C56Bl/6 age groups were compared ($p=0.001$). The 3-month mean was 19% greater than at 18 months ($p=0.003$). The 10-month mean was 24% greater than at 18 months ($p=0.012$) (Figure 3.10 – B). The 3-month bone volume fraction (BVf) mean was 41% greater than the 10-month mean ($p<0.001$), 52% greater than the 14-month mean ($p<0.001$), and 58% greater than the 18-month mean ($p<0.001$) (Figure 3.10 – C). The age group means for anisotropy were overall significantly different ($p<0.001$), with a 14-month mean that was 19% greater than the 3-month mean ($p=0.012$), 26% greater than the 10-month mean ($p=0.004$), and 24% greater than the 18-month mean ($p<0.001$) (Figure 3.10 – D).⁹ The ratio of bone surface to bone volume (BS/BV) was not statistically different between the age groups in the C57BL/6 mice (Figure 3.10 – A). However, trabecular thickness means were different ($p<0.001$). The 3-month mean was 10% greater than the 18-month mean ($p<0.001$) and the 14-month mean was 23% greater than the 18-month mean ($p=0.030$) (Figure 3.11 – B). The average number of trabeculae was also statistically different between age groups ($p<0.001$). The 3-month mean was 44% greater than the 10-month mean ($p<0.001$), 57% greater than the 14-month mean ($p<0.001$), and 60% greater than the 18-month mean ($p<0.001$) (Figure 3.11 – C).

C57Bl/6 Proximal Tibia: Mean tBMD values differed between age groups in the C57BL/6 tibiae ($p<0.001$). The 3-month mean was 19% greater than the 10-month mean ($p=0.002$), 34% greater than the 14-month mean ($p<0.001$), and 33% greater than the 18-month mean ($p<0.001$). The 10-month mean was 18% greater than the 18-month mean ($p=0.034$) (Figure 3.12 – A). Mean tTMD values were also different ($p=0.019$) due to a 9% greater mean in the 3-month mice compared to the 18-month mice ($p=0.042$) (Figure 3.12 – B). The BVf means for the age groups differed with age ($p<0.001$). The 3-month mean was 46% greater than the 10-

⁹ Note: BVf and anisotropy are the only trabecular measures not normalized by weight due to the fact that they are already ratios with the same units, making normalization unnecessary.

month mean ($p<0.001$), 63% greater than the 14-month mean ($p<0.001$), and 55% greater than the 18-month mean ($p<0.001$) (Figure 3.12 – C). Anisotropy measures were not taken for the proximal tibiae. The BS/BV ratio in the tibia did not vary between ages in the C57Bl/6 mice (Figure 3.13 – A). Trabecular thickness of the trabeculae did, however, differ between ages ($p<0.001$). The 3-month mean was 14% greater than the 10-month mean ($p=0.011$) and 16% greater than the 18-month mean ($p<0.001$) (Figure 3.13 – B). In addition to trabecular thickness, the mean trabecular number varied between age groups ($p<0.001$). The 3-month mean was 46% greater than the 10-month mean ($p<0.001$), 65% greater than the 14-month mean ($p<0.001$), and 58% greater than the 18-month mean ($p<0.001$) (Figure 3.13 – C).

CBA/J Distal Femur: The age group mean tBMD values in the CBA/J mice were different ($p=0.003$) with the 3-month mean being 28% greater than the 18-month mean ($p=0.003$) (Figure 3.10 – A). The mean tTMD values were not different in the CBA/J mice when comparing age groups (Figure 3.10 – B). The BVF means, however, were different ($p<0.001$) with the 3-month mean being 65% greater than the 10-month mean ($p<0.001$), 74% greater than the 14-month mean ($p<0.001$), and 67% greater than the 18-month mean ($p<0.001$) (Figure 3.10 – C). Anisotropy was not different between the CBA/J age groups (Figure 3.10 – D). The ratio of BS/BV was not statistically different between the age groups (Figure 3.11 – A). However, trabecular thickness was different between ages ($p=0.038$). The only pairwise comparison that was significant was the 16% greater mean thickness at 3 months than at 18 months ($p=0.054$) (Figure 3.11 – B). The CBA/J trabecular number means were also different ($p<0.001$). The mean at 3 months was 68% greater than that at 10 months ($p<0.001$), 73% greater than at 14 months ($p<0.001$), and 75% greater than at 18 months ($p<0.001$) (Figure 3.11 – C).

CBA/J Proximal Tibia: Means differed for tBMD in the CBA/J tibiae ($p<0.001$). The 3-month tBMD mean was 18% greater than the 10-month mean ($p=0.018$) and 25% greater than both the 14- and 18-month means ($p<0.001$) (Figure 3.12 – A). However, CBA/J tibiae were invariant in mean tTMD (Figure 3.12 – B). The BVF means for the age groups differed by age ($p<0.001$). The 3-month mean was 46% greater than the 10-month mean ($p<0.001$), 72% greater than the 14-month mean ($p<0.001$), and 52% greater than the 18-month mean ($p<0.001$) (Figure 3.12 – C). BS/BV varied between the age groups ($p<0.001$). The 3-month mean

was 27% greater than the 10-month mean ($p=0.010$) and 31% greater than the 18-month mean ($p<0.001$). The 10-month mean was 40% lower than the 14-month mean ($p=0.040$), which was in turn 43% greater than the 18-month mean ($p=0.001$) (Figure 3.13 – A). While trabecular thickness was indistinguishable between age groups (Figure 3.13 – B), trabecular number differed ($p<0.001$). The 3-month mean was 60% greater than the 10-month mean ($p<0.001$), 68% greater than the 14-month mean ($p<0.001$), and 67% greater than the 18-month mean ($p<0.001$) (Figure 3.13 – C).

General Linear Models: Femur

The GLM that we applied was strain+age+strain*age where strain*age is the interaction term. Using this model on tBMD values was significant ($R^2=0.671$, $p<0.001$). Strain and age were significant factors ($R^2=0.278$, $p<0.001$ and $R^2=0.582$, $p<0.001$, respectively). The interaction between strain and age was also significantly influencing the outcomes ($R^2=0.247$, $p=0.002$). The change in means from the 3-month group to 18-month group was significant ($p=0.035$). The slopes from 3 months to 10 months and 14 to 18 months were not statistically different. The slopes between 10 months and 14 months were different between the two strains ($p=0.008$). The C57Bl/6 mice lost relatively more tBMD than the CBA/J mice. The interval most responsible for this difference was from 10 to 14 months, where the C57Bl/6 mice continued to lose tBMD while the CBA/J did not. The change in tBMD in the C57Bl/6 femora began after 3 months and continued to 14 months. The loss of tBMD in the CBA/J femora occurred during the 3 to 10 month interval and then was stable (Figure 3.14 – A).

The model run for tTMD in the femur was also significant ($R^2=0.442$, $p<0.001$). Strain did not influence outcomes in the model, but age had an effect ($R^2=0.246$, $p=0.002$), as did the interaction of age and strain ($R^2=0.213$, $p=0.005$). The ANOVA demonstrated a lower mean in the C57Bl/6 mice between 3 and 18 months but not in the CBA/J mice. The slopes from 3 to 10 months differed between the strains ($p=0.007$). The 10-to-14 and 14-18 month slopes did not differ. However, the rate of change from 10 to 18 months did differ by strain ($p=0.004$). The C57Bl/6 tTMD was still increasing from 3 to 10 months and then began to decline consistently from 10 to 18 months. The CBA/J mice lost tTMD from 3 to 10 months but rebounded with an

increase in mineral density from 10 to 18 months. This resulted in cumulatively no change in CBA/J means from 3 to 18 months (Figure 3.14 – B).

The overall model was significant for BVF ($R^2=0.782$, $p<0.001$). Strain ($R^2=0.619$, $p<0.001$), age ($R^2=0.659$, $p<0.001$), and the interaction term ($R^2=0.160$, $p=0.025$) were all significant. The slopes of the two strains differed from 3 to 18 months ($p=0.001$), however, none of the smaller intervals were divergent enough to reach significance. Both strains experienced a dramatic loss of trabecular volume from 3 to 10 months. From 10 months on, C57BL/6 mice seemed to steadily lose more volume than the CBA/J mice by the final 18 month time point. CBA/J mice at 3 months had much lower BVF than C57BL/6 mice, so the CBA/J mice may have hit a lower limit in BVF earlier than C57BL/6 mice due to the lower starting point. (Figure 3.17 – C).

The model for anisotropy was significant ($R^2=0.344$, $p<0.001$). Strain was the only factor that influences the outcome values ($R^2=0.220$, $p<0.001$). The interaction term did not significantly contribute to the model. The ANOVA for anisotropy showed no difference between 3 and 18 months in either strain. Therefore, differences in anisotropy between C57BL/6 and CBA/J mice were due to CBA/J mice initially having greater levels of anisotropy at 3 months (Figure 3.17 – D).

The model was significant when applied to BS/BV ratios ($R^2=0.306$, $p=0.005$). Strain and the interaction term were significant factors of the model ($R^2=0.082$, $p=0.034$ and $R^2=0.221$, $p=0.004$, respectively), but age was not a significant factor. The overall rate of change was different in the strains from 3 to 18 months ($p=0.001$). The only sub-interval that had diverging slopes was from 14 to 18 months ($p=0.002$). During this interval, C57BL/6 increased BS/BV, which could have occurred due to thinning of the trabeculae. A second explanation that could not be addressed with these data is that there was a greater preponderance of trabecular plates than rods (Figure 3.15 – A).

The model for trabecular thickness was significant ($R^2=0.495$, $p<0.001$) with strain ($R^2=0.188$, $p=0.001$) and age ($R^2=0.380$, $p<0.001$) as influencing factors. The interaction term was not significant. The lack of significance in the interaction term was likely due to the consistent means in both strains from 3 to 14 months. The lack of variation in these intervals

masked the difference in the 14 to 18 month interval. During this time span, C57Bl/6 mice had a marked drop in trabecular thickness but there was little change in the CBA/J mean. This was supported by running the model on a subset of data including only the 14- and 18-month data. In this analysis, the interaction was highly significant ($p=0.001$) (Figure 3.18 – B).

The model for trabecular number was significant ($R^2=0.800$, $p<0.001$). Strain ($R^2=0.657$, $p<0.001$) and age ($R^2=0.675$, $p<0.001$) were significant factors in the model, but the interaction did not reach significance. Not surprisingly, the changes in trabecular number paralleled those measured in the BVF. There was a significant drop from 3 to 10 months in both strains with the C57Bl/6 starting much higher (Figure 3.15 – C).

General Linear Models: Tibia

The linear model was significant for tibial tBMD ($R^2=0.792$, $p<0.001$). Strain ($R^2=0.510$, $p<0.001$) and age ($R^2=0.661$, $p<0.001$) were significant factors, as was the interaction between strain and age ($R^2=0.157$, $p<0.001$). The C57Bl/6 and CBA/J slopes from 3 to 18 months differed ($p<0.001$) with much of the divergence occurring in the interval between 3 and 14 months ($p=0.043$). Both strains experienced a drop in tibial tBMD from 3 to 10 months but only the C57Bl/6 strain lost further tBMD from 10 to 14 months, leading to a relatively greater loss in tBMD by 18 months for the C57Bl/6 mice than the CBA/J mice. This was consistent with the changes occurring in the femoral trabecular compartment (Figure 3.16 – A).

The model applied to tTMD was not significant ($p=0.128$). This is due to the lack of variability between strains as well as between ages within both strains (Figure 3.16 – B). The model run for BVF was significant ($R^2=0.855$, $p<0.001$). Strain ($R^2=0.594$, $p<0.001$), age ($R^2=0.724$, $p<0.001$), and the interaction term ($R^2=0.322$, $p<0.001$) were all significant factors. The slopes of the two strains differed from 3 to 18 months ($p<0.001$), with the most divergence occurring between 3 and 10 months ($p=0.001$). This pattern of change coincides with that measured in the femur (Figure 3.16 – C).

The overall model for BS/BV was significant ($R^2=0.568$, $p<0.001$). All three factors were significant – strain ($R^2=0.298$, $p<0.001$), age ($R^2=0.254$, $p<0.001$), and the interaction ($R^2=0.220$, $p<0.001$). The overall rate of change from 3 to 18 months differed between the two strains

($p<0.001$). Significant divergence of the slopes occurred in the 3 to 10 month interval ($p=0.001$) and the 14 to 18 month interval ($p=0.001$) (Figure 3.17 – A).

The model was significant when run for trabecular thickness ($R^2=0.215$, $p=0.002$). Strain was not a significant factor, but both age ($R^2=0.109$, $p=0.014$) and the interaction were ($R^2=0.113$, $p=0.011$). The amount of change differed from 3 to 18 months when comparing the two strains ($p=0.002$). The most divergence of slope occurred in the 3 to 10 month interval ($p=0.032$) and the 14 to 18 month interval ($p=0.054$). The C57Bl/6 trabecular thickness decreased from 3 to 10 months, increased from 10 to 14 months, and decreased from 14 to 18 months. The CBA/J pattern is reverse where the mean increased from 3 to 10 months, decreased from 10 to 14 months, and increased from 14 to 18 months. This resulted in an overall loss of thickness in the C57Bl/6 mice and no change in the CBA/J mice (Figure 3.17 – B).

The model for trabecular number was significant with $R^2=0.903$ ($p<0.001$). Strain ($R^2=0.714$, $p<0.001$), age ($R^2=0.795$, $p<0.001$), and the interaction between strain and age ($R^2=0.392$, $p<0.001$) were all significant factors. The rate of change differed between the C57Bl/6 and CBA/J mice from 3 to 18 months ($p<0.001$). The slopes diverged in the 3 to 10 month interval ($p=0.005$) and 10 to 14 month interval ($p=0.039$). Like BVF patterns, the C57Bl/6 mice lost a significant number of trabeculae during the 3 to 10 month interval and again from 10 to 14 months. The rate at which CBA/J mice lost trabeculae was much slower from 3 to 10 months and then stayed constant from 10 months on (Figure 3.17 – C).

One interesting aspect of the trabecular regions of the C57Bl/6 and CBA/J mice concerned BMD and TMD when regressed against weight. The tBMD-weight regression in the femur was significant for the C57Bl/6 mice ($R=-0.296$, $R^2=0.09$, $p=0.043$) but not for the CBA/J mice (Figure 3.18 – A). The tTMD-weight regression was not significant in the C57Bl/6 mice, but was in the CBA/J mice ($R=0.369$, $R^2=0.142$, $p=0.012$) (Figure 3.18 – B). The same pattern was recorded in the tibiae where tBMD-to-weight regression was significant in the C57Bl/6 mice ($R=-0.309$, $R^2=0.095$, $p=0.033$), but not in the CBA/J mice (Figure 3.18 – C). The regression between tTMD and weight in the tibia was not significant for the C57Bl/6 mice but was significant for CBA/J mice ($R=0.671$, $R^2=0.443$, $p<0.001$) (Figure 3.19 – D).

In both the femur and tibia, there was a pattern in which weight and tBMD were inversely related in the C57Bl/6 mice and unrelated in the CBA/J mice. Conversely, weight and tTMD were positively related in the CBA/J mice but unrelated in the C57Bl/6 mice. This suggests that as weight increased in the C57Bl/6 mice, there was a negative effect on the amount of bone in the trabecular region but not on the mineralization of bone present. This was supported by the negative relationship between weight and BVF in the C57Bl/6 femora ($R=-0.486$, $p=0.001$) and tibiae ($R=-0.430$, $p=0.002$). In the CBA/J mice, as weight increased, there was no change in tBMD, despite the negative relationship between weight and BVF in both the femora ($R=-0.575$, $p<0.001$) and tibiae ($R=-0.422$, $p=0.001$). There was, however, a positive relationship in CBA/J mice between weight and tTMD.

Trabecular and Cortical Relationships

In the C57Bl/6 femora, stiffness was linearly related to tTMD ($R^2=0.299$, $p<0.001$), BVF ($R^2=0.101$, $p=0.032$), and trabecular thickness ($R^2=0.255$, $p<0.001$), but not to anisotropy or trabecular number. Trabecular TMD was not linearly related to cortical geometry, therefore, the stiffness-tTMD relationship was likely due to mineralization of the cortical region. Further supporting this relationship, regression between tTMD and cortical TMD was significant ($R^2=0.319$, $p<0.001$). These relationships suggest that as TMD decreased with age in the cortical compartment, it also decreased in the trabecular region of the femur.

The stiffness of the CBA/J femora did not change with tTMD, anisotropy, trabecular thickness, or trabecular number. However, there was a negative relationship between cortical stiffness and BVF ($R^2=0.108$, $p=0.026$). As stiffness increased, the volume of trabecular bone was decreasing. Differing from C57Bl/6 mice, the BVF of CBA/J mice was inversely related to the I_y ($R^2=0.253$, $p<0.001$) and positively related to cortical TMD ($R^2=0.212$, $p<0.001$). It is possible that aging induced the reduction in trabecular volume and bone mineralization in order to allocate resources to the periosteal bone apposition to maintain ultimate load.

Discussion

The C57Bl/6 and CBA/J mouse strains demonstrate that variation is present in murine aging. C57Bl/6 mice experience a steady decline in ultimate load and stiffness after 10 months. Which is in line with other findings [1]. The drop in ultimate load in the C57Bl/6 femora is primarily due to cortical thinning through marrow expansion without adequate periosteal deposition, as well as reduced tissue mineralization. These changes, in combination, reduce the stiffness. In addition to the mineral and shape changes, there are matrix composition alterations that negatively affect the post-yield properties. Unlike the C57Bl/6 femoral patterns, the tibial decrease in ultimate load is independent of changes to stiffness. The lack of change in stiffness is suggestive of matrix compositional and organizational changes reducing bone strength in the tibia.

The CBA/J strain does not elicit changes in ultimate load or stiffness in 18 months. The femora of CBA/J mice do not undergo dramatic functional change with age. The consistent mechanical properties are due to a rearrangement of tissue to increase I_y , compensating for loss of mineralization and marrow expansion. In the normalized values, there does not appear to be a dramatic increase in the periosteal surface to account for the increase in I_y . However, when the raw values are compared, the 18-month periosteal length is almost double the 3-month mean. The CBA/J mice are able to respond to increasing body size through periosteal expansion. The loss of significance when normalized to weight suggests that periosteal deposition is occurring in order to adapt to increased load from the mouse body. Instead of shape change in order to compensate for a loss of TMD, it is possible that the weight-induced periosteal deposition allows the body to redirect mineral resources without compromising bone mechanical function.

Both strains experience a drop in tissue mineralization. Unique to the CBA/J is the increase in the moment of inertia. The shape changes in the CBA/J mice prevent the loss of stiffness and ultimate load that is evident in the C57Bl/6 mice. The initial cross-section of the C57Bl/6 femur is wide and thin, some might say robust. The cross-sectional geometry of the CBA/J femur is thick and more concentrated near the centroid. Due to differences in geometry, there is greater surface area for endosteal resorption in the C57Bl/6 mice than in the CBA/J mice. Additionally, bone resorption on the endosteal surface of C57Bl/6 will have a greater

influence on moment of inertia due to the greater distance from the centroid. More slender bones in the CBA/J mice may be suppressing remodeling while the more robust C57Bl/6 bones are not [2]. Differences in aging outcomes between the two strains could be a product of bone phenotype upon reaching maturity. This is true in human aging, as well. Peak bone mass is a strong determinant of fracture risk later in life [3]. Due to this similarity between human and mouse aging, comparative studies using the two mouse strains may be helpful in optimizing prevention strategies for a wide range of people with varying bone morphology.

There is a high amount of phenotypic integration in patterns of bone aging [1] including a relationship between age-induced morphology changes and age-induced composition changes in bone. Jepsen and Andarawis-Puri describe the relatedness between changes in tissue modulus and those in geometry in human tibiae. Individuals with greater loss of tissue modulus with age elicit greater periosteal bone apposition [5]. In the mouse strains described in this chapter, tissue modulus was not directly measured. However, bone mineralization greatly influences modulus. In the C57Bl/6 femora, the 18-month mean cortical TMD was 9% lower than the mean at 3 months. This is in contrast to reports showing an increase in TMD in C57Bl/6 males [6]. The discrepancy may be in the inaccuracy of TMD estimates using microCT. The difference in CBA/J represents a 16% lower mean. Cortical area is reduced with aging in the C57Bl/6 strain but not in the CBA/J strain. It is possible that the phenomenon described in human bone is also present in mouse bone aging. The strain with greater loss of TMD maintains cortical area through periosteal deposition while the strains with less severe TMD loss experiences cortical area reduction.

How direct the relationship between TMD and cortical area change is not clear. A possible explanation is that periosteal expansion is modulated to balance the loss of mechanical integrity that results from the lower mineralization. This suggests differential mechanical response in bones that lose more mineral with aging compared with those that have a less dramatic loss of mineral. Conversely, it is possible that the maintenance of cortical area and increase of moment of inertia in the CBA/J mice allows for redirection of expensive resources. Due to the greater mechanical stability these shape changes provide, mineral may not be as necessary to maintain function. Better resolution in the timing of mineral decrease and shape

change may provide insight as to which parameter change precedes the other. The CBA/J femur increases I_y by 10 months. The difference in TMD is not significant until the 18-month time point. The relationship between the timing of these changes suggests that shape change may be a permissive change allowing for reallocation of mineral in the aging animal.

Some of the most frequent sites of fragility fracture occur in trabeculated regions of bones. Therefore, it is important to include the changes that occur to the trabecular bone in the two strains. Compressive tests on the trabecular bone was not possible, therefore, we cannot make direct relationships between the trabecular changes and how these influence whole-bone functionality. Further work including mechanical testing of the trabecular region is necessary to fully understand how age is altering function and the interplay between mechanics of the cortical region and those of the trabecular region.

Age-related changes in mineralization are not uniform throughout the bone. In the sample studied, C57Bl/6 trabecular bone loses TMD with age while the CBA/J bone does not. In the cortical compartments, both strains lose mineral density in the older ages. The loss of mineralization may be an artifact of porosity in the bone. Ashing the bones will help determine if the changes in TMD are real or due to increase in porosity. Assuming ashing reveals the mineralizing decline is real, the C57Bl/6 strategy may be to distribute the demand for limited resources between the cortical and trabecular compartments. The geometry of the C57Bl/6 cortical bone limits the ability to lose large amounts of mineral and still maintain functionality. The CBA/J mechanical integrity is less prone to the loss of mineralization in the cortical region due to shape and size. However, the amount of bone in the trabecular region of CBA/J mice is much lower than that in C57Bl/6 mice. Thus, TMD is only lost from CBA/J cortical bone since extraction from the trabeculae would reduce stability of the trabecular region even more.

The interaction between cortical and trabecular bone is supported by the fact that loss of BVF in the trabecular bone is associated with periosteal expansion in humans [2]. However, of the two mouse strains, both of which lose BVF, only the CBA/J has an associated increase of moment of area. Periosteal expansion, after normalizing for weight, did not demonstrate significant differences. However, using the raw values, there is a 19% increase in the CBA/J femora and a 6% increase in C57Bl/6. Since BVF loss is greater in CBA/J bones, the greater

periosteal expansion demonstrates that variation in mouse bone aging may be regulated in a similar manner as human bone. This pattern integrates changes in the cortical and trabecular bone to satisfy mechanical and resource demands.

Aging changes in the cortical bone mechanical properties are similar in the femur and tibia for both strains. The cortical morphology of the femur and tibia also change in a similar pattern and degree. Age-related loss in trabecular bone is analogous in the C57Bl/6 mice except for a greater degree of TMD loss in the femur than tibia (19% vs. 9%). In the CBA/J mice, the only deviation from the femur patterns of change occurs in the trabecular thickness. There is a 16% decrease in trabecular thickness in the femur and an insignificant difference in the tibia. Overall, both strains seem to share patterns of bone aging between the femur and tibia.

Models for Human Aging

The general trend of bone aging in humans can be described as increased fragility and greater risk of fracture. However, not all individuals undergo these changes [8]. The C57BL/6, vis-à-vis cortical strength and stiffness, is more analogous to the aging patterns in the at-risk aging population (more common in women). CBA/J mice do not appear to lose mechanical integrity by 18 months, potentially making a good model for successful bone aging without increase in risk of failure (more common in men).

Persons considered at greater risks of sustaining a fragility fracture reach this state through a combination of material and morphological changes. The combination of marrow expansion, periosteal expansion, increase in tissue mineralization, and cortical thinning are determine how well the bone maintains strength. Most individuals experience some degree of marrow expansion and increased tissue mineralization [8, 9]. However, variation in functional outcomes is derived from variation in accompanying periosteal expansion. Men are more able to maintain bone strength because of periosteal deposition leading to increased second moment of inertia [5, 8, 9]. The CBA/J male mice demonstrate similar periosteal bone growth, while C57Bl/6 male mice do not. This further supports the use of CBA/J as a correlate for the successful aging often seen in men and of C57Bl/6 as a correlate for potentially problematic bone aging.

Men and women both lose trabecular bone volume during aging progression [9, 10], though it is more extreme in some women. Furthermore, women tend to lose trabecular number and men lose trabecular thickness [11]. The relative trabecular BVF lost with age is similar in the tibia of the two strains. However, there is greater relative loss of BVF in the CBA/J femur compared to the C57Bl/6 mice. The decrease in trabecular number is much greater in the CBA/J femur and tibia (75% and 67%) than the C57Bl/6 femur and tibia (60% and 58%). Trabeculae are thinner in the femora of both strains, but only C57Bl/6 lost trabecular thickness in the tibia. This is consistent with previous findings that C57Bl/6 males are more prone to loss in number of trabeculae rather than thickness of those present [9, 10]. These findings suggest that C57Bl/6 trabecular aging occurs in a more male-like fashion. The CBA/J patterns of trabecular loss is more aligned with those observed in women.

The patterns of bone aging in humans and those described here demonstrate that C57Bl/6 male mice are a good model for poor cortical aging but more successful trabecular aging. Conversely, CBA/J male mice are a good analog for successful cortical aging and poor trabecular aging. We may be able to more accurately predict sites of fracture based on early bone morphology. If the two mouse strains presented are indicative of variation in humans, it is reasonable to suggest that individuals with thicker cortices and undergo periosteal expansion, are at greater risk of fractures located in the trabecular regions. Meanwhile, individuals with thinner, cortices with no periosteal expansion with age are at greater risk for diaphyseal fractures.

The patterns of bone aging described here, while illuminating, are phenomenological. Despite the evident difference in bone aging strategies, these data cannot conclusively inform us as to the physiological mechanisms underlying the variable patterns. Having established the utility of comparing the inbred strains, we can begin to investigate the ultimate causes that yield aging variation.

References: Chapter III

- [1] L. Meakin, G. Galea, T. Sugiyama, L. Lanyon and J. Price, "Age-related impairment of bones' adaptive response to loading in mice is associated with sex-related deficiencies in osteoblasts but no change in osteocytes," *Journal of Bone and Mineral Research*, vol. 29, no. 8, pp. 1859-1871, 2014.
- [2] H. Goldman, N. Hampson, J. Guth and K. Jepsen, "Intracortical remodeling parameters are associated with measures of bone robustness," *Anatomical Record*, vol. 297, no. 10, pp. 1817-1828, 2014.
- [3] R. Heaney, S. Abrams, B. Dawson-Hughes, A. Looker, R. Marcus, V. Matkovic and C. Weaver, "Peak bone mass," *Osteoporosis International*, vol. 11, pp. 985-1009, 2000.
- [4] K. J. Jepsen, "Functional interactions among morphologic and tissue quality traits define bone quality," *Clinical Orthopaedic Related Research*, vol. 469, no. 8, pp. 2150-2159, 2011.
- [5] K. J. Jepsen and N. Andarawis-Puri, "The amount of periosteal apposition required to maintain bone strength during aging depends on adult bone morphology and tissue-modulus degradation rate," *Journal of Bone and Mineral Research*, vol. 27, no. 9, pp. 1916-1926, 2012.
- [6] B. Halloran, V. Ferguson, S. Simske, A. Burghardt, L. Venton and S. Majumdar, "Changes in bone structure and mass with advancing age in the male C57Bl/6J mouse," *Journal of Bone and Mineral Research*, vol. 17, no. 6, pp. 1044-1050, 2002.
- [7] Y. Duan, X. Wang, A. Evans and E. Seeman, "Structural and biomechanical basis of racial and sex differences in vertebral fragility in Chinese and Caucasians," *Bone*, vol. 36, pp. 987-998, 2005.
- [8] C. Ruff and W. Hayes, "Sex differences in age-related remodeling of the femur and tibia," *Journal of Orthopaedic Research*, vol. 6, pp. 886-896, 1988.
- [9] A. Parfitt, "Age-related structural changes in trabecular and cortical bone: cellular mechanisms and biochemical consequences," *Calcified Tissue International*, vol. 36, no. Supp1, pp. S123-127, 1987.
- [10] S. Garn, T. Sullivan, S. Decker, F. Larkin and V. Hawthorn, "Continuing bone expansion and increasing bone loss over a two decade period in men and women from a total community sample," *Journal of Human Biology*, vol. 4, pp. 57-67, 1992.
- [11] S. Khosla, B. L. Riggs, E. J. Atkinson, A. L. Oberg, L. J. McDaniel, M. Holets, J. M. Peterson and L. J. Melton III, "Effects of sex and age on bone microstructure at the ultradistal radius: a population-based noninvasive in vivo assessment," *Journal of Bone and Mineral Research*, vol. 21, no. 1, pp. 124-131, 2006.

Figures: Chapter III

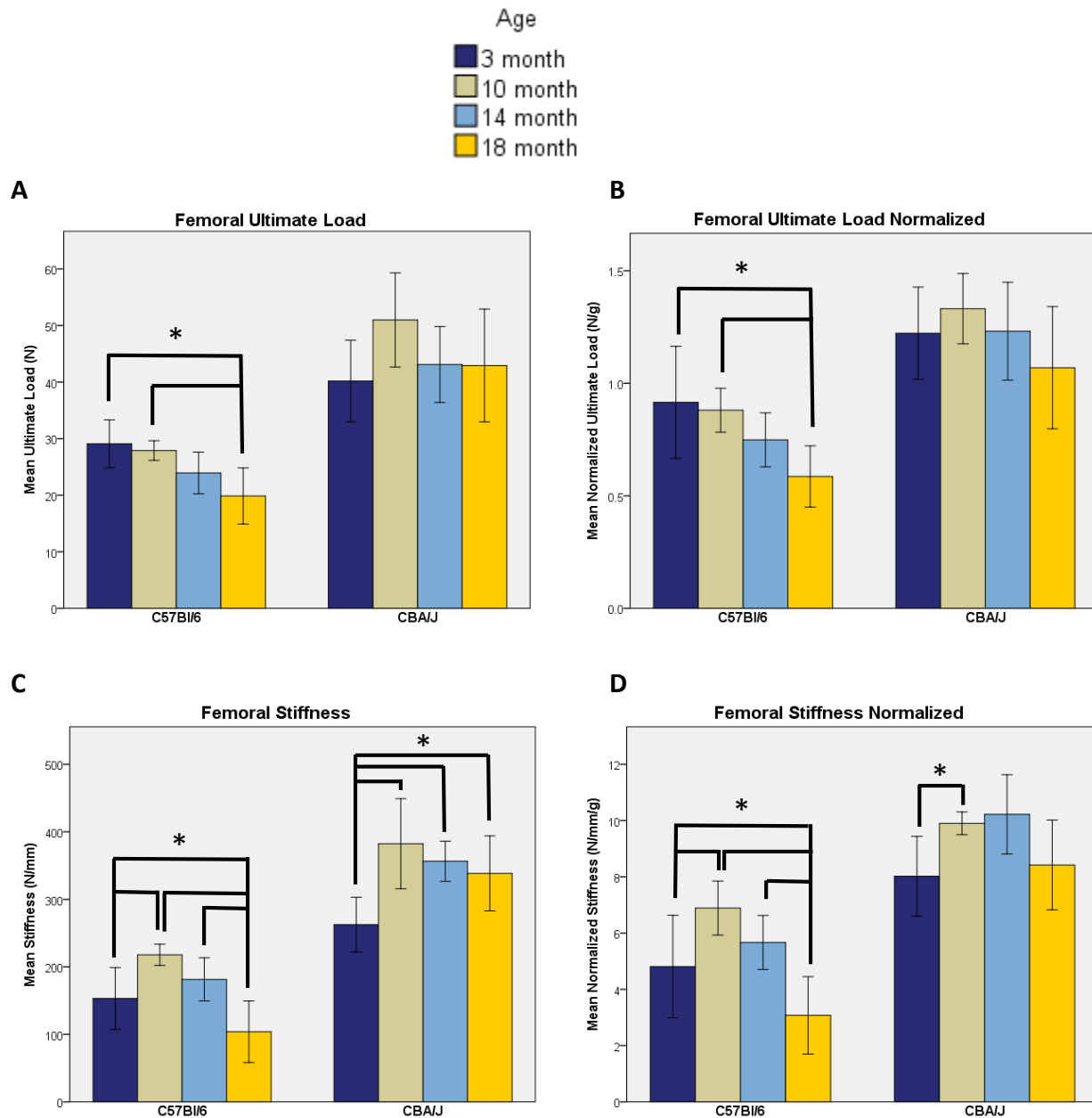


Figure 3. 1 - Femoral mechanical properties.

Results from 4-point testing of the femur in C57Bl/6 and CBA/J mice. **A)** Mean ultimate load (N) values at 3, 10, 14, and 18 months. Mean C57Bl/6 values are 29.09 (± 4.23) N at 3 months, 27.9 (± 1.74) N at 10 months, 23.93 (± 3.69) N at 14 months, and 19.87 (± 4.96) N at 18 months. The overall ANOVA is significant ($p < 0.001$). The 18-month mean is 32% lower than 3-month ($p < 0.001$) and 29% lower than the 10-month means ($p < 0.001$). The means for CBA/J are 40.19 (± 7.22) N at 3 months, 50.98 (± 8.317) N at 10 months, 43.11 (± 6.71) N at 14 months, and 42.92 (± 9.96) N at 18 months. ANOVA shows no difference between the CBA/J means ($p = 0.099$). **B)** Mean ultimate load normalized by weight. Significance of ANOVA results are no different for either C57Bl/6 or CBA/J when using normalized instead of raw ultimate load values. **C)** Mean stiffness values for C57Bl/6 femora are 153.10 (± 45.84)

N/mm at 3 months, 217.93 (± 15.76) N/mm at 10 months, 181.45 (± 32.02) N/mm at 14 months, and 103.87 (± 45.62) N/mm at 18 months. The overall ANOVA is significant ($p < 0.001$) and the 10-month mean is 42% greater than the 3-month mean ($p < 0.001$). The 18-month mean stiffness is 32% lower than the 3-month mean ($p = 0.012$), 52% lower than the 10-month mean ($p < 0.001$), and 43% lower than the 14-month mean ($p = 0.008$). The mean stiffness of the CBA/J mice is 262.48 (± 50.66) N/mm at 3 months, 382.38 (± 66.80) N/mm at 10 months, 356.44 (± 29.73) N/mm at 14 months, and 338.43 (± 55.63) N/mm at 18 months. The general ANOVA is significant in the CBA/J femoral stiffness values ($p < 0.001$). The 3-month mean is 46% less than the 10-month mean ($p = 0.046$), 36% less than the 14-month mean ($p = 0.002$), and 29% less than the 18-month mean ($p < 0.001$). **D)** Mean stiffness values normalized by weight. ANOVA results do not change for the C57Bl/6 femora. The overall ANOVA remains significant for CBA/J normalized stiffness ($p = 0.006$). However, significant differences between 3- and 14-month means as well as the 3- and 18-month means are lost.

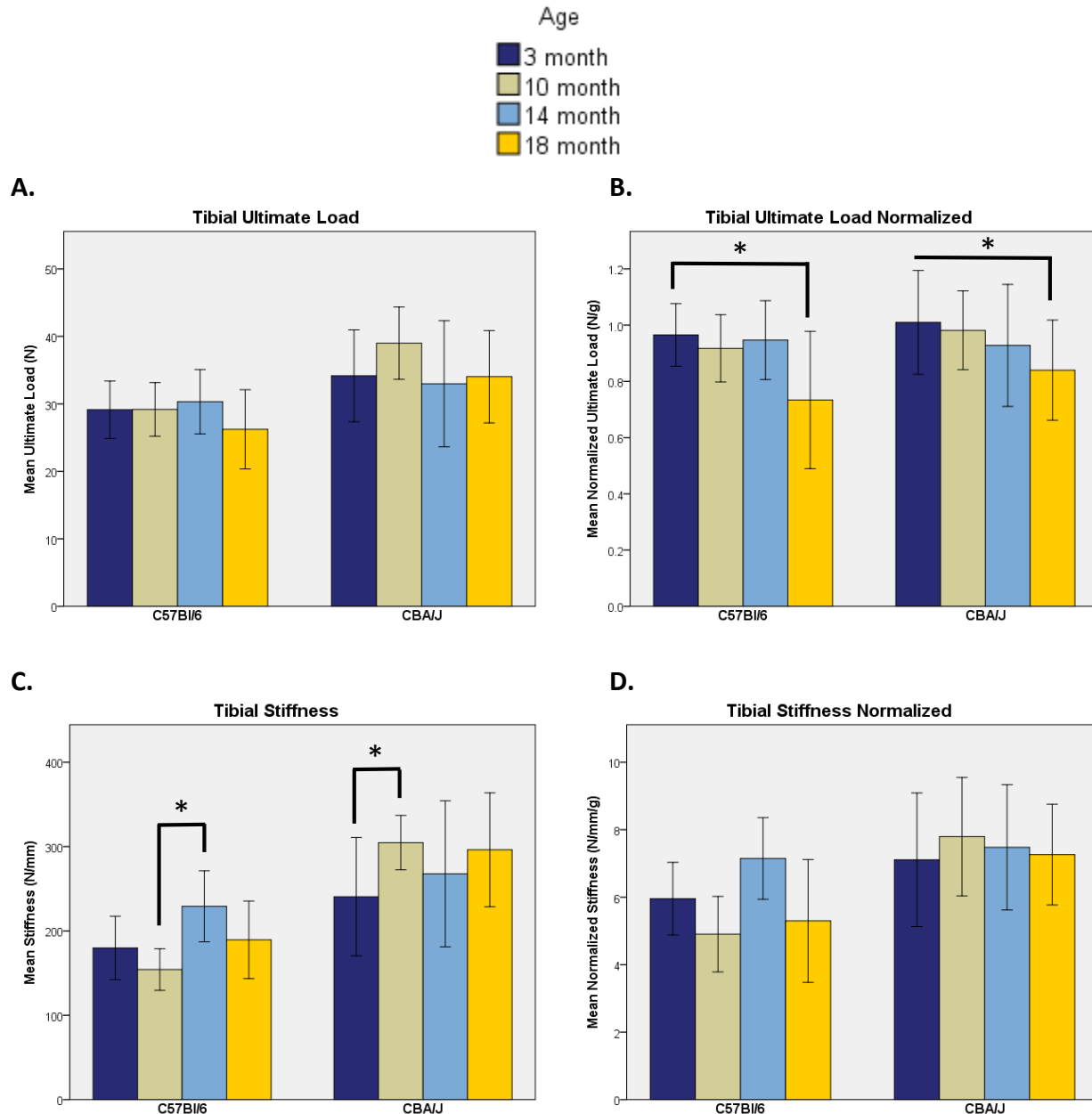


Figure 3. 2 - Tibial mechanical properties.

Results from 4-point testing of the tibia in C57Bl/6 and CBA/J mice for the 3-, 10-, 14-, and 18-month groups. **A)** Mean ultimate load (N) values in C57Bl/6 tibiae are 29.13 (± 4.26) N at 3 months, 29.17 (± 3.97) N at 10 months, 30.32 (± 4.77) N at 14 months, and 26.22 (± 5.87) N at 18 months. These values are not statistically different between age groups ($p=0.234$). The average ultimate load of the CBA/J tibiae is 34.15 (± 6.81) N at 3 months, 38.99 (± 5.35) N at 10 months, 32.98 (± 9.34) N at 14 months, and 34.02 (± 6.84) N at 18 months. ANOVA shows no difference between CBA/J means ($p=0.258$). **B)** Mean ultimate load normalized by weight. ANOVA results for C57Bl/6 tibia are now significant ($p=0.002$) with the 18-month mean being 20% less than the 3-month mean ($p=0.003$). Similarly, the ANOVA for CBA/J becomes significant ($p=0.029$) with the 18-month mean ultimate load being 16% less than the 3-month mean ($p=0.026$). **C)** Mean stiffness values (N/mm) for C57Bl/6 tibiae are 179.84 (± 37.66) N/mm at 3

months, 154.23 (± 24.64) N/mm at 10 months, 229.17 (± 42.12) N/mm at 14 months, and 189.41 (± 46.00) N/mm at 18 months. ANOVA is significant when comparing mean for C57Bl/6 ($p=0.039$). However, the only pair-wise comparison that is significant is the 10 month and 14 month difference ($p=0.047$). The mean stiffness of the CBA/J mice is 240.58 (± 70.20) N/mm at 3 months, 304.70 (± 32.26) N/mm at 10 months, 267.77 (± 86.57) N/mm at 14 months, and 296.20 (± 67.52) N/mm at 18 months. The overall ANOVA is significant ($p=0.034$) with a 10-month mean that is 27% greater than the 3-month mean stiffness ($p=0.012$). **D)** Mean stiffness values normalized by weight in C57Bl/6 remain significant ($p=0.030$), however, no pair-wise comparison between age groups is significant. The ANOVA loses statistical significance for CBA/J tibial stiffness differences when normalized to weight ($p=0.801$).

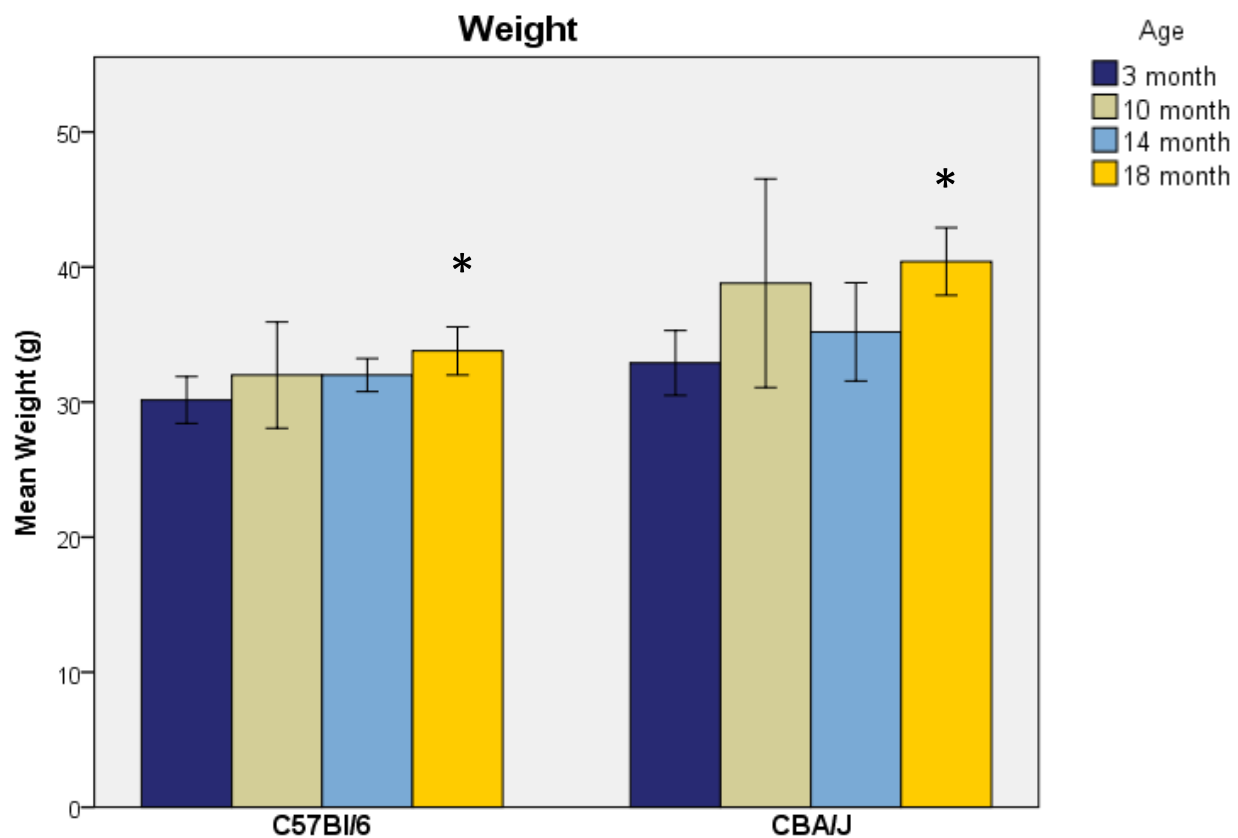


Figure 3. 3 - Average body weights in age groups.

Average body weights for C57Bl/6 are 30.16 (± 1.74) grams at 3 months, 32.00 (± 3.94) grams at 10 months, 32.00 (± 1.23) grams at 14 months, and 33.79 (± 1.78) grams at 18 months. The 18-month body weight is 12% greater than the 3-month group ($p<0.001$) in the C57Bl/6 mice. Average body weights for CBA/J are 32.88 (± 2.41) grams at 3 months, 39.60 (± 6.11) grams at 10 months, 35.20 (± 3.63) grams at 14 months, and 40.41 (± 2.51) grams at 18 months. The 18-month mice are 23% heavier than the 3-month mice ($p<0.001$). * Denotes significant difference to the 3-month mean.

Table 3. 1 - Mean values of mechanical measures in femur and tibia.

Mean values (\pm 1 standard deviation) are presented with the p -values for ANOVA tests.

		C57Bl/6 Means				p -value
		3-month	10-month	14-month	18-month	
Femur	Body Weight (g)	30.16 (\pm 1.74)	32.00 (\pm 3.94)	32.00 (\pm 1.78)	33.79 (\pm 1.78)	<0.001
	Ultimate Load (N)	29.09 (\pm 4.23)	27.9 (\pm 1.74)	23.93 (\pm 3.69)	19.87 (\pm 4.96)	<0.001
	Stiffness (N/mm)	153.10 (\pm 45.84)	217.93 (\pm 15.76)	181.45 (\pm 32.02)	103.87 (\pm 45.62)	<0.001
Tibia	Ultimate Load (N)	29.13 (\pm 4.26)	29.17 (\pm 3.97)	30.32 (\pm 4.77)	26.22 (\pm 5.87)	0.234
	Stiffness (N/mm)	179.84 (\pm 37.66)	154.23 (\pm 24.64)	229.17 (\pm 42.12)	189.41 (\pm 46.0)	0.039
		CBA/J Means				p -value
		3-month	10-month	14-month	18-month	
Femur	Body Weight (g)	32.88 (\pm 2.41)	39.60 (\pm 6.11)	35.20 (\pm 3.63)	40.41 (\pm 2.51)	<0.001
	Ultimate Load (N)	40.19 (\pm 7.22)	50.98 (\pm 8.317)	43.11 (\pm 6.71)	42.92 (\pm 9.96)	0.099
	Stiffness (N/mm)	262.48 (\pm 50.66)	382.38 (\pm 66.80)	356.44 (\pm 29.73)	338.43 (\pm 55.63)	<0.001
Tibia	Ultimate Load (N)	34.15 (\pm 6.81)	38.99 (\pm 5.35)	32.98 (\pm 9.34)	34.02 (\pm 6.84)	0.258
	Stiffness (N/mm)	240.58 (\pm 70.20)	304.70 (\pm 32.26)	267.77 (\pm 86.57)	296.20 (\pm 67.52)	0.034

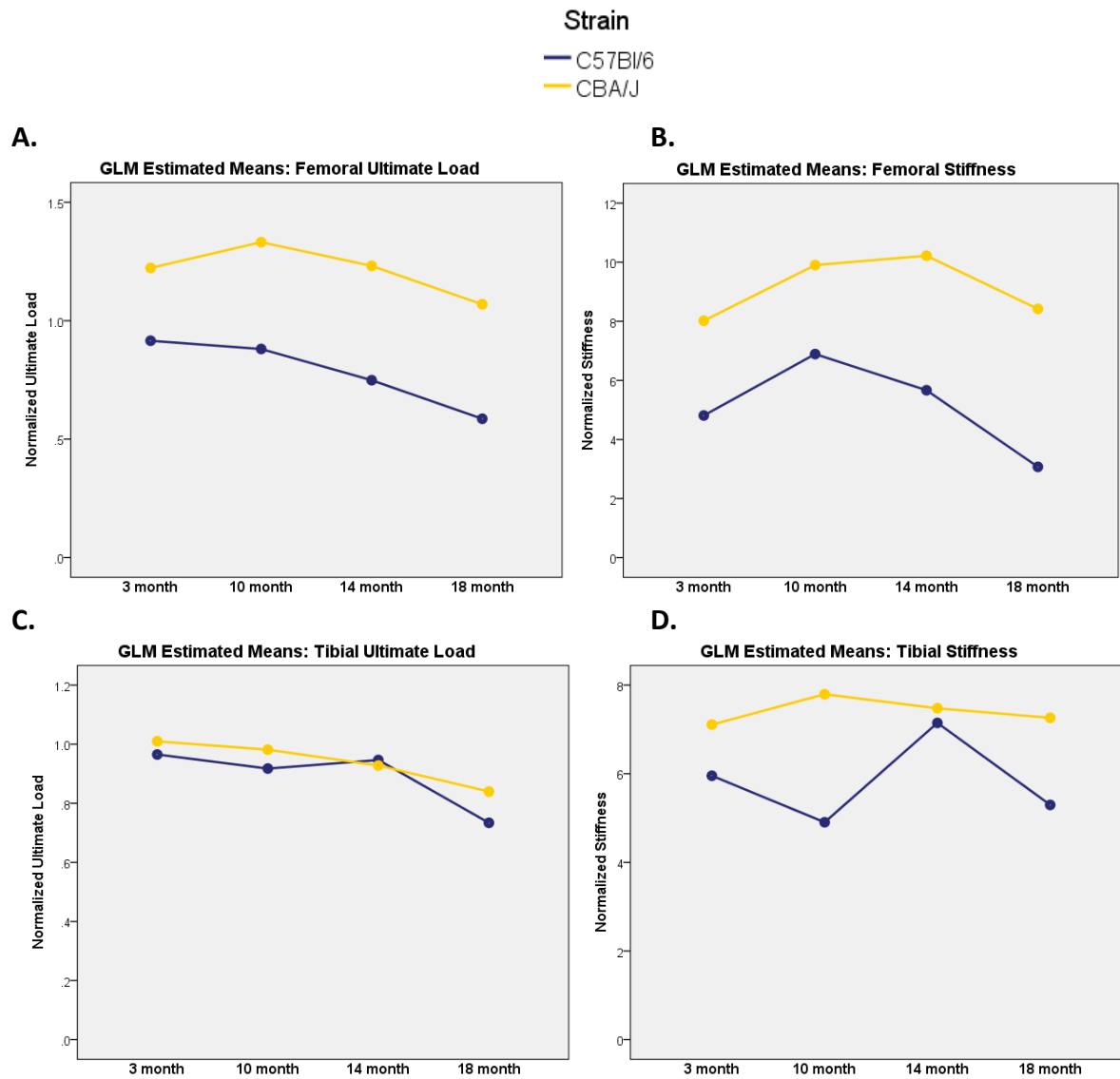


Figure 3. 4 - Graphical representations of general linear models of mechanical properties.

Estimated means of normalized ultimate load and stiffness values are plotted for both strains at 3, 10, 14, and 18 months for a general linear model age+strain+age*strain. **A)** Model for normalized femoral ultimate load is significant ($p<0.001$) with $R^2=0.594$. Strain affects outcome values with $R^2=0.435$ ($p<0.001$). Age affects outcome values with $R^2=0.254$ ($p<0.001$). The interaction term is not significant ($p=0.287$). **B)** Model for normalized femoral stiffness is significant with $R^2=0.733$ ($p<0.001$). Strain affects outcome values with $R^2=0.576$ ($p<0.001$). Age affects outcome values with $R^2=0.291$ ($p<0.001$). The interaction term is significant with $R^2=0.117$ ($p=0.012$). The slopes for C57Bl/6 and CBA/J mice are not distinct between 3 and 10 months ($p=0.854$), 10 and 14 months ($p=0.103$), or 14 and 18 months ($p=0.445$). However, slopes between 3 and 18 months are significantly divergent ($p=0.004$), as are the slopes between 10 and 18 months ($p=0.022$). **C)** Model for ultimate load in the tibia is overall significant ($p<0.001$) with $R^2=0.247$. Age is the only factor significantly influencing the outcome ($p<0.001$, $R^2=0.216$). The slopes are invariant between the strains at all age iterations. **D)** Model for tibial stiffness is overall significant ($p<0.001$) with $R^2=0.260$. Strain is the only factor significantly influencing the model ($p<0.001$, $R^2=0.151$). Slopes are invariant between C57Bl/6 and CBA/J.

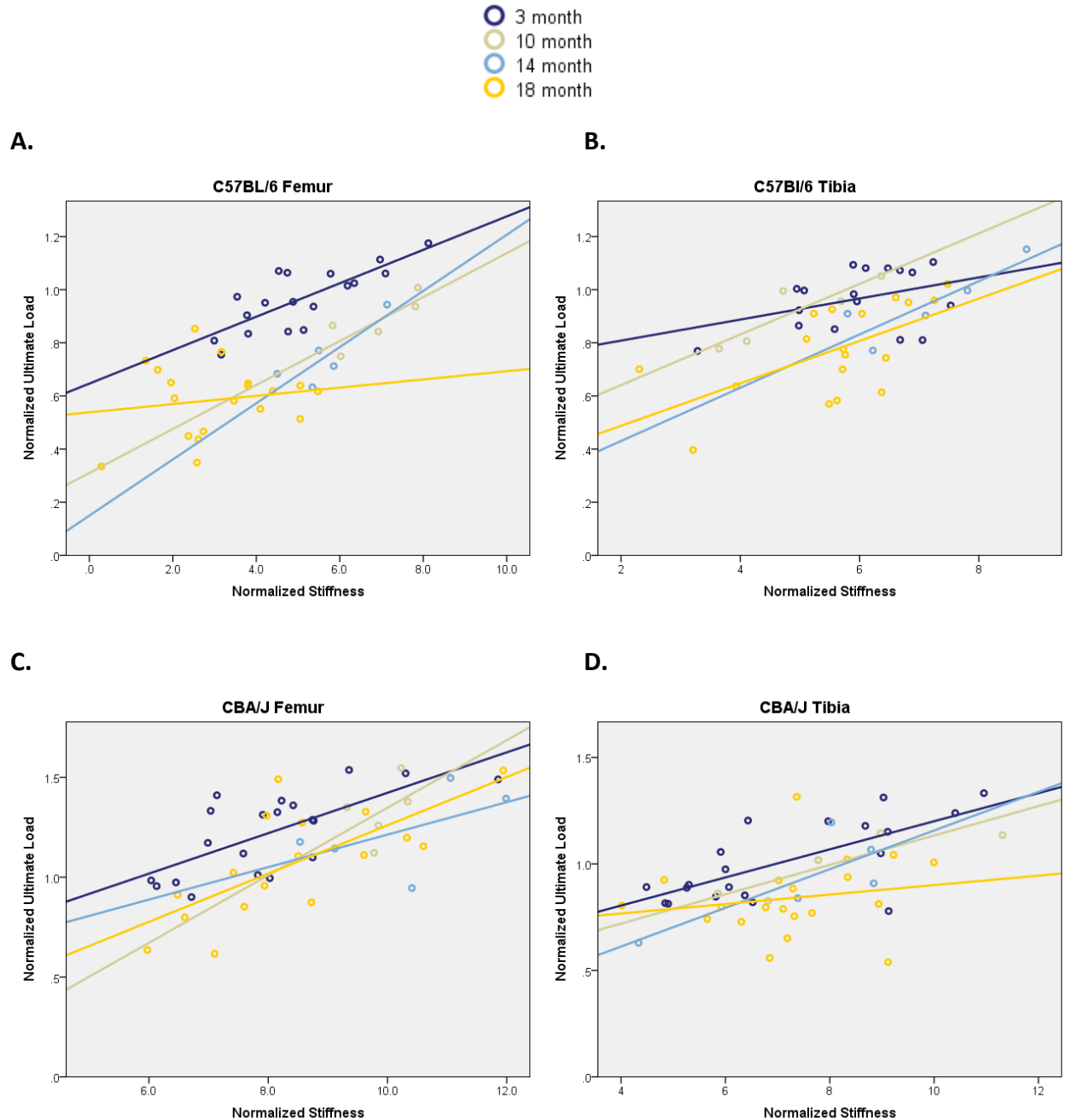


Figure 3. 5 - Linear relationships between stiffness and ultimate load in four age groups.

A) C57BL/6 femoral ultimate load is regressed with stiffness. Regressions are significant in the 3-month mice ($p < 0.001$, $R = 0.779$, $R^2 = 0.606$). Regressions near significance but may lack power in the 10-month ($p = 0.094$, $R = 0.813$, $R^2 = 0.661$) and 14-month mice ($p = 0.072$, $R = 0.844$, $R^2 = 0.713$). The relationship is not significant in the 18-month mice. **B)** Ultimate load of the C57BL/6 tibiae versus stiffness. The linear relationship is significant in the 3-month mice ($p = 0.035$, $R = 0.530$, $R^2 = 0.281$) and the 10-month mice ($p = 0.044$, $R = 0.889$, $R^2 = 0.790$). The 14-month relationship nears significance ($p = 0.059$, $R = 0.865$, $R^2 = 0.747$). The relationship is once again significant in the 18-month mice ($p = 0.007$, $R = 0.616$, $R^2 = 0.379$). **C)** Ultimate load versus stiffness in the CBA/J femora at the four different ages. Relationships are significant in the 3-month mice ($p = 0.001$, $R = 0.701$, $R^2 = 0.492$) and 18-month mice ($p = 0.001$, $R = 0.711$,

$R^2=0.506$). Due to lack of numbers, the 10-month and 14-month regressions are not significant. **D)** Regressions of tibial ultimate load versus stiffness. The relationship is significant in the 3-month ($p<0.001$, $R=0.708$, $R^2=0.501$) and 10-month ($p=0.003$, $R=0.864$, $R^2=0.746$) mice, but not in the 14- or 18-month groups.

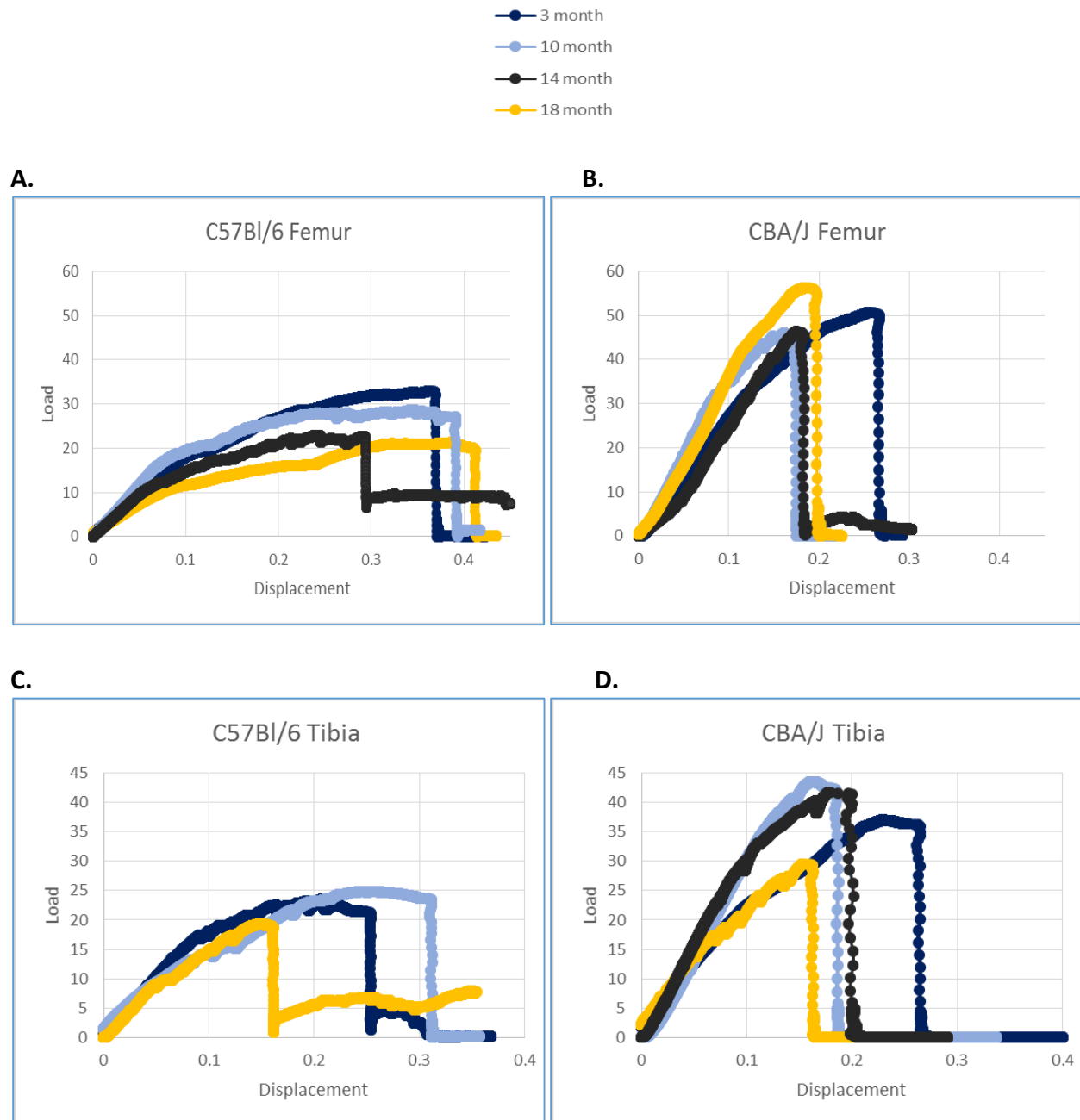


Figure 3. 6 - Representative load-displacement curves for 4-point bending in four age groups.

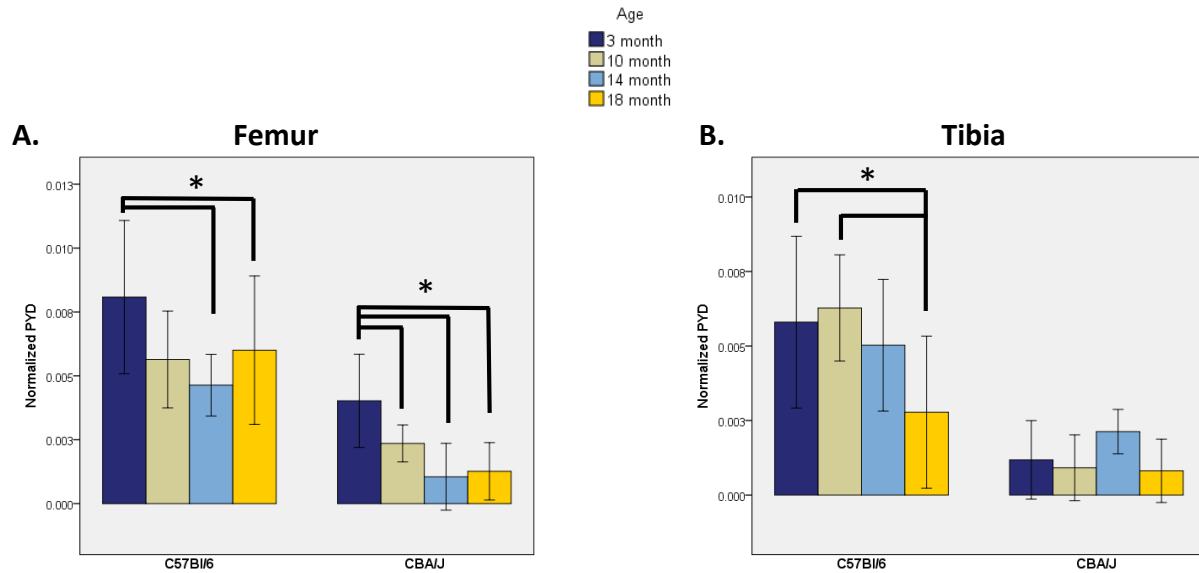


Figure 3. 7 - Post-yield displacement means from 4-point bending.

Bar graphs demonstrate the differences in mean values of each strain in each age group. **A)** Femoral post-yield deflection – PYD is significantly different in C57Bl/6 age groups ($p=0.004$). Compared to the 3-month mean, the 14-month mean is 46% lower ($p=0.001$) and the 18-month mean is 30% lower ($p=0.030$). Femoral PYD in the CBA/J age groups are different ($p<0.001$). Compared to the 3-month mean, the 10-month mice have 41% lower PYD ($p=0.024$), the 14-month mice have 74% lower PYD ($p=0.012$) and the 18-month mice have 69% lower PYD ($p<0.001$). **B)** Tibial PYD – PYD in the C57Bl/6 mice is different when comparing age groups ($p=0.009$). The 18-month mean is 49% lower than the 3-month mean ($p=0.022$) and 53% lower than the 10-month mean ($p=0.035$). The PYD means are not different when the CBA/J age groups are compared ($p=0.164$).

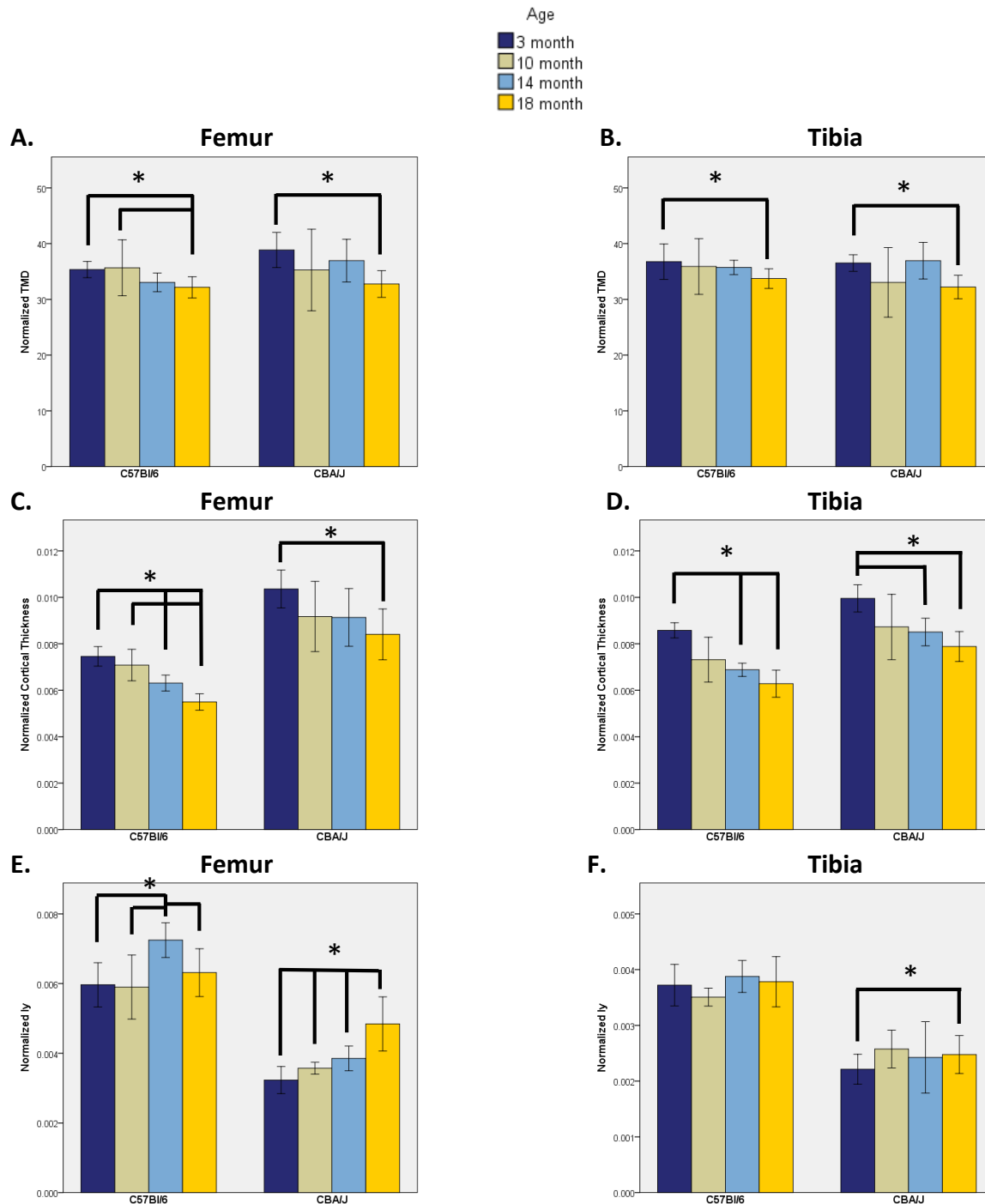


Figure 3. 8 - MicroCT parameters influencing mechanics.

Mineralization and shape parameters are reported in bar graphs. **A)** Femoral TMD – C57Bl/6 TMD means are significantly different between ages ($p < 0.001$) with the 18-month mean being 9% lower than the 3-month mean ($p < 0.001$) and 10% lower than the 10-month mean ($p = 0.018$). CBA/J TMD means are also significantly different between the age groups ($p < 0.001$), however the only significant pairwise comparison is the 16% greater mean in the 3-month mice compared to the 18-month mice. **B)** Tibial TMD – C57Bl/6 Tibial TMD is different when ages are compared ($p = 0.016$) with the 3-month mean being

8% greater than the 18-month mean ($p=0.006$). The CBA/J means are also different between ages ($p<0.001$), with the 3-month mean being 12% greater than the 18-month mean ($p<0.001$). **C)** Femoral cortical thickness – C57BL/6 cortical thickness is different when age groups are compared ($p<0.001$), with the 3-month mean being 15% greater than the 14-month mean ($p<0.001$) and 26% greater than the 18-month mean ($p<0.001$). The 10-month mean is 11% greater than the mean at 14 months ($p=0.035$) and 22% greater than the mean at 18 months ($p<0.001$). The 14-month mean is 13% greater than the 18-month mean ($p=0.002$). The CBA/J femoral cortical thickness means are different when the ages are compared ($p<0.001$) with the 3-month mean being 19% greater than the 18-month mean ($p<0.001$). **D)** Tibial cortical thickness – C57BL/6 age groups have differing mean cortical thickness ($p<0.001$). The 3-month mean is 20% greater than the 14-month mean ($p<0.001$) and 27% greater than the 18-month mean ($p<0.001$). Additionally, the 14-month mean is 9% greater than the 18-month mean ($p=0.026$). The CBA/J means are also different when the age groups are compared ($p<0.001$), with the 3-month mean being 15% greater than the mean at 14-months ($p=0.010$) and 21% greater than the mean at 18-months ($p<0.001$). **E)** Femoral I_y – C57BL/6 age groups have different means for second moment of inertia in the bending direction ($p=0.003$). The only significant differences are when the ages are compared to the spike in the 14-month mean which is 21% greater than the 3-month mean ($p=0.003$), 23% greater than the 10-month mean ($p=0.017$), and 14% greater than the 18-month mean ($p=0.052$). CBA/J means are also significantly different ($p<0.001$), with the 3-month mean being 11% less than the 10-month mean ($p=0.045$), 19% less than the 14-month mean ($p=0.045$), and 50% less than the 18-month mean ($p<0.001$). The 10-month mean is 36% less ($p<0.001$) and the 14-month mean is 26% less ($p=0.005$) than the 18-month mean. **F)** Tibia I_y – C57BL/6 mean values are invariant across age groups ($p=0.446$). However, the CBA/J means are different between the age groups ($p=0.045$), with the 3-month mean being 12% less than the 18-month mean ($p=0.047$).

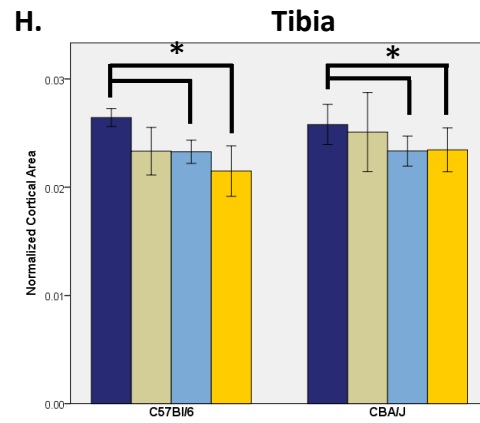
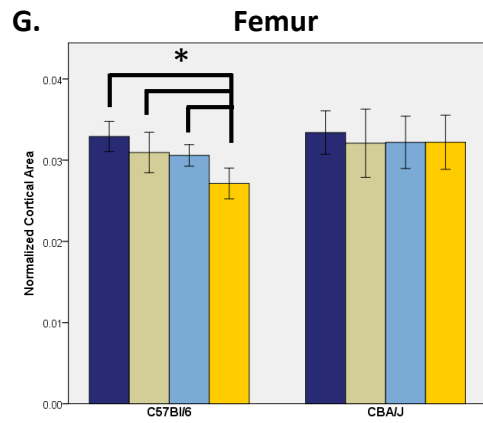
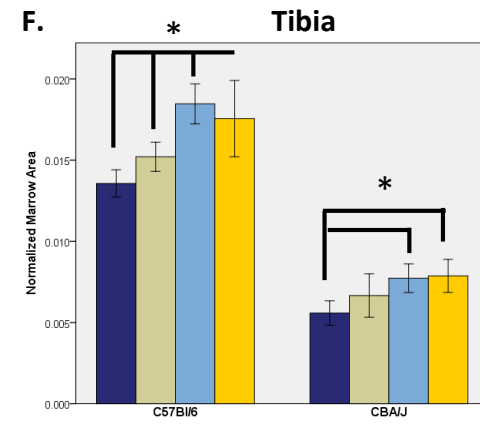
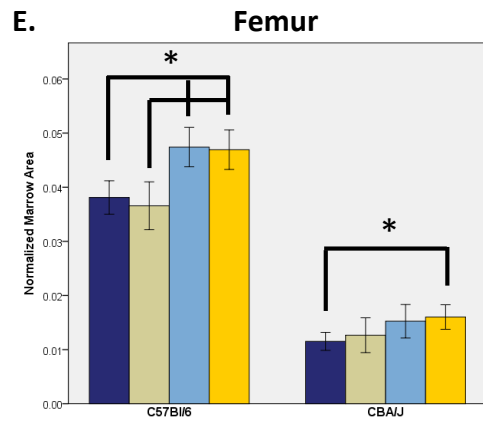
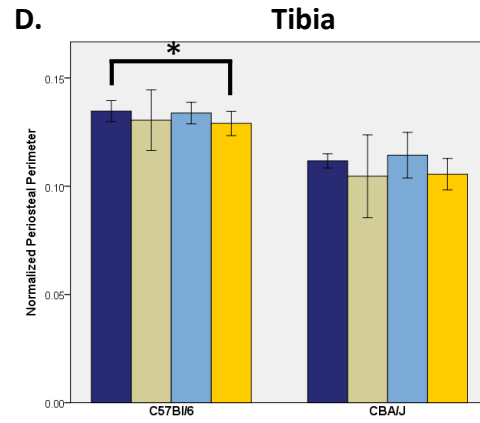
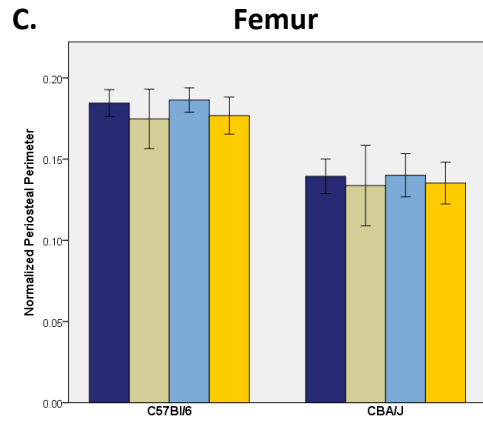
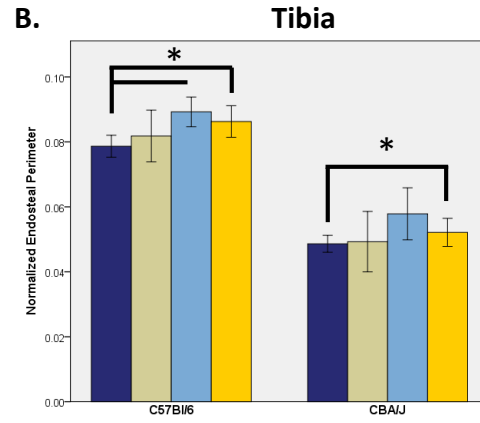
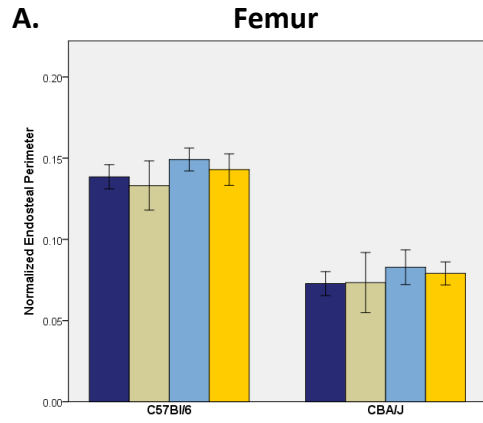


Figure 3. 9 - Cortical bone morphological measures in femur (left) and tibia (right).

Shape parameters are reported in bar graphs from microCT analysis. **A)** Femoral endosteal perimeter – C57Bl/6 means are different according to the overall ANOVA ($p=0.032$), however, none of the pairwise comparisons reached significance. CBA/J mean endosteal perimeter does not quite reach significance when comparing the age groups ($p=0.075$). **B)** Tibial endosteal perimeter – C57Bl/6 means are variant when ages are compared ($p<0.001$). The 3-month mean is 14% less than the 14-month mean ($p=0.016$) and 10% less than the 18-month mean ($p<0.001$). The age groups have different means in the CBA/J mice ($p=0.010$) with the 3-month mean being 7% smaller than the 18-month mean ($p=0.010$). **C)** Femoral periosteal perimeter – C57Bl/6 age groups do not have significantly different means ($p=0.066$). This is also the case in the CBA/J mice ($p=0.705$). **D)** Tibial periosteal perimeter – C57Bl/6 mean perimeter values differ between the age groups ($p<0.001$), with the 3-month mean being 4% greater than the 18-month mean ($p=0.010$). The CBA/J means are not statistically distinguishable ($p=0.141$). **E)** Femoral marrow area – C57Bl/6 means are different between age groups ($p<0.001$). The 3-month mean is 24% less than the 14-month mean ($p<0.001$) and 23% less than the 18-month mean ($p<0.001$). The 10-month mean is 30% lower than the 14-month mean ($p<0.001$) and 28% lower than the 18-month mean ($p<0.001$). The means in the CBA/J mice are also significantly different when comparing the age groups ($p<0.001$), where the 3-month mean is 39% lower than the 18-month mean ($p<0.001$). **F)** Tibial marrow area – C57Bl/6 means are different when age groups are compared ($p<0.001$). The 3-month mean is 12% lower than the 10-month mean ($p=0.039$), 36% lower than the 14-month mean ($p=0.001$), and 29% lower than the 18-month mean ($p<0.001$). The 10-month mean is 21% less than the 14-month mean ($p=0.007$) and 15% less than the 18-month mean ($p=0.012$). The CBA/J means are also significantly different ($p<0.001$). The 3-month mean is 38% lower than the 14-month mean ($p=0.012$) and 41% lower than the 18-month mean ($p<0.001$). **G)** Femoral cortical area – C57Bl/6 mean cortical area is different when comparing the age groups ($p<0.001$). The 18-month mean is 18% lower than the 3-month mean ($p<0.001$), 12% lower than the 10-month mean ($p=0.001$), and 11% lower than the 14-month mean ($p=0.005$). The femoral cortical area is invariant between the age groups of the CBA/J mice ($p=0.634$). **H)** Tibial cortical area – C57Bl/6 means are significantly different between the ages ($p<0.001$). The 3-month mean is 12% greater than the 14-month mean ($p=0.004$) and 19% greater than the 18-month mean ($p<0.001$). The CBA/J age groups have different means, as well ($p=0.007$). The 3-month mean is 9% larger than both the 14-month mean ($p=0.045$) and the 18-month mean ($p=0.003$).

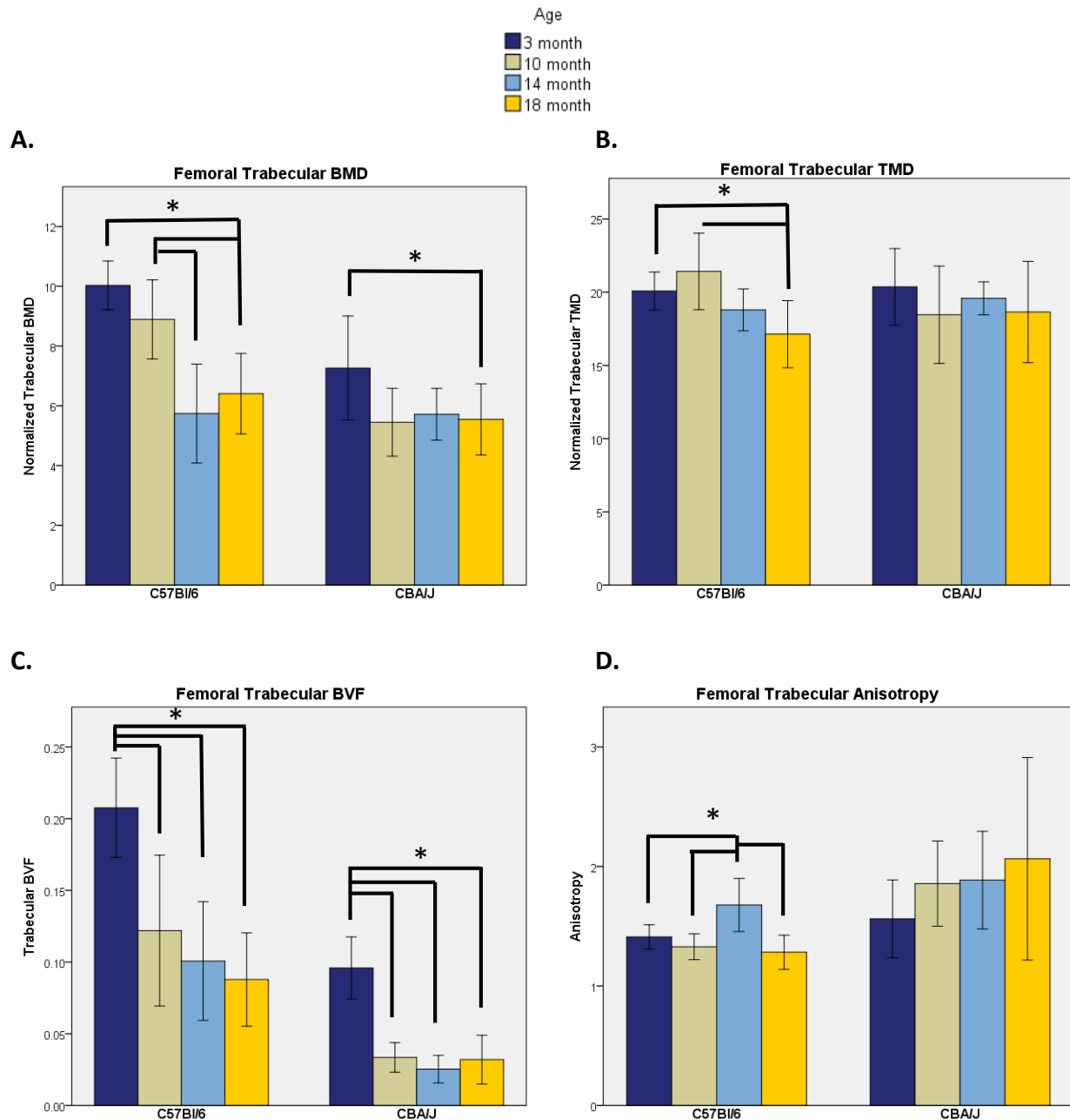
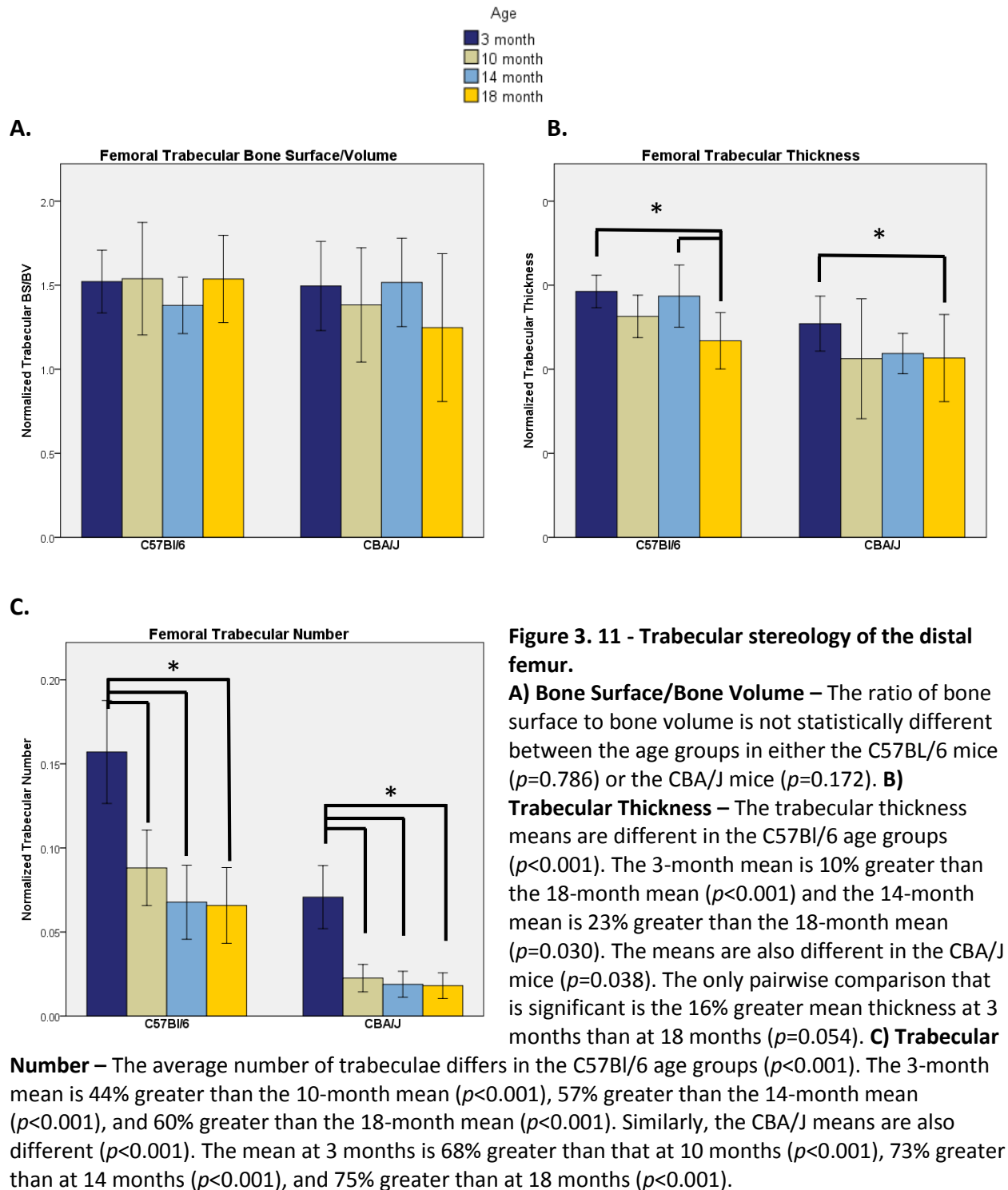


Figure 3. 10 - Trabecular properties of the distal femur.

MicroCT-based measures of the trabecular region in both C57Bl/6 and CBA/J mice in the four age groups. **A) Trabecular BMD** – Mean BMD is different when C57Bl/6 ages are compared ($p<0.001$). The 3-month mean is 43% greater than the 14-month mean ($p<0.001$) and 40% greater than the 18-month mean ($p<0.001$). The 10-month mean is 35% greater than the 14-month mean ($p=0.010$) and 32% greater than the 18-month mean ($p=0.003$). The mean BMD values in the CBA/J mice are also different ($p=0.003$) with the 3-month mean being 28% greater than the 18-month mean ($p=0.003$). **B) Trabecular TMD** – Mean TMD values differ when the C56Bl/6 age groups are compared ($p=0.001$). The 3-month mean is 19% greater than that at 18 months ($p=0.003$). The 10-month mean is 24% greater than that at 18 months ($p=0.012$). The means are not different in the CBA/J mice when comparing age groups

($p=0.207$). **C) Trabecular Bone Volume Fraction (BVF)** – Mean values of BVF are different in the C57Bl/6 mouse strain age groups ($p<0.001$). The 3-month mean is 41% greater than the 10-month mean ($p<0.001$), 52% greater than the 14-month mean ($p<0.001$), and 58% greater than the 18-month mean ($p<0.001$). The CBA/J age groups also differ in mean BVF ($p<0.001$) with the 3-month mean being 65% greater than the 10-month mean ($p<0.001$), 74% greater than the 14-month mean ($p<0.001$), and 67% greater than the 18-month mean ($p<0.001$). **D) Trabecular Anisotropy** – The age group means for anisotropy are overall significantly different ($p<0.001$), however, the only age that differs is the 14-month mean which is 19% greater than the 3-month mean ($p=0.012$), 26% greater than the 14-month mean ($p=0.004$), and 24% greater than the 18-month mean ($p<0.001$). Anisotropy is not different between the CBA/J age groups ($p=0.193$).



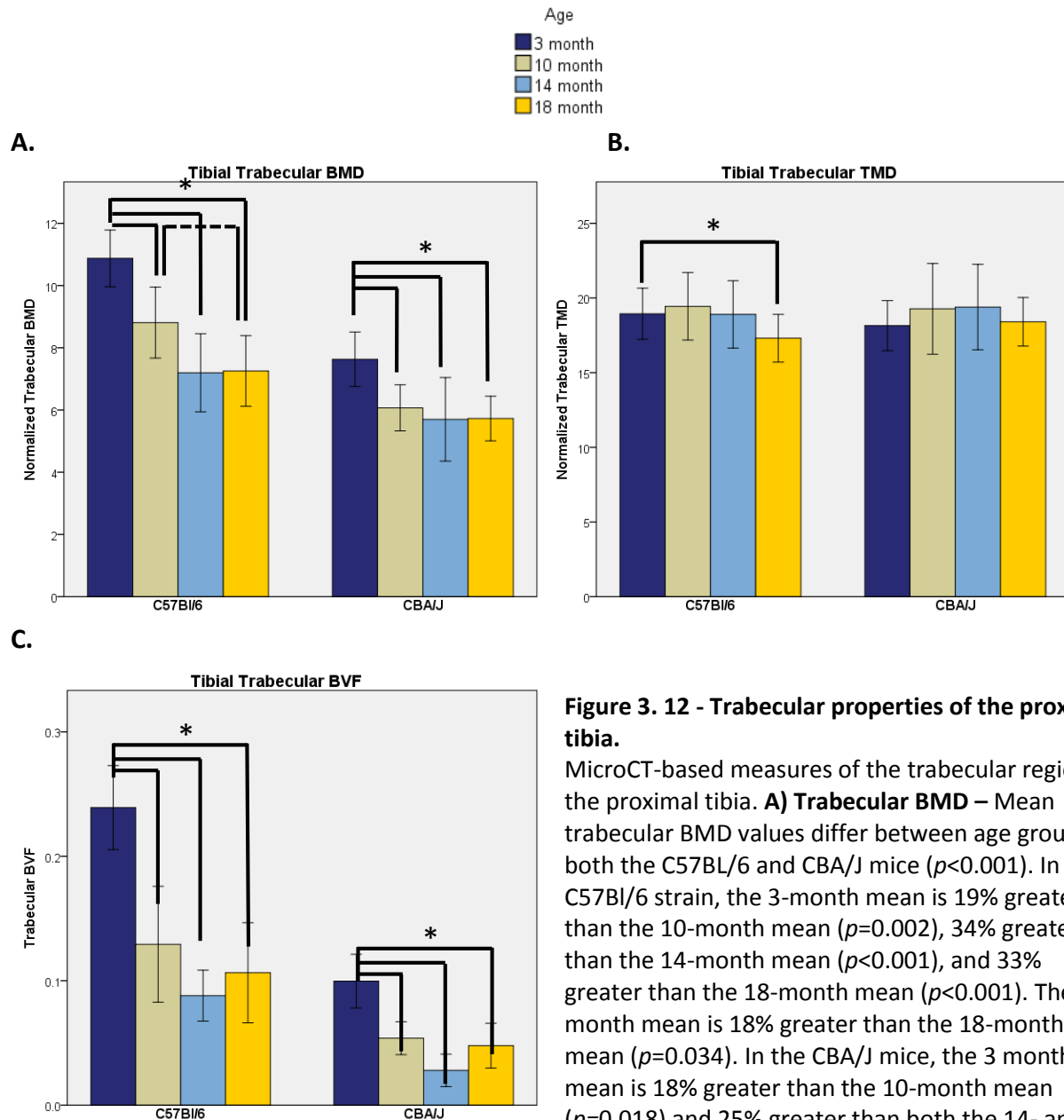


Figure 3. 12 - Trabecular properties of the proximal tibia.

MicroCT-based measures of the trabecular region of the proximal tibia. **A) Trabecular BMD** – Mean trabecular BMD values differ between age groups in both the C57BL/6 and CBA/J mice ($p < 0.001$). In the C57BL/6 strain, the 3-month mean is 19% greater than the 10-month mean ($p = 0.002$), 34% greater than the 14-month mean ($p < 0.001$), and 33% greater than the 18-month mean ($p < 0.001$). The 10-month mean is 18% greater than the 18-month mean ($p = 0.034$). In the CBA/J mice, the 3 month mean is 18% greater than the 10-month mean ($p = 0.018$) and 25% greater than both the 14- and

18-month means ($p < 0.001$). **B) Trabecular TMD** – Mean trabecular TMD values are different in the C57BL/6 mice ($p = 0.019$) but only a 9% greater mean in the 3-month mice compared to the 18-month mice ($p = 0.042$). CBA/J mice are invariant in mean TMD ($p = 0.252$). **C) Trabecular Bone Volume Fraction (BVF)** – The means for the age groups differ in both the C57BL/6 and CBA/J mice ($p < 0.001$). In the C57BL/6 mice, the 3-month mean is 46% greater than the 10-month mean ($p < 0.001$), 63% greater than the 14-month mean ($p < 0.001$), and 55% greater than the 18-month mean ($p < 0.001$). The CBA/J means follow a similar pattern with the 3-month mean being 46% greater than the 10-month mean ($p < 0.001$), 72% greater than the 14-month mean ($p < 0.001$), and 52% greater than the 18-month mean ($p < 0.001$).

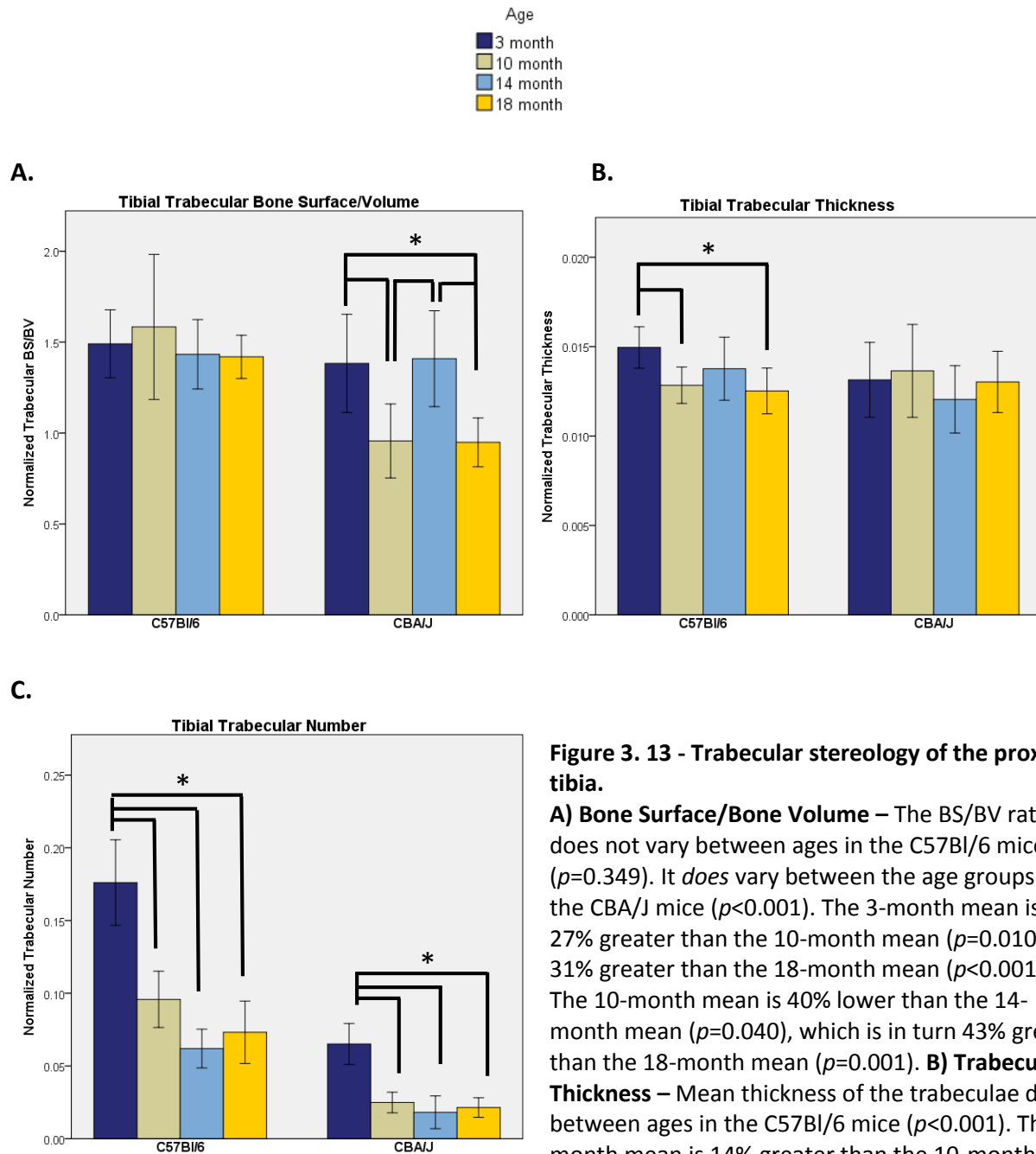


Figure 3. 13 - Trabecular stereology of the proximal tibia.

A) Bone Surface/Bone Volume – The BS/BV ratio does not vary between ages in the C57Bl/6 mice ($p=0.349$). It *does* vary between the age groups of the CBA/J mice ($p<0.001$). The 3-month mean is 27% greater than the 10-month mean ($p=0.010$) and 31% greater than the 18-month mean ($p<0.001$). The 10-month mean is 40% lower than the 14-month mean ($p=0.040$), which is in turn 43% greater than the 18-month mean ($p=0.001$). **B) Trabecular Thickness** – Mean thickness of the trabeculae differ between ages in the C57Bl/6 mice ($p<0.001$). The 3-month mean is 14% greater than the 10-month

mean ($p=0.011$) and 16% greater than the 18-month mean ($p<0.001$). Trabecular thickness does not differ between the age groups in CBA/J mice ($p=0.413$). **C) Trabecular Number** – Both strains have difference in trabecular number when age groups are compared ($p<0.001$). The C57Bl/6 3-month mean is 46% greater than the 10-month mean ($p<0.001$), 65% greater than the 14-month mean ($p<0.001$), and 58% greater than the 18-month mean ($p<0.001$). The CBA/J 3-month mean is 60% greater than the 10-month mean ($p<0.001$), 68% greater than the 14-month mean ($p<0.001$), and 67% greater than the 18-month mean ($p<0.001$).

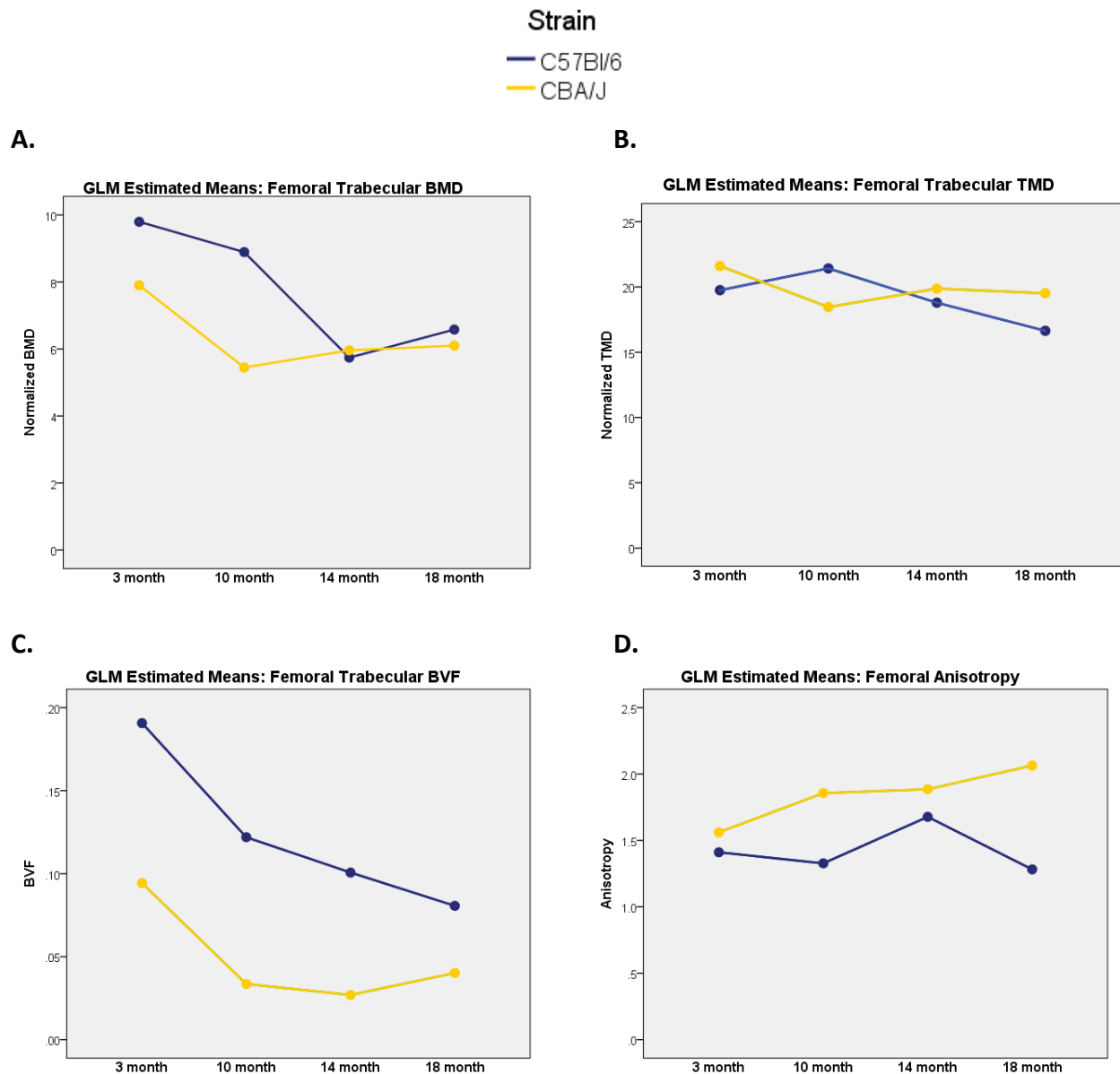


Figure 3. 14 - General linear models of femoral trabecular parameters.

The model run for the trabecular parameters was strain+age+strain*age. Graphs show model-estimated means. **A) Trabecular BMD** – Model is significant with $R^2=0.671$ ($p<0.001$). Strain is a significant factor with $R^2=0.278$ ($p<0.001$). Age, as a factor, is significant with $R^2=0.582$ ($p<0.001$). The interaction between strain and age is also significantly influencing the outcomes ($R^2=0.247$, $p=0.002$). The C57Bl/6 and CBA/J slopes from 3 months to 10 months are not statistically different, but approach significance ($p=0.071$). The slopes between 10 months and 14 months are different between the two strains ($p=0.008$). The change from 14 months to 18 months is not different in the two strains ($p=0.459$). **B) Trabecular TMD** – Model is significant with $R^2=0.442$ ($p<0.001$). Strain does not influence outcomes in the model ($p=0.211$). However, age does influence outcomes ($R^2=0.246$, $p=0.002$), as does the interaction of age and strain ($R^2=0.213$, $p=0.005$). The slopes from 3 to 10 months differ between the strains ($p=0.007$). The 10-to-14 and 14-18 month slopes do not differ. However, the accumulation of change from 10 to 18 months does differ between the strains ($p=0.004$). **C) Trabecular Bone Volume Fraction (BVF)** – The overall model is

significant for BVF with $R^2=0.782$ ($p<0.001$). Strain ($R^2=0.619$, $p<0.001$), age ($R^2=0.659$, $p<0.001$), and the interaction term ($R^2=0.160$, $p=0.025$) are all significant. The slopes of the two strains differ from 3 to 18 months ($p=0.001$), however, none of the smaller intervals are divergent enough to reach significance. **D) Trabecular Anisotropy** – The model for anisotropy is significant with $R^2=0.344$ ($p<0.001$). Strain is the only factor that influences the outcome values ($R^2=0.220$, $p<0.001$). The interaction term does not significantly contribute to the model, however, the slopes from 3 to 18 months differ between C57Bl/6 and CBA/J mice ($p=0.022$). None of the sub-intervals have differing slopes.

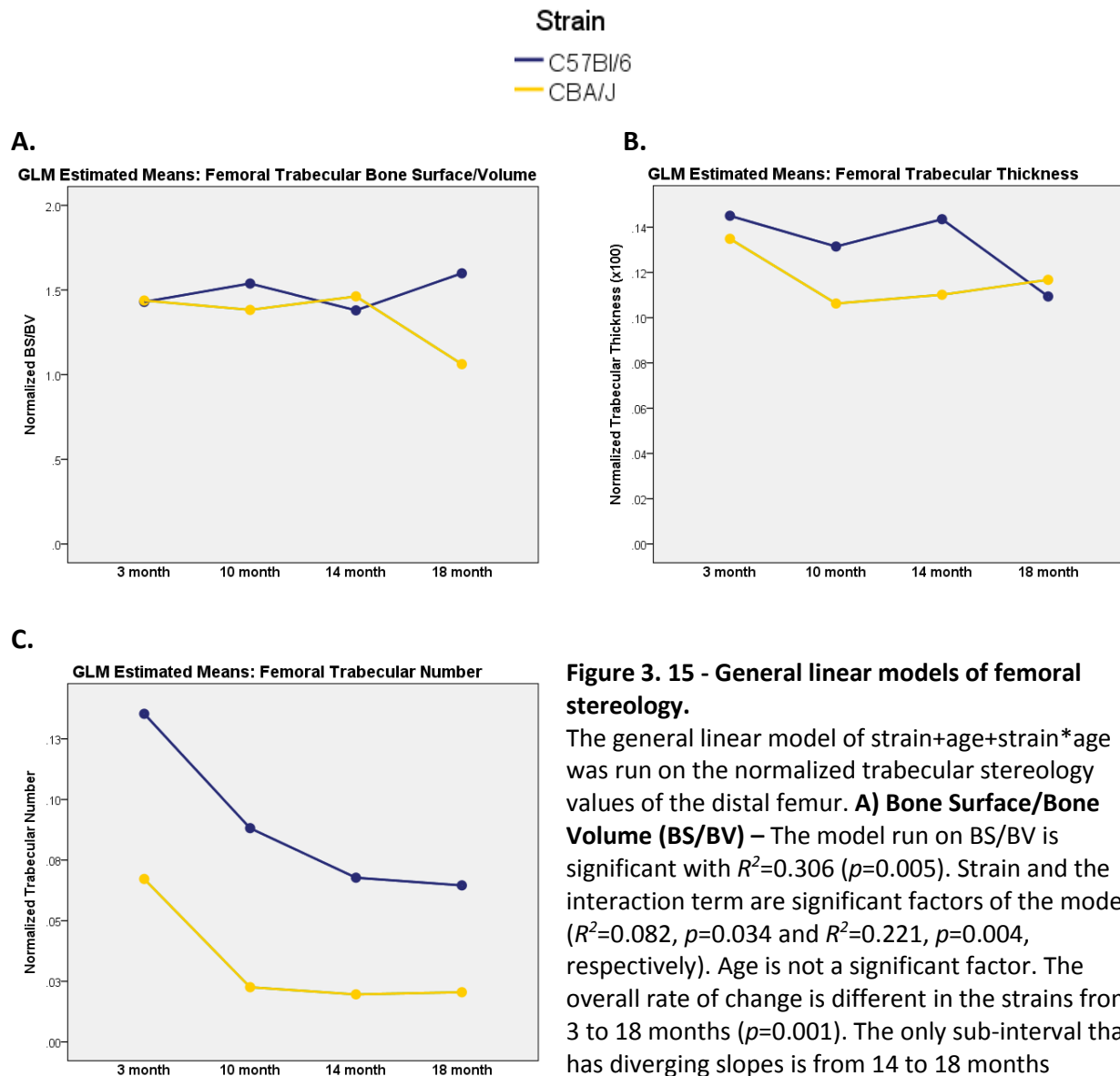


Figure 3. 15 - General linear models of femoral stereology.

The general linear model of strain+age+strain*age was run on the normalized trabecular stereology values of the distal femur. **A) Bone Surface/Bone Volume (BS/BV)** – The model run on BS/BV is significant with $R^2=0.306$ ($p=0.005$). Strain and the interaction term are significant factors of the model ($R^2=0.082$, $p=0.034$ and $R^2=0.221$, $p=0.004$, respectively). Age is not a significant factor. The overall rate of change is different in the strains from 3 to 18 months ($p=0.001$). The only sub-interval that has diverging slopes is from 14 to 18 months ($p=0.002$). **B) Trabecular Thickness** – The model for trabecular thickness is significant ($R^2=0.495$, $p<0.001$) with strain ($R^2=0.188$, $p=0.001$) and age ($R^2=0.380$, $p<0.001$) as influencing factors. The interaction term is not significant. **C) Trabecular Number** – The model for trabecular number is significant with $R^2=0.800$ ($p<0.001$). Strain ($R^2=0.657$, $p<0.001$) and age ($R^2=0.675$, $p<0.001$) are significant factors in the model. The interaction does not reach significance.

trabecular thickness is significant ($R^2=0.495$, $p<0.001$) with strain ($R^2=0.188$, $p=0.001$) and age ($R^2=0.380$, $p<0.001$) as influencing factors. The interaction term is not significant. **C) Trabecular Number** – The model for trabecular number is significant with $R^2=0.800$ ($p<0.001$). Strain ($R^2=0.657$, $p<0.001$) and age ($R^2=0.675$, $p<0.001$) are significant factors in the model. The interaction does not reach significance.

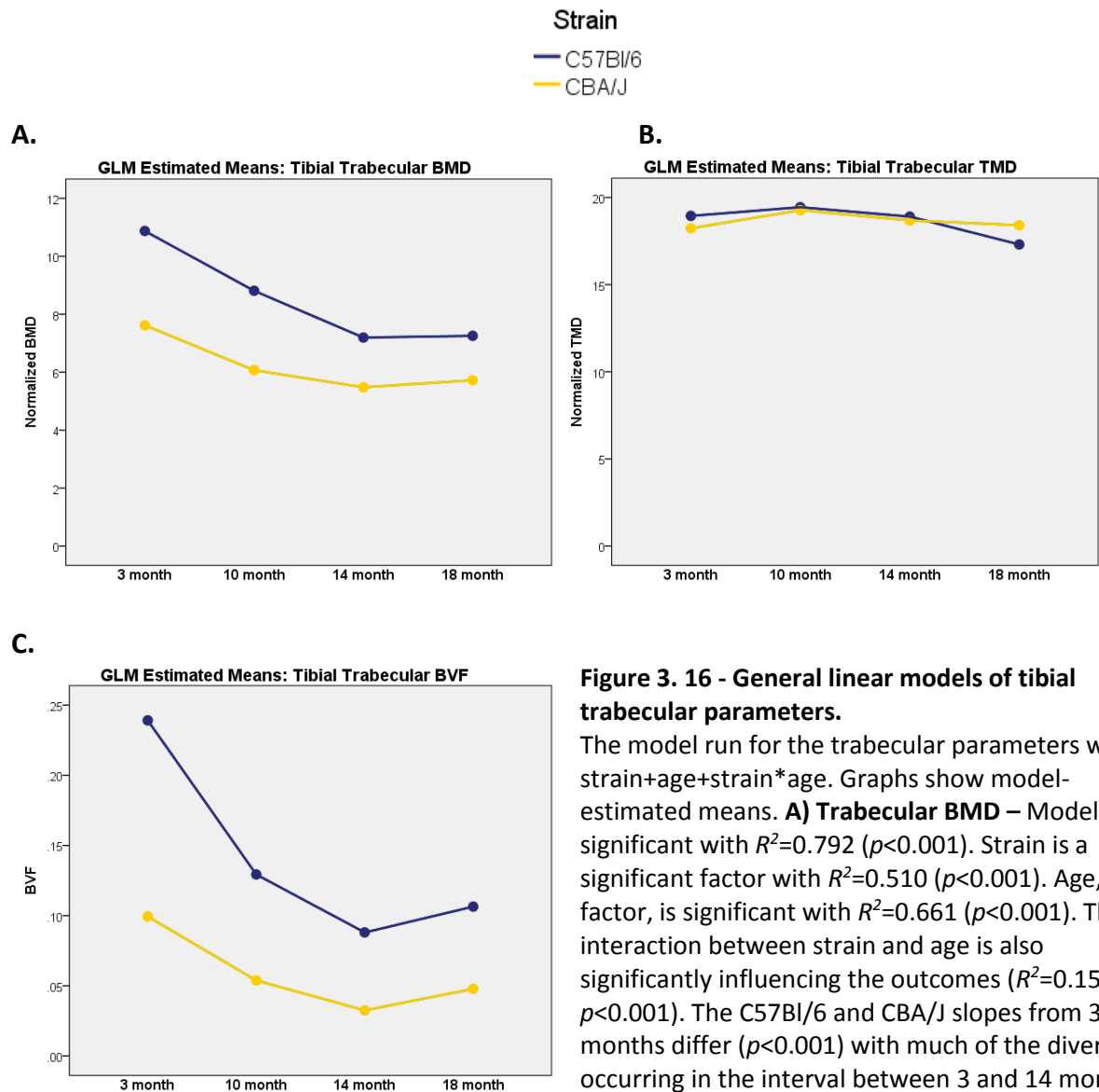


Figure 3. 16 - General linear models of tibial trabecular parameters.

The model run for the trabecular parameters was strain+age+strain*age. Graphs show model-estimated means. **A) Trabecular BMD** – Model is significant with $R^2=0.792$ ($p<0.001$). Strain is a significant factor with $R^2=0.510$ ($p<0.001$). Age, as a factor, is significant with $R^2=0.661$ ($p<0.001$). The interaction between strain and age is also significantly influencing the outcomes ($R^2=0.157$, $p<0.001$). The C57Bl/6 and CBA/J slopes from 3 to 18 months differ ($p<0.001$) with much of the divergence occurring in the interval between 3 and 14 months ($p=0.043$). **B) Trabecular TMD** – The model for TMD

is not significant. **C) Trabecular Bone Volume Fraction (BVF)** – The overall model is significant for BVF with $R^2=0.855$ ($p<0.001$). Strain ($R^2=0.594$, $p<0.001$), age ($R^2=0.724$, $p<0.001$), and the interaction term ($R^2=0.322$, $p<0.001$) are all significant. The slopes of the two strains overall differ from 3 to 18 months ($p<0.001$), with the most divergence occurring between 3 and 10 months ($p=0.001$).

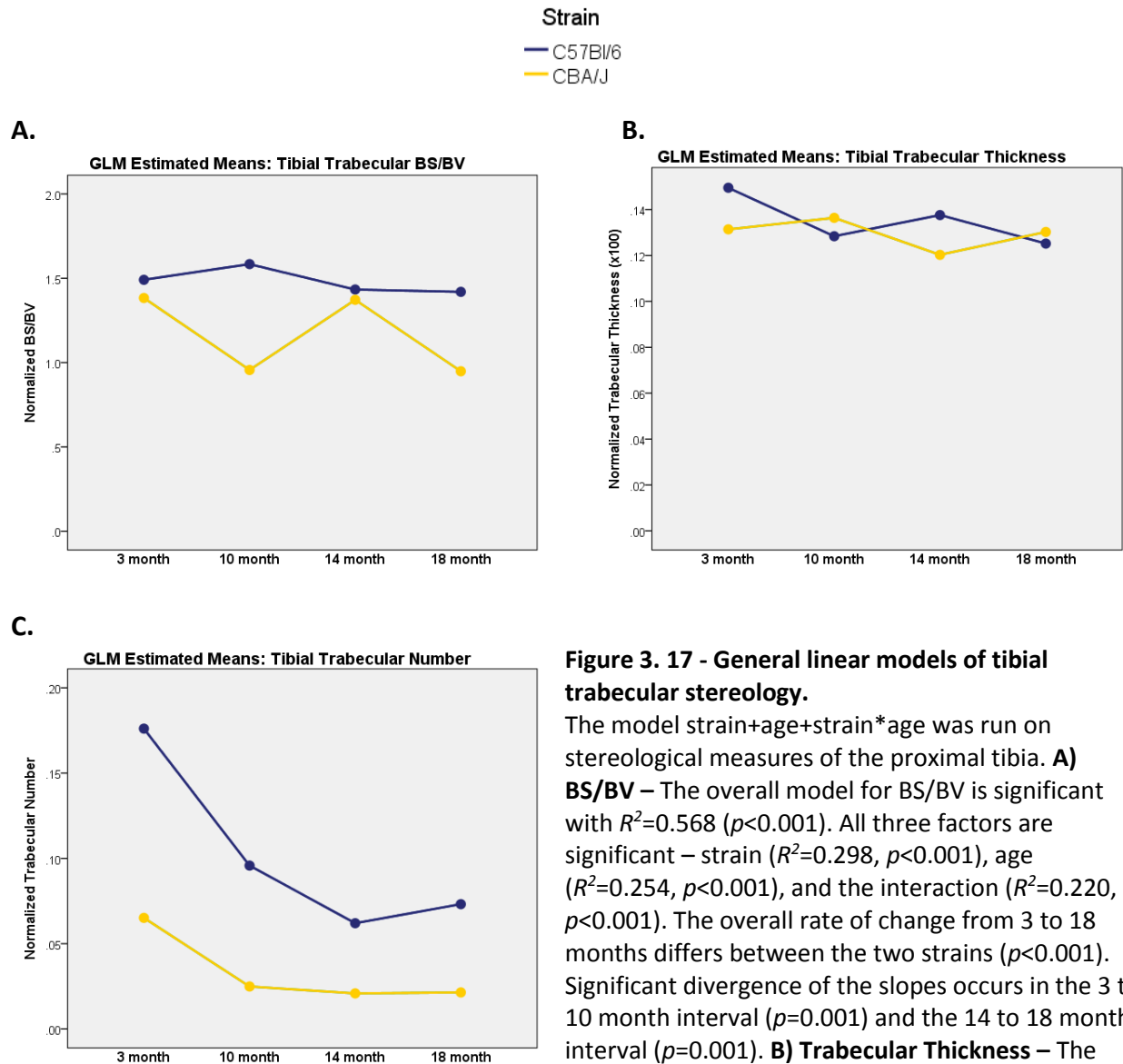


Figure 3. 17 - General linear models of tibial trabecular stereology.

The model strain+age+strain*age was run on stereological measures of the proximal tibia. **A) BS/BV** – The overall model for BS/BV is significant with $R^2=0.568$ ($p<0.001$). All three factors are significant – strain ($R^2=0.298$, $p<0.001$), age ($R^2=0.254$, $p<0.001$), and the interaction ($R^2=0.220$, $p<0.001$). The overall rate of change from 3 to 18 months differs between the two strains ($p<0.001$). Significant divergence of the slopes occurs in the 3 to 10 month interval ($p=0.001$) and the 14 to 18 month interval ($p=0.001$). **B) Trabecular Thickness** – The model is significant when run for trabecular thickness

($R^2=0.215$, $p=0.002$). Strain is not a significant factor, but both age ($R^2=0.109$, $p=0.014$) and the interaction are ($R^2=0.113$, $p=0.011$). The amount of change differs from 3 to 18 months when comparing the two strains ($p=0.002$). The most divergence of slope occurs in the 3 to 10 month interval ($p=0.032$) and the 14 to 18 month interval ($p=0.054$). **C) Trabecular Number** – The model for trabecular number is significant with $R^2=0.903$ ($p<0.001$). Strain ($R^2=0.714$, $p<0.001$), age ($R^2=0.795$, $p<0.001$), and the interaction between strain and age ($R^2=0.392$, $p<0.001$) are all significant factors. The rate of change differs between the C57Bl/6 and CBA/J mice from 3 to 18 months ($p<0.001$). The slopes diverge in the 3 to 10 month interval ($p=0.005$) and 10 to 14 month interval ($p=0.039$).

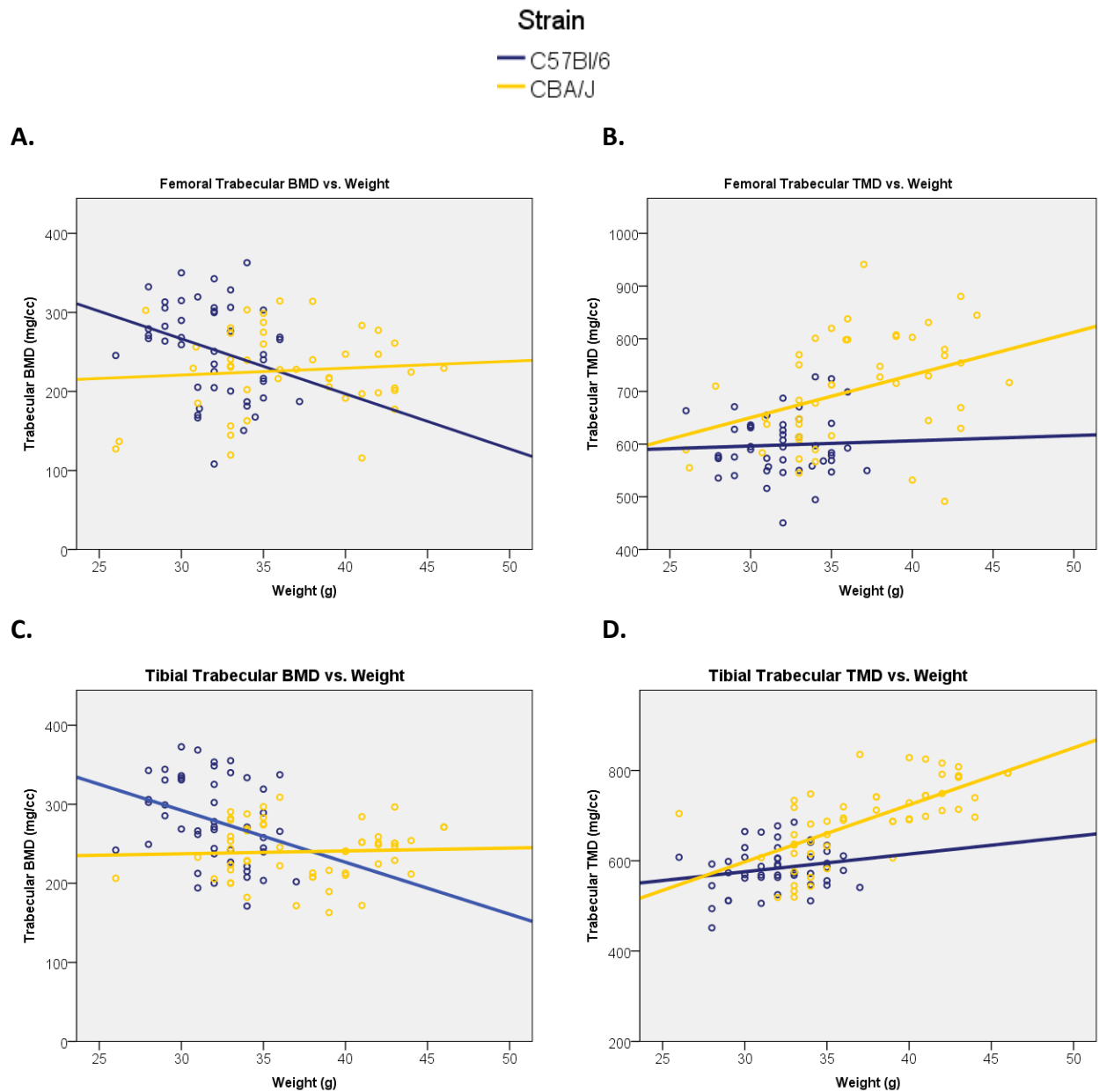


Figure 3. 18 - Trabecular BMD and TMD regressed against weight.

Linear regressions were run comparing trabecular BMD and TMD to weight (values not normalized). **A) Femoral Trabecular BMD** – Regression is significant for the C57Bl/6 mice with a correlation coefficient of $R=-0.296$ ($R^2=0.09$, $p=0.043$). Regression is *not* significant for the CBA/J mice ($p=0.755$). **B) Femoral Trabecular TMD** – Regression is not significant for TMD vs. weight in the C57Bl/6 mice ($p=0.776$). The linear relationship *is* significant in the CBA/J mice with a correlation coefficient of $R=0.369$ ($R^2=0.142$, $p=0.012$). **C) Tibial Trabecular BMD** – Regression is significant in the C57Bl/6 mice with a correlation coefficient of $R=-0.309$ ($R^2=0.095$, $p=0.033$). Regression is *not* significant in the CBA/J mice ($p=0.920$). **D) Tibial Trabecular TMD** – Regression is not significant for the C57Bl/6 mice ($p=0.176$). The regression *is* significant for CBA/J mice with a correlation coefficient of $R=0.671$ ($R^2=0.443$, $p<0.001$).

CHAPTER IV: DIFFERENTIAL AGE-RELATED CHANGES IN MECHANORESPONSE

Introduction

In the previous two chapters, we have demonstrated the variability in aging strategies that can be found in mice. We have also demonstrated how these differences in bone aging may be applicable to trends in human aging. The variable bone-related aging patterns in a mouse model provide a useful research tool for investigating the underlying factors of the bone outcomes. While there are numerous sources that influence bone health with age, we cannot study all of them in one dissertation. One factor stands out from the analyses presented in the previous chapters. Both mouse strains, C57Bl/6 and CBA/J, increase body mass as they age. The positive correlation between body weight and bone mineral density in men [1] and women [2, 3] has been well documented by researchers. The relationship between bone phenotype and weight is partly due to the adaptive response of bones to increase load. Published data have also demonstrated the relationship between body mass and bone mass in C57Bl/6 male mice, specifically [4]. What is not known is whether this relationship is maintained throughout aging.

In the 3-month C57Bl/6 mice, there are strong positive relationships between body weight and ultimate load ($R^2=0.360$, $p=0.009$) as well as weight and cortical area ($R^2=0.350$, $p=0.008$). In the 14- and 18-month C57Bl/6 mice combined, the relationships between weight and ultimate load ($p=0.364$) and weight and cortical area ($p=0.697$) are lost. In the CBA/J 3-month mice, there is a linear relationship between body weight and ultimate load ($R^2=0.361$, $p=0.008$), as well as between body weight and cortical area ($R^2=0.244$, $p=0.037$). Like the C57Bl/6 mice, the weight-ultimate load relationship is lost in the older CBA/J mice ($p=0.861$). However, this strain does maintain a relationship between weight and cortical area ($R^2=0.238$, $p=0.025$). These data lead to the hypothesis that the C57Bl/6 mice lose the ability to respond to

the increase in body weight. The CBA/J mice, however, maintain the mechanoresponsiveness throughout aging and can adapt to the load increase.

Research in the field of skeletal biology supports the notion that mechanical stimulation is necessary for healthy skeletal maintenance and function [5]. Bone is able to respond to mechanical stimuli through a complex, multi-tiered process of mechanotransduction. It is still unclear how aging influences the mechanoresponsiveness of bone. With advanced age, people have reduced bone response to exercise [6, 7]. This suggests that some level of the mechanoresponse system is impaired by senescence.

Studies focused on how aging affects mechanoresponse in rodents have yielded mixed results. A number of findings suggest that mechanoresponse is diminished in older mice [8, 9, 10, 11, 12, 13]. However, the strains and sexes used in these studies are not universal, preventing confidence in drawing conclusions. Rats have also been used to study aging effects on mechanoresponse. Turner *et al.* demonstrate that strain thresholds are increased to elicit a response in the older animals. Furthermore, when eliciting a response, older animals had 16-fold less bone growth than the young adults [14]. Contrary to these findings, other groups have presented data refuting the change in mechanoresponse with age. Therefore, more work needs to be done in order to come to a consensus regarding the relationship between aging and response to mechanical stimuli.

In this chapter, we will compare the *in vivo* response to load in the C57Bl/6 and CBA/J mouse strains using tibial axial compression. Previous studies have demonstrated the ability to elicit an anabolic response using this method in adult mice [10, 13, 15, 16]. In the last chapter, findings were presented suggesting that CBA/J mice maintain mechanical integrity of the cortical bone with aging, whereas C57Bl/6 mice do not. Therefore, we propose that the mechanoresponse in the CBA/J diaphysis will not diminish with age and the C57Bl/6 diaphyseal response will be reduced in the older animals.

In the CBA/J older mice, much of the mechanical stability is derived from the continued periosteal bone apposition. In the C57Bl/6 mice, the periosteal surface fails to expand to maintain mechanical function. Due to these findings, the periosteal tissue will specifically be tested for changes in mechanoresponse. Periosteum has been shown to be integral in bone

formation, growth, repair, and even mechanical response [17, 18, 19, 20]. Periosteal cells are responsive to dynamic fluid pressure by increasing proliferation [21]. Periostin, a critical extracellular protein in periosteal tissue, is upregulated in response to mechanical loading [22]. Periostin and is responsive to increases in both Runx2 [23] and c-Fos [24], both of which are upregulated with mechanical stimulation.

Older humans and rats both have decreased periosteal thickness, micro-vessel density, fibroblasts, osteoblasts, and collagen compared to younger individuals [25, 26, 27, 28]. The periosteal cells' interaction with the underlying bone largely influences its ability to transduce mechanical signals [29, 30, 31]. Due to the age-related changes in both the periosteal tissue and cortical bone, we expect the response to mechanical loading will also be altered with age. This leads to the prediction that the C57Bl/6 mice, which do not have periosteal bone apposition with aging, will lose mechanoresponsiveness in the periosteum. Furthermore, we predict the CBA/J periosteal response will remain constant throughout aging.

The cortical bone from the tibial diaphysis will be measured, as well. It is thought that the osteocyte is one of the primary mechanosensory cells and found in high abundance in the cortical bone [12]. Differences in bone apposition on the periosteal surface may be regulated by the osteocytes of the peripheral cortical bone instead of, or in addition to, the periosteal cells. Therefore, we expect to see maintenance of cortical responsiveness in the CBA/J mice with age, but a decrease in the C57Bl/6 mice.

In addition to the diaphyseal tissue, the epiphyseal region of the proximal tibia will be isolated to look at changes in mechanical response in the trabecular bone. In the trabecular compartment, C57Bl/6 appears to lose trabecular bone volume more slowly than CBA/J mice. Therefore, we hypothesize that both strains will reduce the epiphyseal response to load with age, but the reduction will be more severe in the CBA/J mice.

Materials & Methods

Tibial Loading

Male C57Bl/6 and CBA/J mice were used at 3-, 10-, and 18-months of age. Each group had 10 animals. The right tibia was loaded in a similar manner to experiments done by other investigators [10, 15, 32] (Figure 4.1). Custom platens were designed and manufactured at the

Orthopaedic Research Laboratories at University of Michigan. Loading was conducted on a Bose ElectroForce® 3300 mechanical testing system (Bose Corp., Eden Prairie, MN). Limbs were loaded axially while mice were under anesthesia (isofluorene) as approved by University of Michigan Animal Care.

Strain-matched loads were applied based on pilot strain gaging data. All animals were loaded using a 2 Hz sine wave with a 2 N preload. The 3-month and 10-month old mice of both strains were loaded at 10 N compressive force, approximating 2500 μE . The 18-month mice, in order to match the strain levels, were loaded at 12 N maximum compressive force. Each animal was loaded for 600 cycles with a 100 cycle tow-in period under indirect load-based cyclic feedback control. Animals were euthanized 30 minutes following loading. Both left and right tibiae were extracted immediately following sacrifice and placed in RNA*later* (AMBION, Inc., Austin, TX). Samples were stored at -80°C for at least two days to ensure no cellular response during RNA extraction.

Pilot experiments were run in order to ensure mechanical response was elicited that could be measured with rtPCR. For this pilot test, marrow was flushed and the whole tibia homogenized for RNA extraction. Quantitative rtPCR was run using primers for *c-Fos*, *runx2*, and *Gja1* using *$\beta 2m$* as a housekeeping gene. Six 3-month old C57Bl/6 mice were loaded and sacrificed 15 minutes following load, six 3-month old CBA/J mice were sacrificed 20 minutes post-load, and another six 3-month C57Bl/6 mice were sacrificed 30 minutes post-load. This was done to test for the optimal timing of sacrifice for measuring gene response. Previous work done in the lab demonstrated a drop in response in *c-Fos* and *COX-2* from 30 minutes to 60 minutes post-loading [33].

Results for whole bone gene expression changes demonstrate a 4.5-fold increase of *c-Fos*, 0.99-fold change in *Runx2*, and a 0.67-fold change in *Gja1* at 15 minutes post-load. At 20 minutes post-load, there was a 6.21-fold increase in *c-Fos* expression, 1.07-fold increase in *Runx2*, and a 1.09-fold increase in *Gja1* expression. After 30 minutes post-load, *c-Fos* expression was increased 10.35-fold, *Runx2* expression was increased 1.03-fold, and *Gja1* expression was increased 2.98-fold (Table 4.1). These data validate the use of this loading method for eliciting a mechanical response in both C57Bl/6 and CBA/J tibiae. Furthermore, 30 minutes post-loading is

the ideal time for sacrifice for *c-Fos* expression. *Runx2* expression does not increase during this period, likely due to insufficient time for up-regulation.

Quantitative Real-Time PCR

Bones were removed from the -80°C storage and thawed on ice. All extractions were done using appropriate RNA techniques. Marrow was flushed and collected using 1 mL TRIzol® (AMBION Inc., Austin, TX).¹⁰ Proximal epiphyses were removed just below the proximal tibia-fibula junction and placed in 1 mL Trizol. Periosteum was scraped under a dissection microscope in 0.5 mL DNase/RNase-free water, collected, and added to 0.5 mL Trizol. Remaining cortical bone was rinsed and placed in 1 mL Trizol. All tissue types were homogenized for 30 seconds.

Homogenates were immediately treated with 200 uL of chloroform and shaken for 15 seconds. They were then centrifuged for 20 minutes at 4° C at 12,000 g. The top (clear) layer was extracted. The RNeasy® Mini-kit was then utilized according to manufacturer protocols to further purify the RNA. This included the optional DNase treatment. RNA was eluted from columns using 30 uL RNase-free water warmed to 65° C. Elution was run through twice for cortical and periosteal RNA columns to maximize yield. Two separate elutions of 30 uL were run for the epiphyseal and marrow columns in order to dilute RNA to usable ranges. Extracted RNA was immediately stored at -80° C.

Little work has been done using isolated periosteum for rtPCR. Therefore, pilot work was done to ensure RNA yields were sufficient for downstream quantification. The first trial provided yields of 61.3 ng/uL of cortical RNA, 19.3 ng/uL of periosteal RNA, 333.3 ng/uL of epiphyseal RNA, and 377.8 ng/uL of marrow RNA. Due to the low yield of the periosteal RNA, the extraction method was modified to reduce time between thawing and homogenization in TRIzol. Additionally, trials were run that demonstrated higher yields when combining TRIzol-only and RNeasy-kit® (Qiagen, Valencia, CA) extraction and RNA isolation techniques. Following these changes, a second trial was run and periosteal RNA yield averaged 65.9 ng/uL.

¹⁰ Marrow was run though none of the genes showed expression in any strain or age or treatment, therefore results are omitted.

Following RNA extraction, samples were thawed on ice and yield measured using a NanoDrop system. Reverse transcription was done using qScript cDNA SuperMix (Quanta Biosciences, Inc., Gaithersburg, MD) according to manufacturer's protocol for 30 uL-reaction volume. For cortical, epiphyseal, and marrow RNA, 1 ug of total RNA was used for the RT reaction. Due to lower yields, 500 ng of periosteal RNA was used for the reactions. Pilot work demonstrated that the downstream quantification would still work with this lower concentration of RNA. Real-time PCR was performed in triplicate and quantified using SYBR Green fluorescent markers (Invitrogen, Carlsbad, CA). Beta-2-microglobulin ($\beta 2m$) was used as an internal control due to pilot work comparing other commonly used housekeeping genes. PrimeTime® qPCR primers were obtained (Applied Biosystems, Foster City, CA) for C-Fos (*Fos*), COX-2 (*Ptgs2*), eNOS (*Nos3*), Cx43 (*Gja1*), and $\beta 2m$ (Table 4.2). Expression changes are measured using the $\Delta\Delta C(t)$ method with the left limb as control.

The $\Delta\Delta C(t)$ method is an equation to calculate fold-change in gene expression. For each rtPCR experiment run, a threshold for LOG of the fluorescence is set just the onset of the exponential phase of the fluorescent curve.¹¹ The $C(t)$ -value is the cycle number (point on the x-axis) that intersects with the fluorescent threshold. Following export of the data, we compared the triplicate values to point out possible errors in technique leading to highly variable $C(t)$ values within the three wells. $C(t)$ -values for wells were averaged and the equations used were the following:

$$\Delta C(t)_{limb} = \overline{C(t)}_{gene} - \overline{C(t)}_{\beta 2m}$$

Where each gene of each limb is normalized to the housekeeping gene ($\beta 2m$).

$$\Delta\Delta C(t) = \Delta C(t)_{right} - \Delta C(t)_{left}$$

Such that the $\Delta\Delta C(t)$ of each gene is the difference between the $\Delta C(t)$ of the experimental (loaded/right) limb and the control (unloaded/left).

$$Fold\ change = 2^{-\Delta\Delta C(t)}$$

This equation results in a fold-change value, which is only considered if greater than 1-cycle, or 2-fold up/down-regulation. Values greater than 1 indicate an increase in gene

¹¹ Note: In a LOG graph, linear change is actually exponential, so threshold is set where the LOG graph becomes a straight line.

expression in the loaded limb. Values less than 1 indicate a down-regulation in expression in the loaded limb.

C-Fos (*Fos*) is a commonly reported early mechanoresponse gene [34]. In response to mechanical stimuli, the JNK and ERK pathways are activated, which lead to up-regulation of the Fos-gene family, of which c-Fos is a member. The c-Fos is a major component of the transcription factor activator protein-1 (AP-1) which mediates gene expression in early osteoblastic differentiation [5, 35, 36].

Cyclooxygenase-2 (COX-2/*Ptgs2*) is another early-response transcription factor often reported in bone mechanoresponse studies. COX-2 activity leads to the conversion of arachidonic acid into prostaglandin-E2 (PGE2). COX-2 transcription is upregulated through the ERK and PKA pathways when mechanically stimulated [5, 37]. There is evidence that aged mice have a reduction in the expression of COX-2 compared to young adult mice [38].

Endothelial nitric oxide synthase (eNOS/*Nos3*) and is one of three enzymes that produce active nitric oxide (NO). Nitric oxide suppresses osteoclasts and promotes osteogenesis [5, 39, 40]. Under mechanical stimulation, NO has been shown to be released by both osteoblasts [37, 41, 42, 43, 44] and in bone marrow stromal cells [45, 46, 47]. The inhibition of eNOS significantly impairs load-induced bone osteogenesis [40, 48, 49].

The final gene of interest is connexin-43 (Cx43/*Gja1*). Connexin proteins are involved in the formation of hemi-channels and gap-junctions [50]. Cx43 is a marker of mechanical response that is involved in the mobilization and movement of calcium within and outside the cell [51, 52]. Expression of Cx43 is upregulated in response to mechanical stimulation [53, 54] and promotes osteogenesis along the PGE2-signaling axis [5]. The responsiveness of Cx43 channels to mechanical stimuli is lost with advancing age [55, 56].

Adaptive Loading

In order to assess the downstream adaptive responsiveness in the two strains, an initial long-term loading pilot experiment was run on 3-month-old male C57Bl/6 and CBA/J mice. This experiment used the same tibial loading parameters as described above. However, animals were loaded three days a week for four weeks. Alizarin I-P injections were administered on day

28 of loading. Calcein injections were administered on day 33 and animals were euthanized on day 35.

Bones were excised following sacrifice and prepared for embedding in PMMA. Cortical sections were taken just distal to the tibia-fibula junction. Trabecular regions were taken from just below the proximal tibia-fibula junction. Images were taken using a Zeiss fluorescent microscope and measured using BioQuant® software. Mineralizing surface, mineral apposition rate (MAR), and bone formation rate (BFR) were recorded for both loaded and unloaded limbs.

Statistics

Statistical analyses were run using commercially available SPSS software. Statistics were done on the ddC(t) values due to the lack of linearity and Gaussian distribution inherent in fold-change values. For graphical purposes, the 3-month C57Bl/6 mean fold-change value was set at 1 and all other values offset accordingly. Outliers for the PCR data were only removed if the fold-change exceeded 100 in order to avoid biasing the data. ANOVA was used to compare the 3-, 10-, and 18-month age groups within each strain. T-tests were used to compare C57Bl/6 and CBA/J means at each age. Significance is defined as $p \leq 0.05$. Paired t-tests were used to compare the loaded and unloaded limbs for dynamic histomorphometry. Due to high levels of variability, near-significance was defined as a p -value between 0.055 and 0.01.

Results

Periosteal Gene Expression

In the periosteum of the C57Bl/6 mice, c-Fos was differentially expressed when comparing age groups following loading ($p=0.045$). Though significant, the difference in expression between the 10-month and 18-month means only represented a 1.6-fold increase at 18 months ($p=0.047$) (Figure 4.2 – A). Expression of COX-2 was also variant in the periosteum of C57Bl/6 mice when ages were compared ($p=0.025$). The expression at 18 months was 2.0-fold greater than the expression at 10 months (Figure 4.2 – B). Due to primer issues, data for 3-month COX-2 expression were unavailable. Periosteal expression of eNos and Cx43 (*Gja1*) were not different between age groups (Figure 4.2 – C and D).

The age groups in the CBA/J strain expressed differing levels of c-Fos following loading ($p=0.032$). The difference in expression between 3 and 18 months neared significance and represented a 5.6-fold greater c-Fos expression at 18 months compared to 3 months ($p=0.081$). The difference between the 10-month and 18-month means represented a 5.8-fold greater expression of c-Fos in the 18-month group ($p=0.046$) (Figure 4.2 – A). Difference in COX-2 expression between CBA/J age groups did not reach significance ($p=0.118$). However, qualitatively, the expression at 18 months is much greater than that at 3 and 10 months (Figure 4.2 – B). Statistics returned as not significant due to high levels of variability. Greater sample size and removal of outliers might yield significant results. Expression of eNos is invariant when CBA/J age groups are compared (Figure 4.2 – C). The expression of Cx43 (*Gja1*) was also similar at all ages in the CBA/J periosteum (Figure 4.2 – D).

The expression of c-Fos was similar in the C57Bl/6 and CBA/J strains at 3 and 10 months. However, the 18-month CBA/J mean was significantly greater than the C57Bl/6 18-month mean ($p=0.006$). Similar to c-Fos, expression of COX-2 did not differ between strains at 3 and 10 months. The 18-month CBA/J mean expression was much greater than the C57Bl/6 expression at 18 months ($p=0.003$). Expression of Cx43 (*Gja1*) was greater in the CBA/J 18-month mice compared to the expression of the C57Bl/6 18-month mice ($p=0.016$).

Cortical Gene Expression

In the C57Bl/6 mice, expression differences between age groups were not significant for any of the genes measured (Figure 4.3 – A, B, C, D). Similarly, expression in the CBA/J mice did not differ when ages were compared for the genes of interest (Figure 4.3 – A, B, C, D).

Epiphyseal Gene Expression

Expression of c-Fos was different when C57Bl/6 age groups were compared ($p=0.036$) with the 18-month response showing a 3.2-fold greater expression than the 10-month mice ($p=0.033$) (Figure 4.4 – A). There were also differences in expression of COX-2 when C57Bl/6 age groups were compared ($p=0.008$). The 18-month mean expression is 10.5-fold greater than the 3-month mean ($p=0.026$) and 12.2-fold greater than the 10-month mean ($p=0.012$) (Figure

4.4 – B). Expression of eNos (Figure 4.4 – C) and *Gja1* (Figure 4.4 – D) did not differ when C57Bl/6 ages were compared.

Expression profiles of c-Fos, COX-2, and eNos, in the epiphysis of CBA/J mice, were invariant between age groups (Figure 4.4 – A, B, C). Comparisons between the age groups for *Gja1* expression in CBA/J mice neared significance ($p=0.072$) with the 3- and 18-month difference in expression falling just outside the range of significance ($p=0.081$) (Figure 4.4 – D).

Periosteal Dynamic Histomorphometry

There was no difference in periosteal mineralizing surface (MS) or mineralizing surface/bone surface (MS/BS) when comparing the C57Bl/6 loaded and unloaded limbs. There was a significant increase in MS in the CBA/J tibiae when loaded ($p=0.048$). The ratio of MS/BS was not significantly different in the CBA/J loaded and unloaded groups (Figure 4.5). Neither strain produced double labeling on the periosteal surface. For this reason, mineral apposition and bone formation rates were not measurable.

Endosteal Dynamic Histomorphometry

The averages for MS and MS/BS in the C57Bl/6 left (control) limbs were significantly greater than the average in the loaded limbs ($p=0.042$, $p=0.053$) (Figure 4.6 – A, B). The average mineral apposition rate (MAR) for the C57Bl/6 was not statistically different when comparing the loaded and unloaded limbs (Figure 4.6 – C). Additionally, the bone formation rate (BFR) was not different when the sides were compared (Figure 4.6 – D).

The CBA/J control limbs had a significantly lower mean MS and MS/BS than the loaded side ($p=0.021$ and $p=0.028$, respectively) (Figure 4.6 – A, B). The mean MAR values was greater in the loaded limb than the contralateral controls ($p=0.031$) (Figure 4.6 – C). However, the mean BFR was not different in the loaded and unloaded limbs (Figure 4.6 – D).

Metaphyseal Dynamic Histomorphometry

In the trabecular region of the tibial metaphysis, the MS/BS and MAR averages were not different in the C57Bl/6 loaded and unloaded limbs (Figure 4.7 – A, B). However, the BFR in the loaded C57Bl/6 limb was significantly greater than the BFR of the unloaded limb ($p=0.019$) (Figure 4.7 – C).

The mean MS/BS of the CBA/J control limbs was invariant from the mean of the loaded limb. (Figure 4.7 – A). The mean MAR in the CBA/J tibiae was significantly greater in the loaded limb compared to the unloaded limb ($p=0.015$) (Figure 4.7 – B). The mean BFR was, however, not different in the loaded and unloaded CBA/J limbs (Figure 4.7 – C).

Discussion

A number of researchers in the field have proposed that age-related bone loss and fragility is due to inappropriate adaptation to mechanical loading [12, 57]. In the first hypothesis of this chapter, we estimated that the C57Bl/6 periosteum was expected to lose response to load with aging. The data do not support these projections. The expression in the C57Bl/6 periosteal tissue is not greatly affected by age. Despite significance between the 10-month and 18-month mean fold change in c-Fos and COX-2 expression, the actual fold change is not above 2x. The 3-month periosteal tissue did not demonstrate an upregulation in the genes tested for. Therefore, a loss of expression could not be measured.

Due to the continued periosteal expansion, we predicted that CBA/J mice would experience a consistent response to loading regardless of age. Instead of maintaining expression levels, the CBA/J response markedly increased with age in c-Fos and COX-2. It is possible that as the periosteal tissue is displaced further from the neutral bending axis, the strain each cell experiences is greater due to increased moment. This would suggest that the cells are not altering the responsiveness, but rather the response is scaled to the level of strain the mechanosensory cells experience. Another explanation is that the extracellular matrix of the periosteum is losing ductility due to collagen cross-linkage. This would lead to increased strain experienced by the cells. Since the C57Bl/6 periosteal cells do not seem to increase response, it is more likely that the location away from the neutral axis is having a greater effect on the increase in change measured in CBA/J mice.

The cortical bone response in the C57Bl/6 mice was expected to be decreased in the older aged animals. Statistically, there are no differences in the gene expression profiles. However, the expression for c-Fos (2.18-fold increase) and COX-2 (2.67-fold increase) fall below the 2-fold threshold for relevance in the 10-month and 18-month animals. It is possible that

these data do, in fact, represent a loss in response, but is masked by the high degree of variation.

The CBA/J cortical bone also does not appear to have any statistically different expression values. The 3-month mean c-Fos and COX-2 expression is upregulated due to loading over the 2-fold criterion. The lack of significant change in expression at 10- and 18-months suggests that the response is maintained with age. However, the c-Fos 18-month mean does dip slightly below the 2-fold threshold.

We hypothesized that the C57Bl/6 epiphyseal expression would decrease slightly but less so than the CBA/J mice. The data disprove this hypothesis but still provide interesting results. The epiphyseal upregulation of c-Fos, COX-2, and eNOS due to loading are all increased in the 18-month C57Bl/6 mice. The CBA/J mice do not appear to have any change in the gene expression profiles with age, with all ages having low amounts of upregulation due to loading.

While these data do not match exactly the proposed outcomes, they do support the idea that the two strains of mice undergo varying changes to loading response with age. The C57Bl/6 mice either maintain or reduce the ability to respond to load in the diaphyseal region, possibly leading to the lack of periosteal deposition that is evident in this strain's older mice. This aligns with the proposition that C57Bl/6 mice do not increase bone mass and second moment due to weight increase because they lack the ability to respond to load in the diaphyseal bone. Conversely, the CBA/J mice have a large increase in response in the periosteum and maintain load-induced upregulation in the cortex. These results are indicative of the continued or increased deposition of bone in response to greater loads from body mass.

The reason for the increase in trabecular response in the C57Bl/6 older mice could be due to the decreased cortical bone at the diaphysis. The increase in trabecular response could be a compensatory mechanism to prevent further loss of bone. Since there is an overall reduction in the amount of trabecular bone in the old C57Bl/6 mice, it is possible that the remaining trabecular bone is taking on greater responsibility for load bearing leading to per cell response increasing.

These results are not consistent with previous reports of decreasing mechanoresponse with age in mice [8, 9, 10, 11, 12, 13, 58]. However, most of the previous work has been

conducted on C57Bl/6 or BALB/c mice and focused on the cortical bone. Based on the data presented here, it is not surprising that a loss in mechanoresponse has been reported. By adding the CBA/J mice to the analysis, we demonstrate that aging does not influence mechanoresponse universally in all strains of mice. Furthermore, a loss of mechanoresponse in the cortical bone does not necessitate a loss in response in the trabecular region.

The high amounts of variability in the expression profiles within each strain is concerning. Prior to the experiment, a power analysis was run using similar PCR data from a tibial loading model from our lab. The levels of variability from those data led to our calculation of 7-8 mice per group. However, the variability in the data we present in this chapter is well above that from the previous work. One potential explanation for this discrepancy is due to the use of old mice in our study. Age inherently increases variability, likely leading to a greater range of outcomes regarding gene expression. Another possible reason for the large variability in the PCR outcomes arises from the separation of periosteal, cortical, and epiphyseal tissue. This method reduces the RNA yield, making the outcomes more sensitive to minor variations. In order to account for the heightened variation in measures, larger sample sizes are necessary. Additionally, quality control using RIN values could provide insight into influence of handling and processing on RNA quality.

One interesting observation relates to the curvature of the tibiae in the two strains. The CBA/J tibiae are clearly much more curved than those of the C57Bl/6 mice. The differing curvature suggests different concentrations of stressors in the whole bone. The C57Bl/6 tibia is almost straight, with little bowing. With the greater curvature of the tibiae in the CBA/J mice, strain experienced is different than the C57Bl/6 diaphysis due to altered 3-D stress state. These geometry patterns would help explain the greater mechanical response in the C57Bl/6 epiphysis and the CBA/J periosteum and cortex.

One drawback to this study is the lack of information on the fibula. The fibulae were all removed and discarded prior to RNA extraction. The tibiae in the C57Bl/6 mice may be much straighter but the fibulae much more bowed. This would put a greater demand on the fibula and alleviate the amount of strain required in the tibia. Future work should include analysis of the gene profiles in the tibiae, as well. Another complication could be in the pilot strain-gaging

data that provided load estimates for the strain-matched model. Whole-bone mechanics might be altered by the absence of periosteal tissue [59]. In order to adhere the gages to the surface of the bones, periosteum is stripped. This could lead to altered *in vivo* strain in the tibiae. Unfortunately, there are currently no methods for direct gage application without removal of the periosteal tissue. However, future strain measures might be taken using visual/infrared tracking of stable points to get more accurate measures.

Another critical limitation of this work is the inability to assess the functional implications of the gene expression changes. The mechanoreponse system is comprised of four mechanisms. Age could influence any or all levels, leading to an ultimate reduced adaptive response to load. The first step in the mechanoreponse system is the transmission of load through the tissue [60, 61]. The previous chapters demonstrated age-related changes in mineralization, shape, and post-yield properties in both strains. Increased collagen crosslinks have been reported to influence aging bone stiffness and post-yield properties in both human and rodents [9, 62]. These changes will alter the transmission and propagation of through the bones. Furthermore, substrate stiffness has been shown to alter cell fate [59, 63, 64, 65, 66]. Alterations in the end results of mechanical load could be due to material level properties altering direction and concentration of loads and how the cells receive the mechanical signals.

The next steps in the mechanical response process is the sensation of load by sensory cells and the transduction of the physical signal into bioelectric or biochemical signals [61, 67]. Experimentally, these two processes are difficult to distinguish as cell response is the only *in vivo* method to assess cell sensation. Using *in vitro* methods, there is evidence that older bone cells have decreased response to mechanical challenges compared to younger cells [47, 58, 68]. Aging cells may lose the ability to sense and/or respond to load due to general senescence. Telomere shortening could prevent appropriate production of upregulated genes necessary to elicit an adequate remodeling response. DNA error rates increase in each successive replication cycle. Therefore, older cells may have difficulty in transcription factor binding and/or correct translation.

One intriguing finding of this work was the tendency for some individual mice to elicit a down-regulation in response to loading. This would not be surprising in a long-term loading

study. However, 30 minutes is a short timespan for reducing presence of mRNA. One explanation that bear future study is that potential role of epigenetic effects on mechanoreponse. miRNA's have the ability to inhibit protein production from transcribed RNA. These can be fast-acting molecules and have been suggested as influencing dysfunction leading to osteoporosis [69]. Therefore, miRNA and other post-transcriptional and post-translational modifications should be investigated and may be important regulatory mechanisms for bone loading response.

This study is able to assess the mechanical response through the early parts of the third step. However, the immediate response profiles are not necessarily indicative of down-stream changes to bone adaptation. The final step in the ability for bone to respond to load is the effector cells' response to transmitted signals. A large percentage of mechanotransduction work related to aging has focused on the long-term effects of loading. Many of these studies suggest an overall drop in mechanoreponse based on reduced bone formation in the older animals in response to load [10, 14, 16]. These findings combined with the results presented in this paper suggest that the loss of mechanotransduction may be primarily caused by senescence of the responding cells or their ability to receive the signal.

Klein Nulend *et al.* discovered aging cells had no change or increased response to load *in vitro* but a reduction in cell growth and proliferation [70]. Other studies have demonstrated that older age has no effect on the load-induced osteocyte response but reduces the osteoblastic proliferation *in vitro* [12, 71]. These studies suggest that the impaired osteo-adaptive response to load is a product of effector cell senescence rather than mechanosensation. In order to compare these findings to those presented here, long-term loading experiments should be run looking at both gene regulation and bone deposition through dynamic histomorphometry.

Initial work was started on investigating the long-term effects of loading in both strains, however, only 3-month animals have been tested thus far. In the preliminary work, the CBA/J mice demonstrated an increase in mineralizing surface on the periosteal side due to loading. The C57Bl/6 mice showed no significant difference. The lack of response in the C57Bl/6 mice is conducive to results presented previously [15]. On the endosteal surface, the C57Bl/6 mice

decreased MS and MS/BS values but had no change in MAR or BFR. The CBA/J mice had a significant load-induced increase in MS, MS/BS, MAR, and BFR.

These data suggest that even at the young adult stage, the CBA/J mice are more responsive in the mid-diaphysis. The lack of significance to the increase in MS/BS, MAR, and BFR in the C57Bl/6 metaphysis is likely due to the low number of animals used for the pilot work. This is supported by Holguin *et al*'s findings that trabecular bone increased in C57Bl/6 young adults [13]. More work needs to be done to verify the difference in initial response to long-term loading in the strains as well as how the ability to respond may change with age.

The PCR and initial long-term adaptive response data, together, suggest that there is a large range of variation in the mechanoresponse patterns of bone even at 3-months of age. The aging process likely does not affect all individuals in the same manner. If the C57Bl/6 mice, as proposed previously, are a good model for mid-shaft fracture risk in humans, the lack of responsiveness may indicate that load-bearing exercises in this population of the elderly may not be an effective preventative measure. The CBA/J mice, as a model for successful cortical bone aging, could demonstrate that loading exercises may not ease risk of fracture in trabecular regions.

References: Chapter IV

- [1] R. Hoxha, H. Islami, H. Qorraj-Bytyqi, S. Thaci and E. Bahtiri, "Relationship of weight and body mass index with bone mineral density in adult men from Kosovo," *Mareria Socio Medica*, vol. 26, no. 5, pp. 306-308, 2014.
- [2] D. Felson, Y. Zhang, M. Hannan and J. Anderson, "Effects of weight and body mass index on bone mineral density in men and women: the framingham study," *Journal of Bone and Miineral Research*, vol. 8, no. 5, pp. 567-573, 1993.
- [3] S. Morin, J. Tsang and W. Leslie, "Weight and body mass index predict bone mineral density and fracture in women aged 40 to 59 years," *Osteoporosis Internationaal*, vol. 20, pp. 363-370, 2009.
- [4] U. Iwaniec, M. Dube, S. Boghossian, H. Song, W. Helferich, R. Turner and S. Kalra, "Body mass influence cortical bone mass independent of leptin signaling," *Bone*, vol. 44, no. 3, pp. 404-412, 2009.

- [5] D. Papachristou, K. Papachroni, E. Basdra and A. Papavassiliou, "Signaling networks and transcription factors regulating mechanotransduction in bone," *BioEssays*, vol. 31, pp. 794-804, 2009.
- [6] S. Srinivasan, T. Gross and S. Bain, "Bone mechanotransduction may require augmentation in order to strengthen the senescent skeleton," *Aging Research Reviews*, vol. 11, no. 3, pp. 353-360, 2012.
- [7] A. Parfitt, "Bone remodeling in type I osteoporosis," *Journal of Bone and Mineral Research*, vol. 6, pp. 95-7, 1991.
- [8] V. Ferguson, R. Ayers, T. Bateman and S. Simske, "Bone development and age-related bone loss in male C57Bl/6 mice," *Bone*, vol. 33, pp. 387-398, 2003.
- [9] M. Willingham, M. Brodt, K. Lee, A. Stephens, J. Ye and M. Silva, "Age-related changes in bone structure and strength in female and male BALB/c mice," *Calcified Tissue International*, vol. 86, pp. 470-483, 2010.
- [10] M. Brodt and M. Silva, "Aged mice have enhanced endocortical response and normal periosteal response compared with young-adult mice following 1 week of axial tibial compression," *Journal of Bone and Mineral Research*, vol. 25, no. 9, pp. 2006-2015, 2010.
- [11] S. Srinivasan, S. Agans, K. King, N. Moy, S. Poliachik and T. Gross, "Enabling bone formation in the aged skeleton via rest-inserted mechanical loading," *Bone*, vol. 33, no. 6, pp. 946-955, 2003.
- [12] L. Meakin, G. Galea, T. Sugiyama, L. Lanyon and J. Price, "Age-related impairment of bones' adaptive response to loading in mice is associated with sex-related deficiencies in osteoblasts but no change in osteocytes," *Journal of Bone and Mineral Research*, vol. 29, no. 8, pp. 1859-1871, 2014.
- [13] N. Holguin, M. Brodt, M. Sanchez and M. Silva, "Aging diminishes lamellar and woven bone formation induced by tibial compression in adult C57Bl/6," *Bone*, vol. 65, pp. 83-91, 2014.
- [14] C. Turner, Y. Takano and I. Owan, "Aging changes mechanical loading thresholds for bone formation in rats," *Journal of Bone and Mineral Research*, vol. 10, no. 10, pp. 1544-1549, 1995.
- [15] R. De Souza, M. Matsuura, F. Eckstein, S. Rawlinson, L. Lanyon and A. Pitsillides, "Non-invasive axial loading of mouse tibiae increases cortical bone formation and modifies trabecular organization: a new model to study cortical and cancellous compartments in a single loaded element," *Bone*, vol. 37, pp. 810-818, 2005.
- [16] M. Silva, M. Brodt, M. Lynch, A. Stephens, D. Wood and R. Civitelli, "Tibial loading increases osteogenic gene expression and cortical bone volume in mature and middle-aged mice," *PLoS One*, vol. 7, p. e34980, 2012.
- [17] K. Manzos and L. Paptheodorou, "The healing potential of the periosteum molecular aspects," *Injury*, vol. 36, no. Suppl 3, pp. S13-S19, 2005.
- [18] A. Eyre-Brook, "The periosteum: its function reassessed," *Clinical Orthopaedic Related Research*, pp. 300-307, 1984.

- [19] E. Seeman, "Periosteal bone formation - a neglected determinant of bone strength," *New England Journal of Medicine*, vol. 349, pp. 320-323, 2003.
- [20] B. Merle and P. Garnero, "The multiple facets of periostin in bone metabolism," *Osteoporosis International*, vol. 23, pp. 1199-1212, 2012.
- [21] D. Saris, A. Sanyal, K. An, J. Fitzsimmons and S. O'Driscoll, "Periosteum responds to dynamic fluid pressure by proliferating in vitro," *Journal of Orthopaedic Research*, vol. 17, p. 668, 1999.
- [22] N. Bonnet, K. Standley, E. Bianchi, V. Stadelmann, M. Foti, S. Conway and S. Ferrari, "The matricellular protein periostin is required for sost inhibition and the anabolic response to mechanical loading and physical activity," *Journal of Biological Chemistry*, vol. 284, pp. 35939-35950, 2009.
- [23] M. Stock, H. Schafer, M. Fliegauf and F. Otto, "Identification of novel genes of the bone-specific transcription factor Runx2," *Journal of Bone and Mineral Research*, vol. 19, pp. 959-972, 2004.
- [24] T. Kashima, T. Nishiyama, K. Shimazu, M. Shimazaki, I. Kii, A. Grigoriadis, M. Fukayama and A. Kudo, "Periostin, a novel marker of intramembranous ossification, is expressed in fibrous dysplasia and in c-Fos-overexpressing bone lesions," *Human Pathology*, vol. 40, pp. 226-237, 2009.
- [25] W. Fan, R. Crawford and Y. Xiao, "Structural and cellular differences between metaphyseal and diaphyseal periosteum in different aged rats," *Bone*, vol. 42, pp. 81-89, 2008.
- [26] E. Tonna, "Electron microscopic study of bone surface changes during aging. The loss of cellular control and biofeedback," *Journal of Gerontology*, vol. 33, pp. 163-177, 1978.
- [27] C. Squier, S. Ghoneim and C. Kremenak, "Ultrastructure of the periosteum from membrane bone," *Journal of Anatomy*, vol. 171, pp. 233-239, 1990.
- [28] S. O'Driscoll, D. Saris, Y. Ito and J. Fitzsimmons, "The chondrogenic potential of periosteum decreases with age," *Journal of Orthopaedic Research*, vol. 19, pp. 95-103, 2001.
- [29] D. Li, J. Zhou, F. Chowdhury, J. Cheng, N. Wang and F. Wang, "Role of mechanical factors in fate decisions of stem cells," *Regenerative Medicine*, vol. 6, p. 229, 2011.
- [30] R. Carpenter and D. Carter, "The mechanobiological effects of periosteal surface loads," *Biomechanics and Modeling in Mechanobiology*, vol. 7, p. 227, 2008.
- [31] M. Knothe Tate, T. Falls, S. McBride, R. Atit and U. Knothe, "Mechanical modulation of osteochondroprogenitor cell fate," *International Journal of Biochemistry and Cell Biology*, vol. 40, p. 2720, 2008.
- [32] J. Fritton, E. Myers, T. Wright and M. van der Meulen, "Loading induces site-specific increases in mineral content assessed by microcomputed tomography of the mouse tibia," *Bone*, vol. 36, pp. 1030-1038, 2005.

- [33] C. Soves, "The potential role of megakaryocytes in mechanically mediated bone adaptation," *Thesis for Ph.D. in Biomedical Engineering in the University of Michigan*, 2010.
- [34] D. Kletsas, E. Basdra and A. Papavassiliou, "Effect of protein kinase inhibitors on the stretch-elicited c-Fos and c-Jun up-regulation in human PDL osteoblast-like cells," *Journal of Cell Physiology*, vol. 190, pp. 313-321, 2002.
- [35] L. Chang and M. Karin, "Mammalian MAP kinase signaling cascades," *Nature*, vol. 37, pp. 37-40, 2001.
- [36] M. Karin, "The regulation of AP-1 activity by mitogen-activated protein kinases," *Journal of Biological Chemistry*, vol. 270, pp. 16483-16486, 1995.
- [37] A. Liedert, D. Kaspar, R. Blakytyn, L. Claes and A. Ignatius, "Signal transduction pathways involved in mechanotransduction in bone cells," *Biochemical and Biophysical Research Communications*, vol. 349, pp. 1-5, 2006.
- [38] A. Naik, C. Xie, M. Zuscik, P. Kingsley, E. Schwarz, H. Awad, R. Guldberg, H. Drissi, J. Puzas, B. Boyce, X. Zhang and R. O'Keefe, "Reduced COX-2 expression in aged mice is associated with impaired fracture healing," *Journal of Bone and Mineral Research*, vol. 24, no. 3, pp. 251-264, 2009.
- [39] S. Wimalawansa, "Nitric oxide and bone," *Annals of the New York Academy of Sciences*, vol. 1192, pp. 391-403, 2010.
- [40] G. Zaman, A. Pitsillides, S. Rawlinson, R. Suswillo, J. Mosley, M. Cheng, L. Platts, M. Hukkanen, J. Polak and L. Lanyon, "Mechanical strain stimulates nitric oxide production by rapid activation of endothelial nitric oxide synthase in osteocytes," *Journal of Bone and Mineral Research*, vol. 14, no. 7, pp. 1123-1131, 1999.
- [41] S. Fox and J. Chow, "Nitric oxide synthase expression in bone cells," *Bone*, vol. 23, pp. 1-6, 1998.
- [42] S. Fox, T. Chambers and J. Chow, "Nitric oxide is an early mediator of the increase in bone formation by mechanical stimulation," *American Journal of Physiology*, vol. 270, no. 6 Pt.1, pp. E955-E960, 1996.
- [43] J. Klein-Nulend, C. Semeins, N. Ajubi, P. Nijweide and E. Burger, "Pulsating fluid flow increases nitric oxide (NO) synthesis by osteocytes but no periosteal fibroblasts - correlation with prostaglandin upregulation," *Biochemical and Biophysical Research Communications*, vol. 217, no. 2, pp. 640-648, 1995.
- [44] J. Rubin, T. Murphy, L. Zhu, E. Roy, M. Nanes and X. Fan, "Mechanical strain differentially regulates endothelial nitric-oxide synthase and receptor activator of nuclear kappa B ligand expression via ERK 1/2 MAPK," *Journal of Biological Chemistry*, vol. 278, pp. 34018-34025, 2003.
- [45] C. Punjabi, D. Laskin, D. Heck and J. Laskin, "Production of nitric oxide by murine bone marrow cells: inverse correlation with cellular proliferation," *Journal of Immunology*, vol. 149, pp. 2179-2184, 1992.
- [46] E. Burger and J. Klein-Nulend, "Response of bone cells to biomechanical forces in vitro," *Advances in Dental Research*, vol. 13, pp. 93-98, 1999.

- [47] J. Sterck, J. Klein-Nulend, P. Lips and E. Burger, "Response of normal and osteoporotic human bone cells to mechanical stress in vitro," *American Journal of Physiology*, vol. 274, no. 6 Pt.1, pp. E1113-E1120, 1998.
- [48] A. Pitsillides, S. Rawlinson, R. Suswillo, S. Bourrin, G. Zaman and L. Lanyon, "Mechanical strain-induced NO production by bone cells: a possible role in adaptive bone (re)modeling?," *The FASEB Journal*, vol. 9, no. 15, pp. 1614-1622, 1995.
- [49] C. Turner, Y. Takano, I. Owan and G. Murrell, "Nitric oxide inhibitor L-Name suppresses mechanically induced bone formation in rats," *American Journal of Physiology*, vol. 270, no. 4 Pt.1, pp. E634-E639, 1996.
- [50] T. Zappitelli and J. Aubin, "The "connexin" between bone cells and skeletal functions," *Journal of Cellular Biochemistry*, vol. 115, pp. 1646-1658, 2014.
- [51] S. Lloyd, A. Loiselle, Y. Zhang and H. Donahue, "Shifting paradigms on the role of Connexin43 in the skeletal response to mechanical load," *Journal of Bone and Mineral Research*, vol. 29, no. 2, pp. 275-286, 2014.
- [52] S. Lloyd and H. Donahue, "Gap junctions and biophysical regulation of bone cells," *Clinical Review of Bone and Mineral Metabolism*, vol. 8, pp. 189-200, 2010.
- [53] A. Alford, C. Jacobs and H. Donahue, "Oscillating fluid flow regulates gap junction communication in osteocytic MLO-Y4 cells by an ERK1/2 MAP kinase-dependent mechanism," *Bone*, vol. 33, pp. 64-70, 2003.
- [54] B. Cheng, S. Zhao, J. Luo, E. Sprague, L. Bonewald and J. Jiang, "Expression of functional gap junctions and regulation by fluid flow in osteocyte-like MLO-Y4 cells," *Journal of Bone and Mineral Research*, vol. 16, pp. 249-259, 2001.
- [55] F. Asumda and P. Chase, "Age-related changes in rat bone-marrow mesenchymal stem cell plasticity," *BMC Cell Biology*, vol. 12, p. 44, 2011.
- [56] D. Genetos, Z. Zhou, Z. Li and H. Donahue, "Age-related changes in gap junctional intercellular communication in osteoblastic cells," *Journal of Orthopaedic Research*, vol. 30, pp. 1979-1984, 2012.
- [57] L. Lanyon and T. Skerry, "Postmenopausal osteoporosis as a failure of bone's adaptation to functional loading: a hypothesis," *Journal of Bone and Mineral Research*, vol. 16, no. 11, pp. 1937-1947, 2001.
- [58] S. Donahue, C. Jacobs and H. Donahue, "Flow-induced calcium oscillations in rat osteoblasts are age, loading frequency, and shear stress dependent," *American Journal of Physiology - Cell Physiology*, vol. 281, pp. C1635-C1641, 2001.
- [59] S. Evans, H. Chang and M. Knothe Tate, "Elucidating multiscale periosteal mechanobiology: a key to unlocking the smart properties and regenerative capacity of the periosteum?," *Tissue Engineering: Part B*, vol. 19, no. 2, pp. 147-159, 2013.
- [60] L. McNamara, A. Edvernn, C. Lyons, C. Price, M. Schaffler, H. Weinans and P. Prendergast, "Strength of cancellous bone trabecular tissue from normal, ovariectomized and drug-treated rats over the course of ageing," *Bone*, vol. 39, pp. 392-400, 2006.

- [61] B. Mulvihill and P. Prendergast, "Mechanobiological regulation of the remodelling cycle in trabecular bone and possible biomechanical pathways for osteoporosis," *Clinical Biomechanics*, vol. 25, pp. 491-498, 2010.
- [62] H. Isaksson, M. Malkiewicz, R. Nowak, H. Helminen and J. Jurvelin, "Rabbit cortical bone tissue increases its elastic stiffness but becomes less viscoelastic with age," *Bone*, vol. 47, pp. 1030-1038, 2010.
- [63] T. Popowics, Z. Zhu and S. Herring, "Mechanical properties of the periosteum in the pig, *Sus scrofa*," *Archives of Oral Biology*, vol. 47, p. 733, 2002.
- [64] S. McBride and M. Knothe-Tate, "Modulation of stem cell shape and fate B: mechanical modulation of cell shape and gene expression," *Tissue Engineering Part A*, vol. 14, p. 1573, 2008.
- [65] M. Song, D. Dean and M. Knothe-Tate, "In situ spatiotemporal mapping of flow fields around seeded stem cells at the subcellular length scale," *PLoS One*, vol. 5, p. e12796, 2010.
- [66] J. Zimmerman and M. Knothe-Tate, "Structure-function relationships in the stem cell's mechanical world A: seeding protocols as a means to control shape and fate of live stem cells," *Molecular and Cellular Biomechanics*, vol. 8, p. 275, 2011.
- [67] H. Frost, "Bone's mechanostat: a 2003 update," *The Anatomical Record. Part A, Discoveries in Molecular, Cellular, and Evolutionary Biology*, vol. 275, pp. 1081-1101, 2003.
- [68] C. Neidlinger-Wilke, I. Stalla, L. Claes, R. Brand, I. Hoellen, S. Rubenacker, M. Arand and L. Kinzl, "Human osteoblasts from younger normal and osteoporotic donors show differences in proliferation and TGF beta-release in response to cyclic strain," *Journal of Biomechanics*, vol. 28, no. 12, pp. 1411-1418, 1995.
- [69] A. van Wijnen, J. van de Peppel, J. van Leeuwen, J. Lian, G. Stein, J. Westendorf, M.-J. Oursler, H.-J. Im, H. Taipaleenmaki, E. Hesse, S. Riester and S. Kakar, "MicroRNA functions in osteogenesis and dysfunctions in osteoporosis," *Current Osteoporosis Report*, vol. 11, pp. 72-82, 2013.
- [70] J. Klein-Nulend, J. Sterck, C. Semeins, P. Lips, M. Joldersma, J. Baart and E. Burger, "Donor age and mechanosensitivity of human bone cells," *Osteoporosis International*, vol. 13, pp. 137-146, 2002.
- [71] J. Cao, L. Venton, T. Sakata and B. P. Halloran, "Expression of RANKL and OPG correlates with age-related bone loss in male C57Bl/6 mice," *Journal of Bone and Mineral Research*, vol. 18, pp. 270-277, 2003.

Figures: Chapter IV



Figure 4. 1 - Axial compressive loading system.

From DeSouza *et al* 2005 [15].

Table 4. 1 - Preliminary results for mechanoreponse in tibial loading.

Values represent fold-changes in gene expression compared to unloaded control limb.

	c-fos	Runx2	Gja1
C57 (15 min)	4.50	0.99	0.67
CBA (20 min)	6.21	1.07	1.09
C57 (30 min)	10.35	1.03	2.98

Table 4. 2 – PrimeTime® qPCR primers and sequences.

Target	Gene Name	RefSeq Number	IDT Assay Name	Sequence
c-Fos	<i>Fos</i>	NM_010234	Mm.Pt.56a.29988214	5'-GGCACTAGAGACGGACAGAT-3' 5'-ACAGCCTTTCCTACTACCATTTC-3'
COX-2	<i>Ptgs2</i>	NM_011198	Mm.PT.58.14196835	5'-ACATTGTAAGTAGGTGGACTGTC-3' 5'-GCACTACATCCTGACCCACT-3'
eNOS	<i>Nos3</i>	NM_008713	Mm.PT.58.12579546	5'-TGGTCCACTATGGTCACTTTG-3' 5'-CTTGAGGATGTGGCTGTGT-3'
Cx43	<i>Gja1</i>	NM_010288	Mm.PT.56a.5955325	5'-GACCTTGTCCAGCAGCTTC-3' 5'-CCTTTGACTTCAGCCTCCAA-3'
β 2m	<i>B2m</i>	NM_009735	Mm.PT.39a.22214835	5'-GGGTGGAAGTGTGTTACGTAG-3' 5'-TGGTCTTTCTGGTGCTTGTC-3'

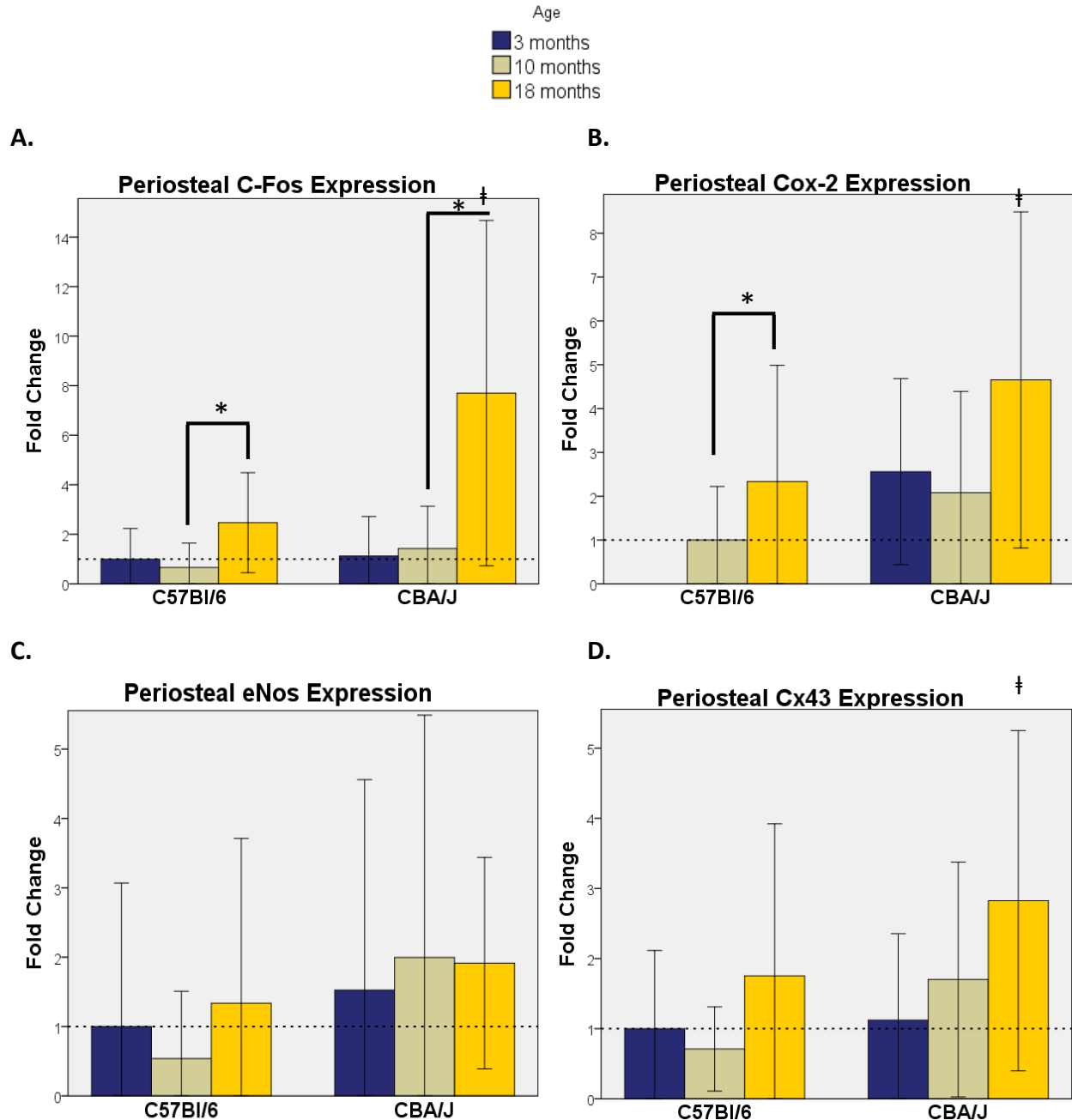


Figure 4. 2 - Periosteal gene expression.

Graphs represent fold change in gene expression with $\beta 2m$ as housekeeping gene and the left (unloaded) limb as control. Fold changes are normalized to the C57Bl/6, 3 month mean for reference. One-way ANOVA are run within strains on the ddC(t) values. T-tests are run between strains at the same age. * signifies p -value ≤ 0.05 in pairwise comparisons within strains. † signifies p -value ≤ 0.05 in t-tests between strains at the same age. **A) Periosteal *c-fos*** – Differences in expression are significant in C57Bl/6 ($p=0.045$). The difference in expression between 10 and 18 months is a 1.62-fold increase ($p=0.047$). Difference in expression in CBA/J is significant ($p=0.032$). The expression at 18 months is 5.6-fold greater than expression at 3 months ($p=0.081$) and 5.8-fold greater than expression at 10 months ($p=0.046$). Periosteal expression of *c-fos* is significantly greater in the CBA/J 18-month group than the

C57Bl/6 18-month group ($p=0.006$). **B) Periosteal *cox-2*** – Differences in expression between the 10-month and 18-month means are significant in C57Bl/6 mice, representing a 2.03-fold increase ($p=0.025$). Since there is no 3-month group, C57Bl/6 10-month mean is used as reference. In the CBA/J mice, difference in expression does not quite reach significance ($p=0.118$). Periosteal *cox-2* expression is significantly greater in the CBA/J 18-month mice than the C57Bl/6 18-month mice ($p=0.003$). **C) Periosteal *eNos*** – Differences between C57Bl/6 age groups is not significant ($p=0.406$). The CBA/J mean differences are also not significant ($p=0.368$). **D) Periosteal *Cx43 (gja1)*** – Age groups are not significantly different in C57Bl/6 mice ($p=0.183$) or in CBA/J mice ($p=0.202$). However, t-test comparison of 18-month means demonstrate a significantly greater level of expression in the CBA/J mice compared to the C57Bl/6 mice ($p=0.016$).

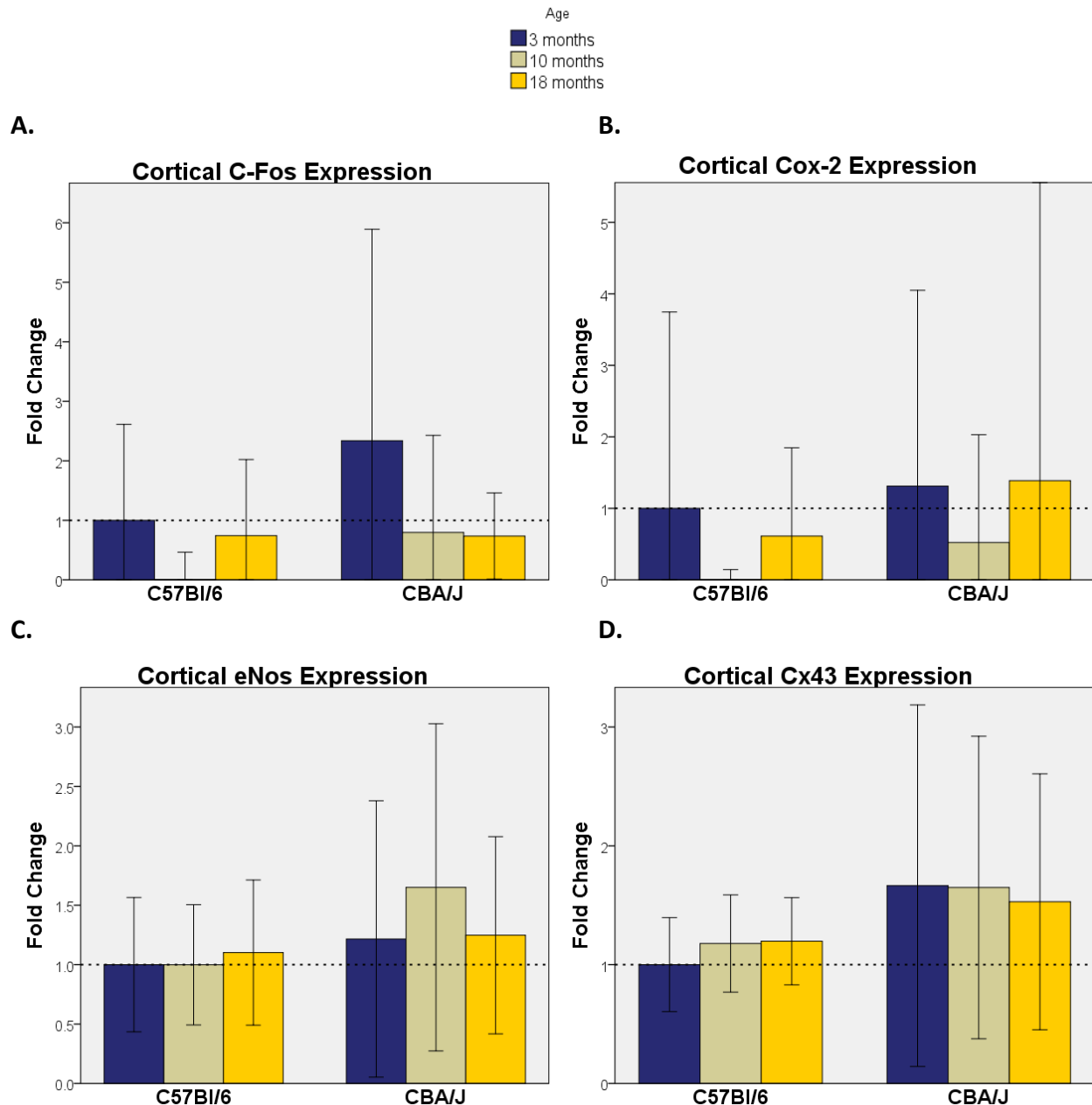


Figure 4. 3 - Cortical gene expression.

Graphs represent fold change in expression with $\beta 2m$ as housekeeping gene and unloaded limb as control. Fold changes normalized to C57Bl/6, 3-month mean for reference. One-way ANOVA are run within strains on the ddC(t) values. T-tests are run between strains at the same age. * signifies p -value ≤ 0.05 for ANOVA pair-wise comparisons. † signifies p -value ≤ 0.05 in t-tests between strains at the same age. **A) Cortical *c-fos*** – Differences in expression in C57Bl/6 mice are not significant ($p=0.171$). The differences in CBA/J mice are also not significant ($p=0.345$). **B) Cortical *cox-2*** – Differences in expression in C57Bl/6 mouse age groups are not significant ($p=0.163$). The differences are also not significant in the CBA/J mice ($p=0.861$). **C) Cortical *eNos*** – Differences between the age groups are not significant in either the C57BL/6 mice ($p=0.926$) or the CBA/J mice ($p=0.848$). **D) Cortical Cx43 (*gja1*)** – Expression is not significantly different between age groups in C57BL/6 mice ($p=0.431$) or CBA/J mice ($p=0.992$).

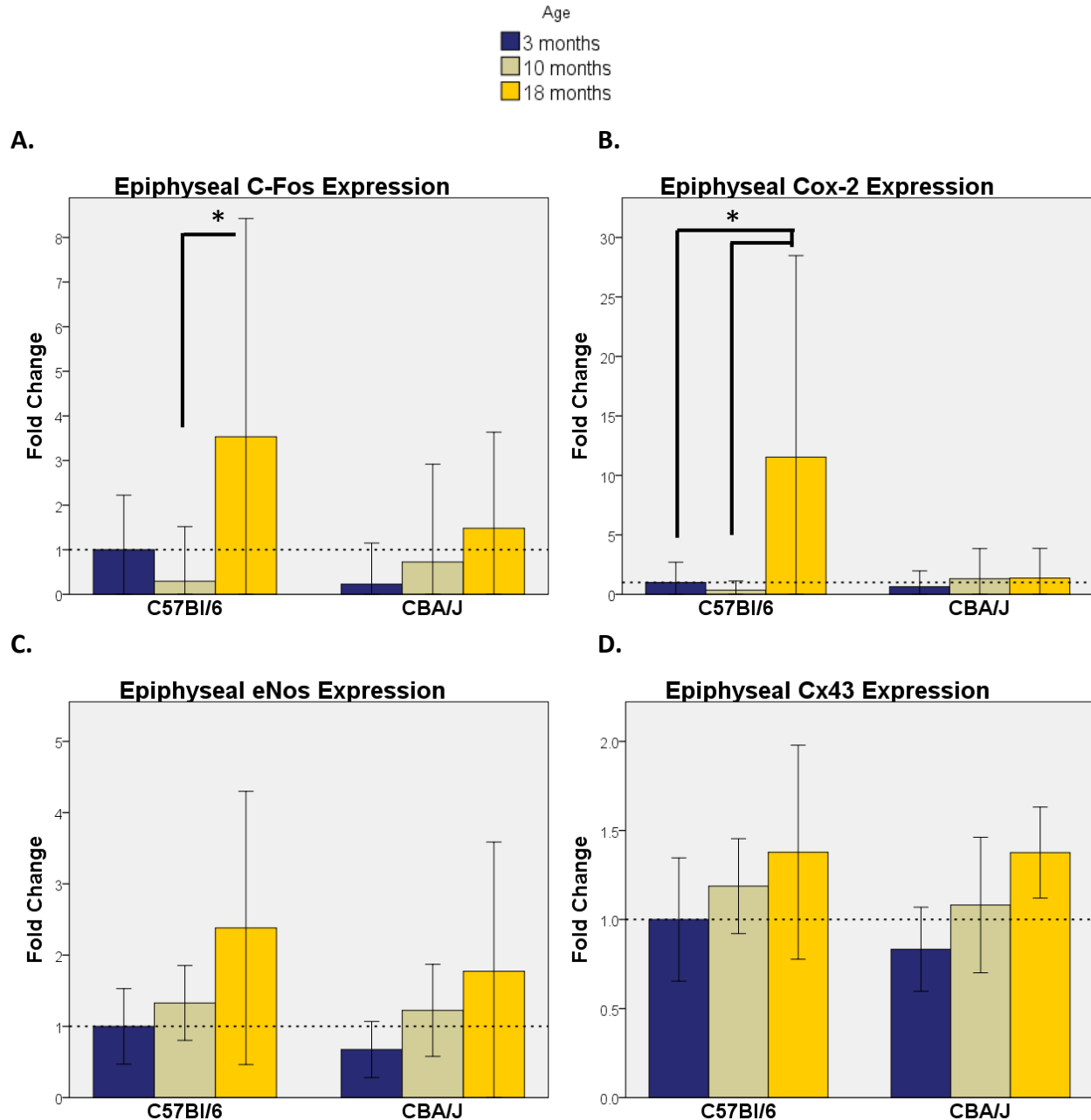


Figure 4. 4 - Epiphyseal gene expression.

Graphs represent fold change in gene expression with $\beta 2m$ as housekeeping gene and the left (unloaded) limb as control. Fold changes are normalized to the C57Bl/6, 3 month mean for reference. One-way ANOVA are run within strains on the ddC(t) values. T-tests are run between strains at the same age. * signifies p -value ≤ 0.05 in pairwise comparisons within strains. † signifies p -value ≤ 0.05 in t-tests between strains at the same age. **A) Epiphyseal *c-fos*** – Differences in expression are significant in C57Bl/6 ($p=0.036$). With the 10-month and 18-month difference in means representing a 3.23-fold difference in expression ($p=0.033$). Expression in the CBA/J age groups is invariant ($p=0.562$). **B) Epiphyseal *cox-2*** – The difference in expression between ages in the C57Bl/6 strain is significant ($p=0.008$). The 18-month expression is 10.54-fold greater than the 3-month expression ($p=0.026$) and 12.19 -fold greater than the 10-month expression ($p=0.012$). There is no difference in expression in the

CBA/J age groups ($p=0.885$). **C) Epiphyseal *eNos*** – Differences between C57Bl/6 age groups is not significant ($p=0.153$), nor are the differences in the CBA/J age groups ($p=0.229$). **D) Epiphyseal *Cx43 (gja1)*** – Age groups are not significantly different in C57Bl/6 mice ($p=0.148$). The differences in the CBA/J mice near significance ($p=0.072$) with the difference between 3- and 18-month means not quite reaching the level of significance ($p=0.081$).

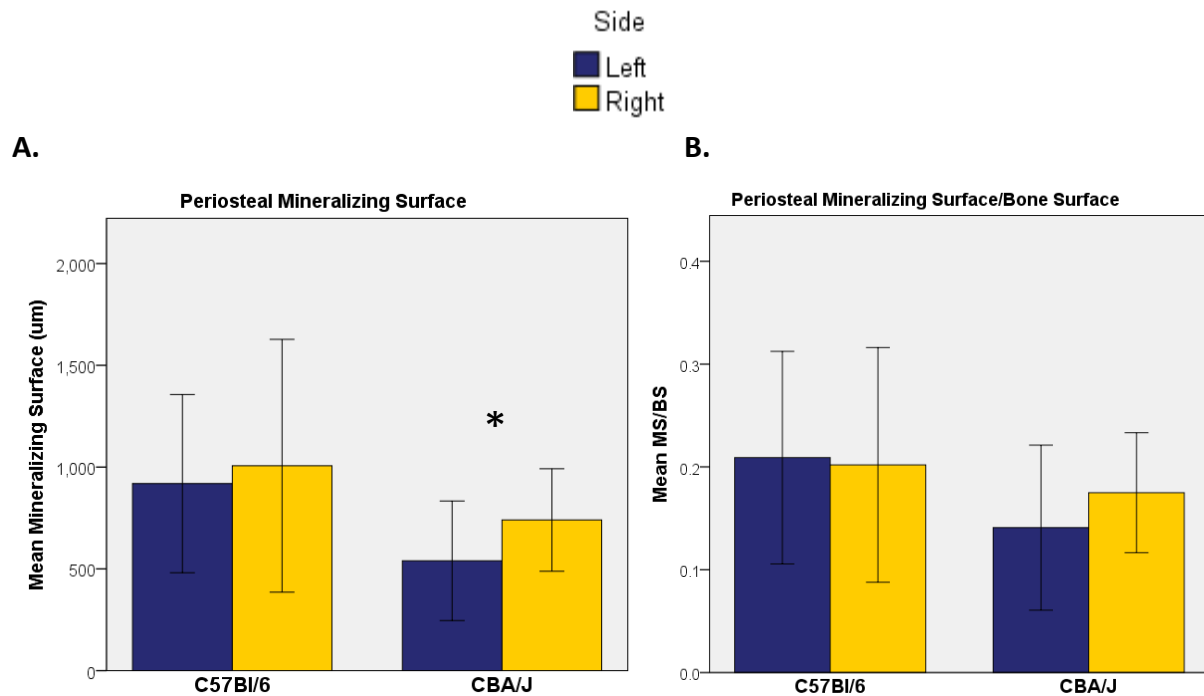


Figure 4. 5 - Periosteal dynamic histomorphometry.

Graphs demonstrate the comparisons between loaded (right) and unloaded control (left) tibiae in 3-month C57Bl/6 and CBA/J mice. Paired t -tests are run to test for differences in means within strains. * signifies significant difference between loaded and unloaded means. **A) Periosteal Mineralizing Surface** – In the C57Bl/6 mice, means for mineralizing surface of the periosteum are 918.93 (± 437.68) μm in the left limb and 1006.6 (± 620.94) μm in the right limb. This is not a significant difference ($p=0.702$). There is a significant increase in mineralizing surface in the CBA/J tibiae when loaded ($p=0.048$). The mean for the left tibiae is 539.93 (± 293.67) μm . The right tibia mean is 740.27 (± 251.83) μm . **B) Periosteal Mineralizing Surface/Bone Surface (MS/BS)** – The mean MS/BS for C57Bl/6 control limb is 0.209 (± 0.103). The mean of the loaded limb is 0.202 (± 0.114). This is not a significant difference between loaded and unloaded limbs ($p=0.849$). The CBA/J MS/BS means are also not significantly different ($p=0.295$) with a control mean of 0.141 (± 0.080) and a loaded mean of 0.175 (± 0.058).

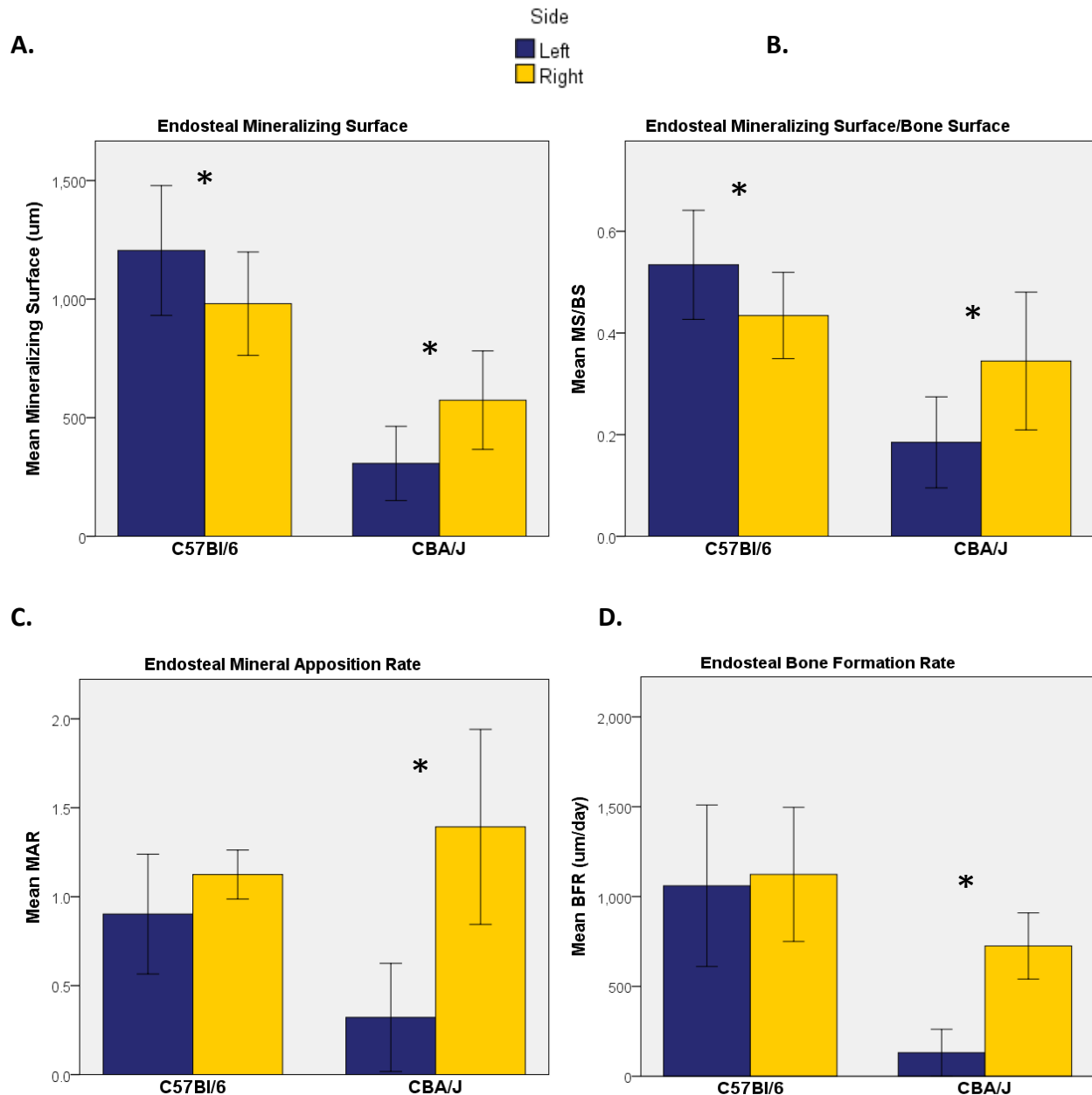


Figure 4. 6 - Endosteal dynamic histomorphometry.

Graphs demonstrate comparisons between loaded (right) and unloaded control (left) tibiae in 3-month C57Bl/6 and CBA/J mice. Paired *t*-tests are run to test for differences in means within strains. * signifies significant difference between loaded and unloaded means. **A) Endosteal Mineralizing Surface (MS)** – Average MS in the C57Bl/6 left (control) limb is 1204.92 (± 273.55) μm . The average MS of the right (loaded) limb is 980.76 (± 218.03) μm . This is a significant drop in MS on the endosteal surface of C57Bl/6 mice following the experimental loading ($p=0.042$). There is also a significant difference in loaded and unloaded means in the CBA/J mice ($p=0.021$). However, in this strain, the unloaded mean of 306.93 (± 156.49) μm is less than the loaded mean of 573.88 (± 207.51) μm . **B) Endosteal MS/BS** – There is a significantly lower MS/BS ratio in the C57Bl/6 loaded limbs—with a mean of 0.434 (± 0.085)—compared

to the unloaded, control limbs that had a mean of $0.534 (\pm 0.107)$ ($p=0.053$). Conversely, in the CBA/J strain, the mean MS/BS of the loaded limbs is $0.345 (\pm 0.140)$ greater than that of the unloaded limbs (0.185 ± 0.090) ($p=0.028$). **C) Endosteal Mineral Apposition Rate (MAR)** – The average MAR for the C57Bl/6 unloaded limbs is $0.902 (\pm 0.337)$ $\mu\text{m/day}$ and for the loaded limbs is $1.124 (\pm 0.138)$ $\mu\text{m/day}$. There is not a significant difference between the MAR of loaded and unloaded limbs in the C57Bl/6 mice ($p=0.264$). MAR in the CBA/J tibiae is significantly greater in the loaded limb (1.393 ± 0.548 $\mu\text{m/day}$) compared to the unloaded limb (0.322 ± 0.304 $\mu\text{m/day}$) ($p=0.031$). **D) Endosteal Bone Formation Rate (BFR)** – Bone formation rate is not different in the C57Bl/6 loaded (1123.39 ± 373.43 $\mu\text{m/day}$) and unloaded (1060.10 ± 449.17 $\mu\text{m/day}$) limbs ($p=0.693$). The average BFR of the CBA/J loaded (724.97 ± 183.91 $\mu\text{m/day}$) and unloaded (131.73 ± 130.25 $\mu\text{m/day}$) limbs are significantly different ($p=0.001$).

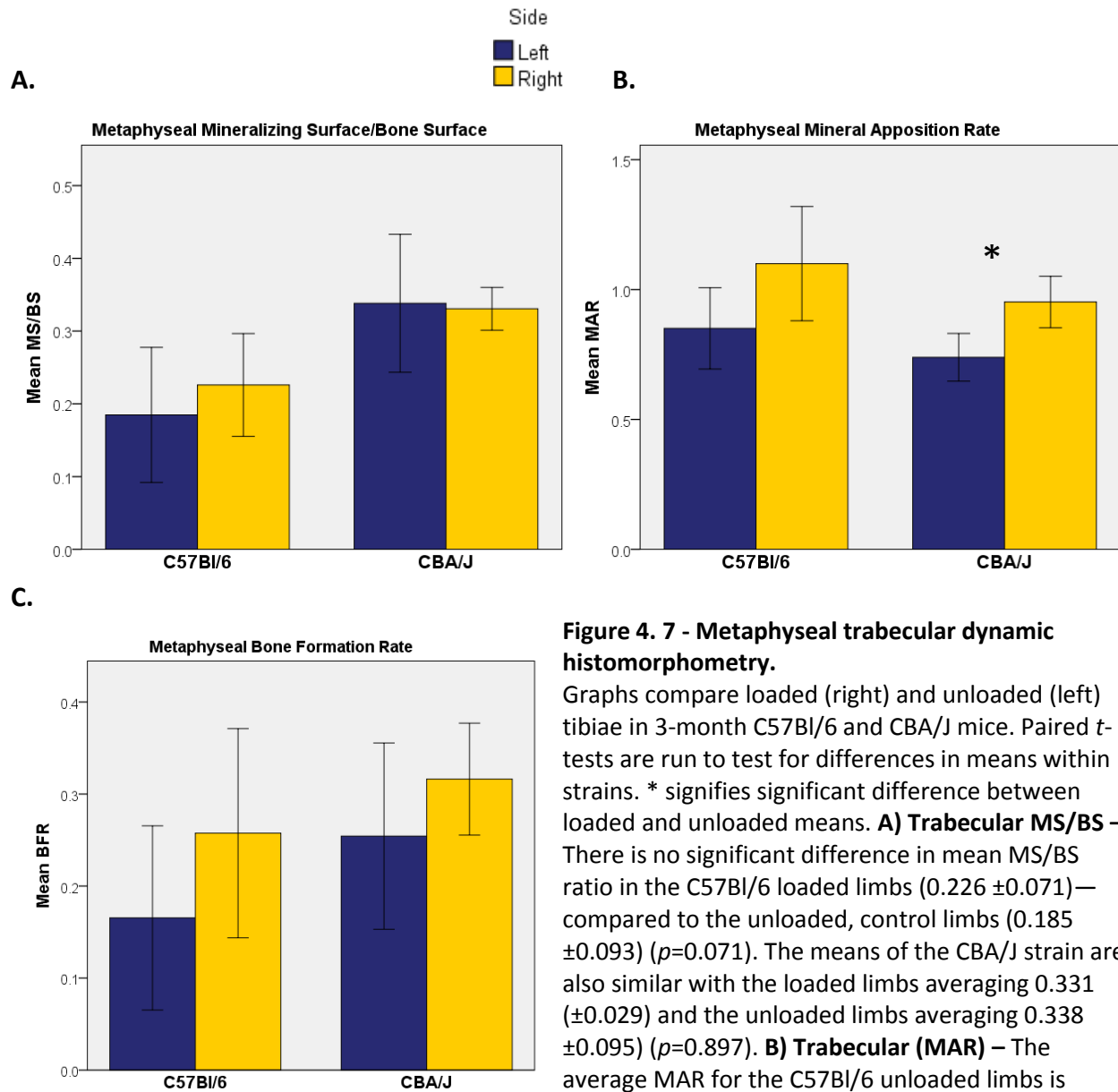


Figure 4. 7 - Metaphyseal trabecular dynamic histomorphometry.

Graphs compare loaded (right) and unloaded (left) tibiae in 3-month C57Bl/6 and CBA/J mice. Paired *t*-tests are run to test for differences in means within strains. * signifies significant difference between loaded and unloaded means. **A) Trabecular MS/BS** – There is no significant difference in mean MS/BS ratio in the C57Bl/6 loaded limbs (0.226 ± 0.071)—compared to the unloaded, control limbs (0.185 ± 0.093) ($p=0.071$). The means of the CBA/J strain are also similar with the loaded limbs averaging $0.331 (\pm 0.029)$ and the unloaded limbs averaging 0.338 ± 0.095 ($p=0.897$). **B) Trabecular (MAR)** – The average MAR for the C57Bl/6 unloaded limbs is $0.851 (\pm 0.157) \mu\text{m/day}$ and for the loaded limbs is

$1.100 (\pm 0.220) \mu\text{m/day}$. There is not a significant difference between the MAR of loaded and unloaded limbs in the C57Bl/6 mice ($p=0.092$). MAR in the CBA/J tibiae is significantly greater in the loaded limb ($0.952 \pm 0.099 \mu\text{m/day}$) compared to the unloaded limb ($0.739 \pm 0.092 \mu\text{m/day}$) ($p=0.015$). **C) Trabecular (BFR)** – Bone formation rate is greater in the C57Bl/6 loaded limbs ($0.257 \pm 0.114 \mu\text{m/day}$) and unloaded ($0.165 \pm 0.100 \mu\text{m/day}$) limbs ($p=0.019$). The average BFR of the CBA/J loaded ($0.316 \pm 0.061 \mu\text{m/day}$) and unloaded ($0.254 \pm 0.101 \mu\text{m/day}$) limbs are not significantly different ($p=0.275$).

Control (Left)



Loaded (Right)

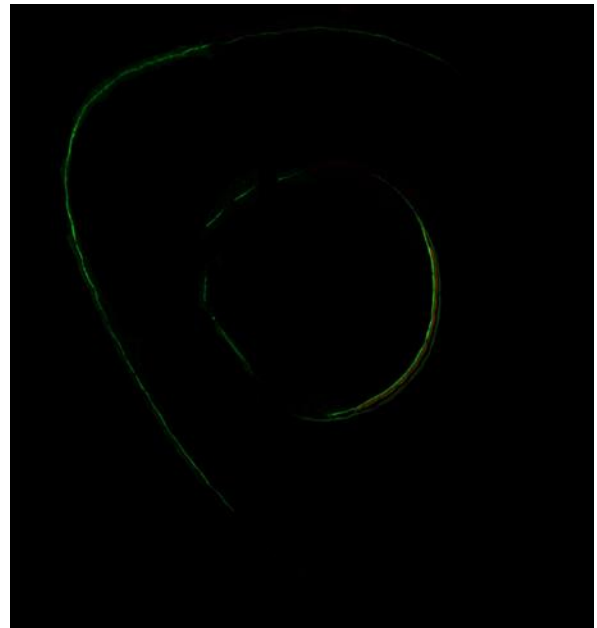


Figure 4. 8 - Representative images of CBA/J diaphysis in control (left) and loaded (right) limbs.

CHAPTER V: CONCLUSIONS AND FUTURE WORK

Mouse Model for Human Bone Aging

Humans are unique amongst other most organisms in their ability to live beyond reproductively viable years. This has only been witnessed in a handful of other species, and many of these only in captivity [1]. Only recently have humans achieved this ability which is largely due to increased cultural advancements preventing earlier death [1]. The term “aging” is used here to describe the process of decline in biological function that occur after reaching maturity. How and why the aging process occurs has been debated in the field. One argument states that age-related loss of function is a stochastic process due to an accumulation of errors in cells over time [2, 3, 4, 5]. The molecular views of aging include the somatic mutation, telomere loss, mitochondrial, altered protein, waste accumulation, and ROS theories [3]. Many of these concepts are based on the biophysicist notion that the processes involved in aging are products of imperfect repair and replication leading to an increase in entropy [6].

Weismann’s theory of “programed death” is another highly debated view of aging. This theory states that natural selection has resulted in aging in order to remove competing members of a population to make way for the next generations [3]. Another approach was presented by Medawar and attributes aging to the declining effectiveness of natural selection to act on the post-reproductive population [2, 5]. Natural selection acts on the breeding population leading to the more successful biological variants reproducing more effectively. Therefore, natural selection is unable to influence adaptations that promote living after an individual’s reproductive years [5,7].

The theory of aging ascribed to here argues that senescence is a byproduct of earlier developmental and life history patterns [3, 8, 9] that have evolved through selection. These early life adaptation, with little selective force acting late in life, ultimately lead to maladaptive

traits in old age. Humans have evolved to survive highly heterogeneous environments and as a k-selective species. In order to accommodate these demands, humans have evolved a high level of plasticity in order to acclimate to changing environments [10]. This, in combination with parental investment requiring long lifespans, has led to a biological system capable of change and repair.

In order to acclimate to changing environments, humans have adapted a high level of plasticity. One example of this capacity can be found in bone biology. Bone has evolved as a repository for resources such as calcium and phosphate that can be accessed for use and deposited for storage [11, 12]. During times of scarcity or when demands on resources are high (e.g. pregnancy and lactation) the body can access these stored nutrients for use. Once the demand on resources has alleviated, new bone can be added in anticipation for the next period of need. Bone is also responsible for biomechanical functions in support and movement. As mechanical demands change, bone is able to acclimate in order to most efficiently prevent fracture [13, 14]. Vast amounts of research have focused on bone adaptive response to increased loading and mechanical demand [15, 16, 17, 18]. Additionally, when bone is not as critical in locomotion (e.g. prolonged bed rest or microgravity environments) it is resorbed so resources are not tied up in superfluous bone mass [16, 19, 20].

As an organism ages, this adaptive mechanism loses efficacy due to cellular and molecular senescence [2]. The remodeling ability of bone, previously critical to survival, loses regulation leading to unbalanced resorption and deposition [21, 22, 23]. These changes result in excess resorption relative to deposition and an overall loss in bone leading to increased risk of fragility fractures. However, not all humans experience the same patterns of bone aging. Cummings and Melton estimate that 40-50% of women [24, 25] and 13% of men [26] over the age of 50 will have a fragility fracture in their remaining lifetime.

Aging is highly dependent upon an individual's life history, as well. Organisms with shorter life expectancy due to predation, disease, or environmental stresses are more likely to have an early investment in reproduction. Humans, evolving with lower predation and highly variable environments, developed a reproductive strategy that includes long-term parental investment, leading to increased life expectancy [1]. Hayflick asserts that organisms that

expend energy and resources quickly and early retain lower excess resources to put towards longevity [1]. Therefore, early biological demands determine the ability and patterns of aging later in life.

There is evidence for this pattern of early-life determinism of aging in the relationship between peak bone mass and aging-induced skeletal fragility [27, 28]. An interesting avenue for research includes investigating the correlation between peak bone mass and longevity. Men have shortened life expectancy than women but have also been reported to maintain skeletal function better [29]. Women have higher reproductive investment than men and may therefore have less resources available for bone maintenance upon reaching old age.¹² Men also are 2.9 times more likely to sustain a fracture between the ages of 15-59 [30]. The greater need to repair bone during reproductively active ages in men may have protective consequences later in life. The maintenance of the remodeling system is might be more efficient in older aged men than women, but at the energetic cost of lifespan. These trends may be indicative of a trade-off between energetic demands on bone homeostasis and resources allocated to prolong life expectancy.

While interesting theories, there is a severe lack of research into the life history and evolutionary trade-offs involved in human age progression. The study of human aging is exceedingly difficult and time intensive. The high levels of genetic and environmental heterogeneity make the influences of aging hard to isolate and interpret. Furthermore, humans have a relatively long lifespan, making longitudinal studies difficult. Cross-sectional studies have been used but have their own inherent flaws when making inferences from the data. For these reasons, there currently is insufficient understanding of the variability in how human bones age. The murine model of variation in aging presented in this thesis is an attempt to demonstrate the need for further study of differences within a species.

Mouse models provide reduction in confounding variables and high levels of experimental control, however, using mice as a proxy for human aging is an imperfect approach as variable patterns of aging have been recorded even within littermates [31]. These models fall

¹² The terms “men” and “women” are used here to describe chromosomal sex and are used for clarity when referencing humans and not animal models.

short based on the quite obvious fact that mice and humans are not synonymous. Aging studies often use species with short lifespans due to the increased rate of senescence. Yet the very reason these models are so attractive to researchers is also why they are not necessarily indicative of human aging. Wild mice have evolved under extreme predation pressures and therefore have a life history pattern of rapid maturation with large and early investment in offspring until death. For this reason, mice have not evolved with a need to conserve resources for later in life. Investigators must approach murine models of geriatric studies with caution, recognizing the inherent differences between the physiologies of the species that arose due to very different selective pressures.

The goal of the first aim of this thesis was to determine if the femora of four different inbred strains of mice change differently with age, with the intent to provide models of intraspecies aging variation. We found that two of the strains, BALB/c and C57Bl/6 have lower mean ultimate loads under 4-point bending in the 18-month mice compared to the 3-month mice. The CBA/J strain had higher mean ultimate loads in the 18-month group when compared to the 3-month group. The fourth strain, DBA/2, had no difference in mean ultimate load values between the two age groups.

In the BALB/c strain, the combination of mechanical and morphological data indicates a loss of strength due to non-geometric changes. The reduced strength is due to the lower mineralization and matrix changes reducing post-yield properties. In the C57Bl/6 old mice, mechanical data demonstrate a reduction in strength, stiffness, and ductility. The loss of strength can be attributed to both the mineralization and matrix changes, as in BALB/c, but also to geometric changes. The loss of strength and stiffness is partly due to the marrow expansion without adequate periosteal compensation. In contrast to the first two strains, the CBA/J mice increase ultimate load with age. Stiffness is also greater in the older animals compared to the 3-month mice. The mineralization, matrix, and endosteal changes are compensated for by periosteal expansion in CBA/J aging. Lastly, the DBA/2 mice had no change in ultimate load with aging. As with the CBA/J mice, stiffness was greater in the older animals. Unique to the DBA/J mice, the older animals did not experience altered PYD or TMD. This indicates minimal changes to the composition of the bone throughout the aging process. Similar to the CBA/J mice, the

DBA/2 strain is able to compensate for the endosteal resorption by adding bone to the periosteal surface.

With respect to bone aging, specifically, there are additional reasons for caution in using mouse models. There is the obvious issue of difference in locomotor patterns. Latimer argues that the shift to bipedality has, in fact, increased our risk of age-induced fragility due to a greater need for trabecular bone which is easily resorbed later in life [32]. So we cannot assume the same functional demands in mice and humans. Mice do not employ BMU-based remodeling as do larger mammals [33]. Bone fragility in older humans is largely a product of unbalanced remodeling [21] and this could provide concerns with inferences taken from mouse studies of aging.

Despite the inevitable drawbacks to using rodent models as a proxy for human biology, the ability to compare inbred strains provides insight into the energetic and life history approach to aging. The use of mice allows researchers to investigate the intraspecies variation and how genetic and environmental factors influence aging. In the C57Bl/6 and CBA/J strains, the C57Bl/6 mice have significantly longer average lifespans [34, 35]. Applying the resource investment approach, it is not surprising that the C57Bl/6 mice also experience reduced bone strength due to unbalanced remodeling. The wide and thin diaphysis of the C57Bl/6 long bones provides greater surface area for endosteal resorption, providing more rapid access to resources required to sustain the animal. Conversely, the maintenance of bone in the CBA/J strain may come at the expense of life span.

The second aim of this work was to look more closely at the C57Bl/6 and CBA/J strains, and determine when age-related changes initiate. In addition to this question, we sought to determine if aging changes of the femur are the same in the tibia. The final goal of this section was to correlate changes in the cortical bone to changes in the trabecular region with age. C57Bl/6 mice experience a steady decline in ultimate load and stiffness after 10 months. Unlike the C57Bl/6 femoral patterns, the tibial decrease in ultimate load is independent of changes to stiffness. The lack of change in stiffness is suggestive of matrix compositional and organizational changes reducing bone strength in the tibia. The CBA/J strain does not elicit changes in ultimate load or stiffness in 18 months. The consistent mechanical properties are due to a

rearrangement of tissue to increase I_y , compensating for loss of mineralization and marrow expansion. The C57Bl/6 strain experienced less bone loss in the trabecular regions than the CBA/J mice. This pattern may represent a trade-off between periosteal deposition and trabecular resorption in the CBA/J mice. The C57Bl/6 strain experiences bone loss in both the cortical and trabecular region and may represent a strategy to disperse the bone loss between the compartments.

Both mouse strains have developmental patterns that produce operational bone phenotypes. Without selection acting on the older animals, these phenotypes are optimized for younger life stages and may be suboptimal upon senescence. The initial shape of the C57Bl/6 diaphyseal bone provides greater endosteal surface area for potential resorption. In order to not over tax this region of bone, some resorption occurs in the trabecular regions, as well. Upon reaching senescence in the CBA/J mice, due to low surface area on the marrow side, less resorption can take place leading to less severe bone loss. This strain also appears to continue periosteal deposition on bone throughout aging. The addition of bone may come at the expense of the already sparse trabecular bone. These represent two very different strategies to maintain bone function during aging that is partly regulated by the morphology of the bones while young.

Young adult bones of humans and mice are designed to be responsive to environmental stimuli. Just as humans have evolved in highly heterogeneous environments, mice also live on every continent except Antarctica [36, 37]. Thus, mice provide a good model in the sense that they also have evolved with the need for acclimation to various environments. Human fragility fractures are in large part due to the unbalanced resorption and deposition of bone [2, 21, 22, 23]. As in humans [15, 16, 17, 18], mice are able to alter bone phenotype in response to various stressors. One of the best studied demand for remodeling is the responsiveness to changes in mechanical loading [38, 39].

The third aim acts as a preliminary study approaching the question of how changes in the mechanoresponse could be influencing the variable bone aging patterns in C57Bl/6 and CBA/J strains. A method of axial tibial loading was employed and rtPCR used to measure the difference in responsiveness to load in the various age groups. Due to the continued periosteal

expansion, we predicted that CBA/J mice would experience a consistent response to loading regardless of age in the periosteal and cortical regions. The lack of periosteal expansion in the C57Bl/6 mice led to our prediction that the response in these regions would be lost with age. In the trabecular region, the C57Bl/6 mice had less dramatic trabecular bone loss than the CBA/J, leading to our prediction that C57Bl/6 mice would retain trabecular responsiveness better than CBA/J mice.

No difference in expression of mechanoresponsive genes was measured in the cortical and marrow regions. The CBA/J 18-month animals had a significant increase in response in the periosteum. The C57Bl/6 mice had an increase in expression in the 18-month epiphyseal sample. The predictions were correct by estimating a greater response in the periosteum of the CBA/J and epiphysis of the C57Bl/6. However, the original prediction of not losing response was not supported. Instead of maintaining response with age, the regions increased response in the 18-month groups. The increased response might provide a buffer preventing more severe bone loss. Future work must look at the down-stream effects of these response patterns.

Future Work

This work has contributed to the understanding of phenotypic variability within a single species with respect to bone aging. To add to the confidence in the outcomes, the next step should be to include female mice in the study, as well as run the analyses conducted in Aim 2 on all four strains and in both sexes. Additionally, functional measures from trabecular compression tests should be included. This study utilized very distinct mouse phenotypes by looking at inbred strains. However, the continuum of variation provided by a heterogeneous mouse population would allow increased resolution of correlated factors.

The work here demonstrates the variance in aging, but this study is primarily phenomenological in nature. Future studies should advance on the results demonstrating the variable aging patterns. The model for known aging differences will allow experimental designs aimed at investigating the physiological mechanisms underlying the aging variability. Broadly, comparisons between the strains could be made looking for patterns of aging associated with

genetics¹³, nutrition, activity, hormones, and drug treatments. The different variables could influence bone aging differently in the various strains. Hypothetically, an experiment could be run comparing exercise-based fracture prevention protocols in the C57Bl/6 and CBA/J strains. If one strain reacts well to the protocol and the other does not, it may indicate that exercise treatments are not suitable for all aging humans, as well.

Aim 3 was an attempt to begin to investigate the mechanisms behind the aging differences. Useful information was gained by measuring short-term response and how it differs by strain and location. However, in order to fully comprehend the functional implications of these differences, long-term loading studies must be undertaken. These studies should look at gene regulation following consistent loading protocols to assess bone anabolic response. More importantly, the functional understanding of these responses demands dynamic histomorphometric comparisons of young and old adults, as well as mechanical tests following loading. These results will provide a more comprehensive view of the actual physiologic outcomes of this variation.

Future work should also look more closely at the role of periosteal tissue in the remodeling and aging processes. It is clear from these data that periosteum is a mechanically responsive tissue under some conditions. However, little work has focused on the whole-bone and micro-level periosteum mechanics. Additional studies concerning variation in cellular response and function with aging between the strains would be enlightening, as well. This would require *in vitro* methods. On top of the variation in cell response to aging, the role of ECM aging change on the cellular functionality would provide insight into how cell senescence and the protein-mineral changes with age influence aging independently and in concert.

Finally, more investigation into the amount and sources of variability in human aging is recommended. Currently, diagnostics and treatments are conducted and administered universally. However, there is likely a large degree of variation that these broad-spectrum approaches overlook. People with different bone phenotypes following maturation may require variant preventative and treatment protocols to reduce the risk of fragility fractures in each

¹³ See Appendix Table 3 for list of SNPs.

individual. Once the degree of variability has been established, the mouse models can be utilized to prescribe approaches more specific to individual physiologies.

References: Chapter V

- [1] L. Hayflick, "How and why we age," *Experimental Gerontology*, vol. 33, no. 7/8, pp. 639-653, 1998.
- [2] J. Mitteldorf, "Aging is not a process of wear and tear," *Rejuvenation Research*, vol. 13, no. 2-3, pp. 322-327, 2010.
- [3] T. Goldsmith, "Aging as an evolved characteristic - Weismann's theory reconsidered," *Medical Hypotheses*, vol. 62, pp. 304-308, 2004.
- [4] T. Kirkwood, "Understanding the odd science of aging," *Cell*, vol. 120, pp. 437-447, 2005.
- [5] C. Rauser, L. Mueller and M. Rose, "The evolution of late life," *Ageing Research Reviews*, vol. 5, pp. 14-32, 2006.
- [6] A. Danchin, "Natural selection and immortality," *Biogerontology*, vol. 10, pp. 503-516, 2009.
- [7] T. Garland Jr. and S. Kelly, "Phenotypic plasticity and experimental evolution," *The Journal of Experimental Biology*, vol. 209, pp. 2344-2361, 2009.
- [8] J. a. C. G. de Magalhaes, "Genomes optimize reproduction: aging as a consequence of the developmental program," *Physiology*, vol. 20, pp. 252-259, 2005.
- [9] R. Walker, "Developmental theory of aging revisited: focus on causal and mechanistic links between development and senescence," *Rejuvenation Research*, vol. 14, no. 4, pp. 429-436, 2011.
- [10] D. Nelson, S. Agarwal and L. Darga, "Bone health from an evolutionary perspective: development in early human populations," in *Nutrition and Bone Health*, New York, Springer Science, 2015, pp. 3-20.
- [11] Z. Mackiewicz, W. E. Niklińska, J. Kowalewska and L. Chyczewski, "Bone as a source of organism vitality and regeneration," *Folia Histochemica et Cytobiologica*, vol. 49, no. 4, pp. 558-569, 2011.
- [12] A. Ravaglioli, A. Krajewski, G. Celotti, A. Piancastelli, B. Bacchini, L. Montanari, G. Zama and L. Piombi, "Mineral evolution of bone," *Biomaterials*, vol. 17, pp. 617-622, 1996.
- [13] C. Turner, Y. Takano and I. Owan, "Aging changes mechanical loading thresholds for bone formation in rats," *Journal of Bone and Mineral Research*, vol. 10, no. 10, pp. 1544-1549, 1995.
- [14] J. Currey, "The many adaptations of bone," *Journal of Biomechanics*, vol. 36, pp. 1487-1495, 2003.
- [15] J. Schriefer, S. Warden, L. Saxon, A. Robling and C. Turner, "Cellular accommodation and the response of bone to mechanical loading," *Journal of Biomechanics*, vol. 38, pp. 1838-1845, 2005.
- [16] D. Papachristou, K. Papachroni, E. Basdra and A. Papavassiliou, "Signaling networks and transcription factors regulating mechanotransduction in bone," *BioEssays*, vol. 31, pp. 794-804, 2009.
- [17] C. H. Turner and A. G. Robling, "Mechanisms by which exercise improves bone strength," *Journal of Bone and Mineral Metabolism*, vol. 23, no. Supp1, pp. 16-22, 2005.
- [18] C. H. Turner, "Skeletal adaptation to mechanical loading," *Clinical Reviews in Bone and Mineral Metabolism*, vol. 5, pp. 181-194, 2007.
- [19] A. LeBlanc, V. Schneider, H. Evans, D. Engelbretson and J. Krebs, "Bone mineral loss and recovery after 17 weeks of bed rest," *Journal of Bone and Mineral Research*, vol. 5, pp. 843-850, 1990.
- [20] A. LeBlanc, E. Spector, H. Evans and J. Sibonga, "Skeletal responses to space flight and the bed rest analog: a review," *Journal of Musculoskeletal Neuronal Interactions*, vol. 7, pp. 33-47, 2007.

- [21] F. Syed and A. Ng, "The pathophysiology of the aging skeleton," *Current Osteoporosis Reports*, vol. 8, pp. 235-240, 2010.
- [22] A. Birkhold, H. Raxi, G. Duda, R. Weinkamer, S. Checa and B. Willie, "The influence of age on adaptive bone formation and bone resorption," *Biomaterials*, vol. 35, pp. 9290-9301, 2014.
- [23] S. Srinivasan, B. Ausk, J. Prasad, D. Threet, S. Bain, T. Richardson and T. Gross, "Rescuing loading induced bone formation at senescence," *PLoS Computational Biology*, vol. 6, no. 9, p. e1000924, 2010.
- [24] S. Cummings and L. Melton, "Epidemiology and outcomes of osteoporotic fractures," *Lancet*, vol. 359, no. 9319, pp. 1761-1767, 2002.
- [25] B. L. Clarke and S. Khosla, "Physiology of bone loss," *Radiologic Clinics of North America*, vol. 48, pp. 483-495, 2010.
- [26] A. Tosteson and C. Hammond, "Quality of life assessment in osteoporosis: health-status and preference-based measures," *Pharmacogenomics*, vol. 20, no. 5, pp. 289-303, 2002.
- [27] J. Center and J. Eisman, "Genetics of osteoporosis," in *Primer on the Metabolic Bone Diseases and Disorders of Mineral Metabolism*, C. Rosen, Ed., Washington DC, American Society for Bone and Mineral Research, 2008, pp. 213-219.
- [28] R. Heaney, S. Abrams, B. Dawson-Hughes, A. Looker, R. Marcus, V. Matkovic and C. Weaver, "Peak bone mass," *Osteoporosis International*, vol. 11, pp. 985-1009, 2000.
- [29] J. Lambert, M. Zaidi and J. Mechanick, "Male osteoporosis: epidemiology and the pathogenesis of aging bones," *Current Osteoporosis Reports*, vol. 9, pp. 229-236, 2011.
- [30] B. Singer, J. McLauchlan, C. Robinson and J. Christie, "Epidemiology of fractures in 15,000 adults: the influence of age and gender," *Journal of Bone and Joint Surgery*, vol. 80, pp. 243-248, 1998.
- [31] F. vom Saal, C. Finch and J. Nelson, "Natural history and mechanisms of reproductive aging in humans, laboratory rodents, and other selected vertebrates," in *The Physiology of Reproduction*, Second Edition ed., J. N. E. Knobil, Ed., New York, Raven Press, Ltd., 1994, pp. 1213-1314.
- [32] B. Latimer, "The perils of being bipedal," *Annals of Biomedical Engineering*, vol. 33, no. 1, pp. 3-6, 2005.
- [33] P. Marie, "Bone cell senescence: mechanisms and perspectives," *Journal of Bone and Mineral Research*, vol. 29, no. 6, pp. 1311-1321, 2014.
- [34] R. Yuan, C. Ackert-Bicknell, B. Paigen and L. L. Peters, "Aging study: Lifespan and survival curves for 31 inbred strains of mice," 2007. [Online]. Available: <http://phenome.jax.org/db/q?rtn=projects/projdet&reqprojid=234>. [Accessed 12 December 2014].
- [35] Y. Duan, X. Wang, A. Evans and E. Seeman, "Structural and biomechanical basis of racial and sex differences in vertebral fragility in Chinese and Caucasians," *Bone*, vol. 36, pp. 987-998, 2005.
- [36] R. Berry, "The natural history of the house mouse," *Field Studies*, vol. 3, pp. 219-262, 1970.
- [37] G. Musser and M. Carleton, "Superfamily Muroidea," in *Mammalian Species of the World: a taxonomic and geographic reference*, Third Edition ed., Baltimore, Johns Hopkins University Press, 2005, pp. 894-1531.
- [38] N. Holguin, M. Brodt, M. Sanchez, A. Kotiya and M. Silva, "Adaptation of tibial structure and strength to axial compression depends on loading history in both C57BL/6 and BALB/c mice," *Calcified Tissue International*, vol. 93, pp. 211-221, 2013.
- [39] M. Lynch, R. Main, Q. Xu, D. Walsh, M. Schaffler, T. Wright and M. van der Meulen, "Cancellous bone adaptation to tibial compression is not sex dependent in growing mice," *Journal of Applied Physiology*, vol. 109, pp. 685-691, 2010.

APPENDIX

Table A. 1 - Mean fold change in gene expression

From Chapter IV: Fold change is calculated using $x=2^{\Delta\Delta c(T)}$ with $\beta 2m$ as housekeeping and left (unloaded) limb as control.

Tissue	Gene	C57Bl/6 Fold Change				CBA/J Fold Change			
		3 month	10 month	18 month	p-value	3 month	10 month	18 month	p-value
Periosteal	c-Fos	1.32 ±1.23	0.99 ±0.99	2.8 ±2.02	0.026	1.45 ±1.59	1.75 ±1.71	8.03 ±6.97	0.003
	COX-2	-----	0.91 ±1.22	2.25 ±2.65	0.166	2.47 ±2.12	1.99 ±2.31	4.57 ±3.84	0.174
	eNOS	1.29 ±2.07	0.83 ±0.97	1.63 ±2.38	0.646	1.81 ±3.03	2.28 ±3.48	2.20 ±1.52	0.929
	Cx43	0.86 ±1.11	0.57 ±0.60	1.61 ±2317	0.268	0.98 ±1.23	1.56 ±1.67	2.68 ±2.43	0.151
Cortical	c-Fos	2.18 ±1.61	1.08 ±0.56	1.92 ±1.28	0.133	3.51 ±3.55	1.97 ±1.63	1.91 ±0.72	0.228
	COX-2	2.67 ±2.75	1.17 ±0.64	2.28 ±1.23	0.167	2.98 ±2.74	2.19 ±1.51	3.06 ±4.44	0.794
	eNOS	1.00 ±0.57	0.99 ±0.51	1.10 ±0.61	0.896	1.21 ±1.16	1.64 ±1.38	1.24 ±0.83	0.643
	Cx43	0.84 ±0.40	1.02 ±0.41	1.04 ±0.37	0.472	1.51 ±1.52	1.49 ±1.27	1.37 ±1.08	0.968
Marrow	c-Fos	1.66 ±0.98	1.18 ±0.38	1.52 ±0.54	0.328	1.61 ±0.89	1.25 ±0.39	1.22 ±0.58	0.339
	COX-2	1.85 ±0.89	1.45 ±0.71	1.76 ±0.81	0.552	2.44 ±1.82	1.25 ±0.46	1.69 ±1.02	0.112
	eNOS	1.16 ±0.63	1.21 ±0.52	1.20 ±0.46	0.976	0.88 ±0.43	1.02 ±0.20	1.25 ±0.87	0.363
	Cx43	1.37 ±0.67	1.30 ±0.63	1.22 ±0.33	0.842	0.93 ±0.33	1.15 ±0.21	1.08 ±0.28	0.219
Epiphysis	c-Fos	2.63 ±1.22	1.92 ±1.22	5.16 ±4.88	0.056	1.86 ±0.32	2.36 ±2.19	3.11 ±2.15	0.368
	COX-2	2.63 ±1.70	1.98 ±0.76	13.17 ±16.9	0.028	2.27 ±1.32	2.93 ±2.53	2.99 ±2.50	0.743
	eNOS	1.00 ±0.53	1.33 ±0.52	2.39 ±1.92	0.039	0.68 ±0.39	1.23 ±0.65	1.78 ±1.81	0.143
	Cx43	0.90 ±0.35	1.09 ±0.27	1.28 ±0.60	0.169	0.74 ±0.24	0.98 ±0.38	1.28 ±0.26	0.025

Table A. 2 - Tibial dynamic histomorphometry data

From Chapter IV: Mean values for dynamic histomorphometry in long-term adaptive loading pilot.

Region	Measurement	C57Bl/6			CBA/J		
		Control	Loaded	<i>p</i> -value	Control	Loaded	<i>p</i> -value
Periosteal	Mineralizing surface (µm)	918.93 (±437.68)	1006.6 (±620.94)	0.702	539.93 (±293.67)	740.24 (±251.83)	0.048
	Mineralizing surface/Bone surface	0.209 (±0.103)	0.202 (±0.114)	0.849	0.141 (±0.08)	0.175 (±0.058)	0.295
Endosteal	Mineralizing surface (µm)	1204.92 (±273.55)	980.76 (±218.03)	0.042	306.93 (±156.49)	573.88 (±207.51)	0.021
	Mineralizing surface/Bone surface	0.534 (±0.107)	0.434 (±0.085)	0.053	0.185 (±0.09)	0.345 (±0.14)	0.028
	Mineral apposition rate (µm/day)	0.902 (±0.337)	1.124 (±0.138)	0.264	0.322 (±0.304)	1.393 (±0.548)	0.031
	Bone formation rate (µm/day)	1060.1 (±449.17)	1123.39 (±373.43)	0.693	131.73 (±130.25)	724.97 (±183.91)	0.001
Trabecular	Mineralizing surface/Bone surface	0.185 (±0.093)	0.226 (±0.071)	0.071	0.338 ±0.095)	0.331 (±0.029)	0.897
	Mineral apposition rate (µm/day)	0.851 (±0.157)	1.100 (±0.220)	0.092	0.739 (±0.092)	0.952 (±0.099)	0.015
	Bone formation rate (µm/day)	0.165 (±0.10)	0.257 (±0.114)	0.019	0.254 (±0.101)	0.316 (±0.061)	0.275